


ESKOM
NUCLEAR SITES
SITE SAFETY REPORTS
COASTAL ENGINEERING
INVESTIGATIONS
BANTAMSKLIP
Report No. 1010/3/102
OCTOBER 2009



PRESTEDGE RETIEF DRESNER WIJNBERG (PTY) LTD
CONSULTING PORT AND COASTAL ENGINEERS

Coastal Engineering Investigations - Bantamsklip Report No. 1010/3/102					
Revision	Date	Author	Checked	Status	Approved
00	March 2008	CWK/SAL	AAM/GKP	Draft for Comment	AAM
01	March 2008	CWK/SAL	AAM/GKP	For Use	AAM
02	March 2008	CWK/SAL	AAM/GKP	For Use	AAM
03	October 2009	RLH/CWK/SAL	AAM/GKP	For Use	

Keywords: Nuclear Sites, Coastal Engineering, Bantamsklip

ESKOM

NUCLEAR SITES SITE SAFETY REPORTS

COASTAL ENGINEERING INVESTIGATIONS BANTAMSKLIP

TABLE OF CONTENTS

	PAGE NO.
1. INTRODUCTION.....	1
1.1 Scope of Work	1
1.2 Limitations	2
1.3 Conventions and Terminology	2
2. PHYSIOGRAPHY AND MARINE/COASTAL GEOLOGY	3
2.1 General Site Description	3
2.2 Coastline and Seabed Characteristics	3
3. POSSIBLE CHANGES TO HYDROGRAPHIC CONDITIONS DUE TO CLIMATE CHANGE .4	
3.1 Introduction.....	4
3.2 Adopted Parameters for Long Term Climate Change.....	4
4. HYDROGRAPHIC CONDITIONS.....	5
4.1 Tides	5
4.2 Storm Surge	5
4.3 Long Waves.....	6
4.3.1 Definition	6
4.3.2 Analysis.....	6
4.3.3 General Discussion of Residuals	7
4.3.4 Results for Bantamsklip	8
4.4 Extreme Waves.....	9
4.5 Wave Transformation across the Surf-Zone.....	9
4.6 Wave Set-up.....	9
4.7 Wave Run-up.....	10

4.7.1	Calculation of Run-up from Profile Data	10
4.7.2	Model Input Conditions	10
4.7.3	Analysis of Profile Slopes	10
4.7.4	Results	11
4.8	Seiche	12
5.	INTAKE AND OUTFALL DESIGN CONSIDERATIONS.....	13
5.1	Classification of Intake and Outfall Structures	13
5.2	General Requirements	13
5.2.1	Quantity of Intake Water	13
5.2.2	Quality of Intake Water	14
5.3	Damage to Cooling Water Intakes and Outfall Structures.....	16
5.4	Sedimentation Risk	16
5.4.1	Tsunami Deposition	16
5.4.2	Tsunami Erosion	17
5.5	Blockage of Cooling Water Intake	19
5.5.1	General Considerations	19
5.5.2	Marine Debris.....	20
5.5.3	Biofouling	21
5.6	Sea Temperatures.....	21
6.	MODELLING OF WAVE PENETRATION AND SEICHE IN BASIN LAYOUTS	22
6.1	Introduction	22
6.2	Description of Two Dimensional Boussinesq Wave Model.....	22
6.3	Model Calibration	23
6.3.1	Model Setup	23
6.3.2	Calibration Results	24
6.4	Basin Layouts Modelled.....	25
6.4.1	Model Setup	25
6.4.2	Bathymetry and Breakwater Plan.....	25
6.5	Results	26
6.6	Discussion of Results	29
7.	COMBINATIONS OF MAXIMUM AND MINIMUM WATER LEVELS	30
7.1	Introduction	30
7.2	Design Basis for Extreme Events	30
7.3	Combination of Events.....	31

7.3.1	Reference Water Level and Return Periods	31
7.3.2	Dependant Events.....	32
7.3.3	Independent Events	33
7.3.4	Long Term Sea Level Rise and Climate Change Parameters	34
7.3.5	Confidence Levels.....	34
7.4	Results	35
7.5	Discussion of Results	37
8.	COASTLINE STABILITY AND CROSS-SHORE SEDIMENT TRANSPORT	39
8.1	Introduction	39
8.2	Long-term Coastline Trends from Aerial Photographs.....	40
8.2.1	Physical Process	40
8.2.2	Methodology	40
8.2.3	Accuracy	40
8.2.4	Coastline Trends.....	41
8.2.5	Discussion	42
8.3	Seasonal Variation in Coastline	42
8.3.1	Physical Process	42
8.3.2	Methodology	43
8.3.3	Coastline Trends.....	43
8.3.4	Quantification of Seasonal Variations.....	43
8.4	Storm Event Erosion.....	44
8.4.1	Physical Process	44
8.4.2	Methodology	45
8.4.3	Storm Events	47
8.4.4	Storm Analysis	48
8.5	Long-term Sea level Rise	49
8.5.1	Physical Process	49
8.5.2	Methodology	49
8.5.3	Storm Erosion Including Climate Change.....	51
8.6	Discussion of Results	52
9.	CONCLUSIONS.....	53

REFERENCES

FIGURES

APPENDIX A: Global Climate Change: Consequences for Coastal Engineering Design

LIST OF TABLES

Table 3.1	:	Adopted parameters for climate change to year 2100	4
Table 4.1	:	Predicted tidal levels for Hermanus	5
Table 4.2	:	Long wave data set information	7
Table 4.3	:	Extreme long-wave residuals at five SANHO tide gauge locations around South Africa	7
Table 4.4	:	Extreme long wave residuals at Port Nolloth	8
Table 4.5	:	Significant wave height from deep water to shallow water location used in run-up calculations for Profile 04	9
Table 4.6	:	Profile slopes for run-up calculations	11
Table 4.7	:	Calculated run-up values excluding climate change wave conditions	11
Table 4.8	:	Calculated run-up values including climate change wave conditions	12
Table 5.1	:	Design criteria intake basin	15
Table 5.2	:	Tsunami deposition study: Event identification	16
Table 5.3	:	Summary of deposition thickness	17
Table 5.4	:	Summary of inundation	18
Table 5.5	:	Summary of erosion characteristics	18
Table 6.1	:	Calibration model input parameters	23
Table 6.2	:	BW model results relative to still water level: Proposed Layout 02a	27
Table 6.3	:	BW model results relative to still water level: Proposed Layout 02b	28
Table 6.4	:	BW model results relative to still water level: Proposed Layout 02d	28
Table 7.1	:	Schematic of combination of events	34
Table 7.2	:	Extreme high water level results	35
Table 7.3	:	Extreme low water level results	36
Table 7.4	:	Maximum high and low water during tsunami event	37
Table 8.1	:	Maximum seasonal variations in horizontal displacements of the measured beach profiles	44
Table 8.2	:	SBEACH calibration parameters	46
Table 8.3	:	Maximum storm erosion horizontal displacements - Excluding climate change	48
Table 8.4	:	Parameters for long-term horizontal erosion due to sea level rise	51
Table 8.5	:	Maximum storm erosion horizontal displacements - Including climate change	51
Table 8.6	:	Maximum expected horizontal coastline erosion at Bantamsklip beach for the expected installation life	52

LIST OF FIGURES

- Figure 2.1 : Seabed features
- Figure 4.1 : Locations of SANHO tide gauges used in the extraction of long wave extreme values
- Figure 4.2 : Complete residual of three min data for 5 SANHO tide gauge locations around South Africa
- Figure 4.3 : Comparison of residual values for three long wave events for 3 SANHO tide gauge sites around South Africa
- Figure 4.4 : Comparison of residual values for a meteo-tsunami event for 5 SANHO tide gauge sites around South Africa
- Figure 4.5 : Comparison of residual values for a bound long wave event for 5 SANHO tide gauge sites around South Africa
- Figure 4.6 : Extreme value analysis of negative long wave residuals at Mossel Bay
- Figure 4.7 : Extreme value analysis of positive long wave residuals at Mossel Bay
- Figure 4.8 : Extreme value analysis of negative long wave residuals at Port Nolloth
- Figure 4.9 : Extreme value analysis of positive long wave residuals at Port Nolloth
- Figure 4.10 : Run-up calculations: Plan view of profiles used
- Figure 4.11 : Selected coastline profiles for run-up calculations
- Figure 4.12 : Extreme high water level beach run-up - Excluding climate change
- Figure 4.13 : Extreme high water level beach run-up - Including climate change
- Figure 5.1 : Biofouling plates recovered from Bantamsklip
- Figure 6.1 : Calibration of Boussinesq Wave modelling using existing Koeberg installation: Bathymetry and model layout
- Figure 6.2 : Calibration of Boussinesq Wave modelling using existing Koeberg installation: Settling basin main components (left) and position of calibration outputs (right)
- Figure 6.3 : Calibration of Boussinesq Wave modelling using existing Koeberg installation: Comparison of surface elevation - LIDAR survey (left) and BW model run (right)
- Figure 6.4 : Calibration of Boussinesq Wave modelling using existing Koeberg installation: Comparison of surface elevation - Line output profiles (Refer to Figure 6.2)
- Figure 6.5 : Boussinesq Wave modelling Bantamsklip basin layout: Bathymetry and model orientation
- Figure 6.6 : Boussinesq Wave modelling proposed basin (Layout 02a) results: $H_{m0} = 15.6$ m, $T_p = 24.4$ s - Instantaneous surface elevation (left) Significant wave height (right)
- Figure 6.7 : Boussinesq Wave modelling proposed basin (Layout 02b) results: $H_{m0} = 15.6$ m, $T_p = 24.4$ s - Instantaneous surface elevation (left) Significant wave height (right)
- Figure 6.8 : Boussinesq Wave modelling proposed basin (Layout 02d) results: $H_{m0} = 15.6$ m, $T_p = 24.4$ s - Instantaneous surface elevation (left) Significant wave height (right)
- Figure 6.9 : Logarithmic interpolation of extracted results of H_{m0} along the pump house sea wall as a function of input H_{m0} values from the 95% confidence level

- Figure 6.10 : Logarithmic interpolation of extracted results of maximum surface elevation along the pump house sea wall as a function of input H_{m0} values from the 95% confidence level
- Figure 6.11 : Logarithmic interpolation of extracted results of minimum surface depth along the pump house sea wall as a function of input H_{m0} values from the 95% confidence level
- Figure 7.1 : Comparison of extreme low water levels: Proposed Layout 02a and Proposed Layout 02d
- Figure 7.2 : Comparison of extreme high water levels: Proposed Layout 02a, Proposed Layout 02d and Profile 04 Beach run-up (including climate change parameters)
- Figure 8.1 : Combined image of the Bantamsklip site showing beach locations used for the coastline study
- Figure 8.2 : Plan view of historical coastline trends from aerial photographs - Castle Beach
- Figure 8.3 : Plan view of historical coastline trends from aerial photographs - Castle Beach
- Figure 8.4 : Plan view of historical coastline trends from aerial photographs - Pearly Beach
- Figure 8.5 : Plan view of historical coastline trends from aerial photographs - Pearly Beach
- Figure 8.6 : Plan view of historical coastline trends from aerial photographs - Pearly Beach
- Figure 8.7 : Plan view of historical coastline trends from aerial photographs - Shell Point
- Figure 8.8 : Plan view of historical coastline trends from aerial photographs - Shell Point
- Figure 8.9 : Plan view of historical coastline trends from aerial photographs - Shell Point
- Figure 8.10 : Plan view of historical coastline trends from aerial photographs - Plaatjieskraalbaai
- Figure 8.11 : Plan view of historical coastline trends from aerial photographs - Plaatjieskraalbaai
- Figure 8.12 : Plan view of historical coastline trends from aerial photographs - Jessie se Baai
- Figure 8.13 : Plan view of historical coastline trends from aerial photographs - Jessie se Baai
- Figure 8.14 : Plan view of historical coastline trends from aerial photographs - Jessie se Baai
- Figure 8.15 : Satellite image of the Bantamsklip site showing profile locations used for the coastline study
- Figure 8.16 : Measured beach profiles showing seasonal variations: Profiles 02 to 05 (refer to Figure 8.15 for positions of profiles)
- Figure 8.17 : Measured beach profiles showing seasonal variations: Profiles 06, 07, 10, 12 (refer to Figure 8.15 for positions of profiles)
- Figure 8.18 : Measured beach profiles showing seasonal variations: Profiles 14, 17, 24, 25 (refer to Figure 8.15 for positions of profiles)
- Figure 8.19 : Measured beach profiles showing seasonal variations: Profiles 26, 27, 28, 32 (refer to Figure 8.15 for positions of profiles)
- Figure 8.20 : Measured beach profiles showing seasonal variations: Profiles 33 to 36 (refer to Figure 8.15 for positions of profiles)
- Figure 8.21 : Seasonal erosion/accretion variation from mean: 2008 to 2009 - Distance from beacon at +1 m MSL (northern beaches)
- Figure 8.22 : Seasonal erosion/accretion variation from mean: 2008 to 2009 -Distance from beacon at +1 m MSL (southern beaches)
- Figure 8.23 : Beach profile instability due to extreme storm events

-
- Figure 8.24 : Duynefontein storm erosion model verification: Extrapolation of measured beach Profile 15 from available bathymetric data - Plan view
- Figure 8.25 : Duynefontein storm erosion model verification: Measured wave and water levels April 2008 to July 2008
- Figure 8.26 : Duynefontein storm erosion model verification: Comparison of modelled profile response of SBEACH calibration parameters against measured profile data
- Figure 8.27 : Duynefontein storm erosion model verification: Comparison of measured storm events and modelled storm progressions
- Figure 8.28 : Duynefontein storm erosion model verification: SBEACH modelled beach response profiles for measured storms and modelled storms
- Figure 8.29 : Bantamsklip beach storm erosion Profile 03 - Excluding climate change: Comparison of SBEACH response profiles using varying D_{50} values
- Figure 8.30 : Schematic diagrams of original Bruun's rule and implemented modification
- Figure 8.31 : Coastal morphology: Application of Bruun's rule to Profile 03 from existing bathymetric data
- Figure 8.32 : Bantamsklip beach storm erosion Profile 03 - Including climate change: Comparison of SBEACH response profiles using varying D_{50} values

1. INTRODUCTION

Eskom have embarked on a Nuclear Sites Programme (NSP) as part of their overall Nuclear Programme. The purpose of the NSP is to identify the most suitable nuclear sites to meet the requirements of sufficiency for a “Strategic reserve of banked potential sites” through a Nuclear Siting Investigation programme implemented to internationally accepted standards, according to best practice and in line with authority requirements (e.g. the National Nuclear Regulator) as appropriate.

To this end, Eskom have embarked on a programme to prepare licenceable Site Safety Reports (SSR’s) for three sites, namely Duynefontein, Bantamsklip and Thyspunt. SSR’s are licensing documents that are submitted to the national nuclear regulatory authority in support of obtaining a site licence. The data incorporated into the SSR’s contain site-related information spanning the site life-cycle phases from Nuclear Siting Investigations through construction, commissioning, operation, decommissioning, to site reuse and thereafter.

Prestedge Retief Dresner Wijnberg (Pty) Ltd (PRDW), as part of a multi-disciplinary team preparing the SSR’s, are responsible for the Oceanography and Coastal Engineering Chapter of the Site Safety Report (SSR), which is required to be prepared in accordance with Eskom’s Technical Specification for this work.

This report on the Coastal Engineering Investigations, along with the Numerical Modelling of Coastal Processes Report (PRDW, 2009a), provide details of the studies undertaken in support of the SSR Chapter on Oceanography and Coastal Engineering for the Bantamsklip site. Due to space constraints the SSR chapter summarises the study methodology and results, whilst the two supporting reports provide additional details.

1.1 Scope of Work

The scope of work is to characterise the following parameters at the Bantamsklip site:

- Physiography and marine/coastal geology
- Possible changes to hydrographic conditions due to climate changes
- Hydrographic conditions
- Intake and outfall design considerations
- Calculation of maximum and minimum seiche in basin layouts
- Combinations of maximum and minimum water levels
- Coastline stability and cross-shore sediment transport

1.2 Limitations

As required by Eskom's Technical Specification for this work, this study analyses return periods up to $1:10^6$ years for water levels, waves and beach erosion. Since these predictions are based on measured or hindcast datasets covering periods as short as three years, the predictions for longer return periods needs to be interpreted with extreme caution.

1.3 Conventions and Terminology

The following conventions and terminology are used in this report:

- H_{m0} is the significant wave height, determined from the zeroth moment of the wave energy spectrum.
- T_p is the peak wave period, defined as the wave period with maximum wave energy density in the wave energy spectrum.
- D_N is the diameter for which N% of the sediment, by weight, has a smaller diameter, e.g. D_{50} is the median grain diameter.
- Time is South African Standard Time (Time Zone -2)
- Seabed and water levels are measured relative to Chart Datum, which corresponds to Lowest Astronomical Tide (LAT) for Hermanus. Chart Datum is 0.788 m below Mean Sea Level or Land Levelling Datum (South African Tide Tables, 2009).
- The map projection system is as follows:

Map projection:	Gauss Conformal
Datum:	Hartebeesthoek 94
Spheroid:	WGS84
Scale factor:	1
Central meridian:	19 °E
Reference system:	WG19
Co-ordinates:	Eastings (X, increasing eastwards) Northings (Y, increasing northwards)
Distance units:	International metre

2. PHYSIOGRAPHY AND MARINE/COASTAL GEOLOGY

2.1 General Site Description

Bantamsklip is situated in the Western Cape, approximately 10 km south-east of Pearly Beach. It falls within the Overberg region in the southern-parts of the Western Cape.

The location of Bantamsklip is well contained between two prominent headlands at Danger Point (20 km NW) and Quoin Point (10 km SE). The stretch of coastline forms an isolated cell with no significant sediment feeds or losses into or out of the cell. The sediment transport regime in the vicinity of the Bantamsklip site has been extensively modelled and is discussed in PRDW (2009a). There will be redistribution of sand deposits under storm conditions and high concentration of suspended sediments in the breaker zone. A large reef area situated in front of the headland of Bantamsklip generally induces wave breaking (PRDW, 2001).

2.2 Coastline and Seabed Characteristics

Bantamsklip is situated on the coastal plain to the south- west of a discontinuous line of hills which lies parallel to the coast at a distance of 4 to 5 km. The coastal plain lies generally below the 60 m MSL contour. Refer to Figure 2.1 for details of the Bantamsklip site and seabed features.

The Bantamsklip site is covered by vegetated semi-consolidated dunes with alternating calcarenite and boulder beds overlying the basement rock. The dunes mostly consist of light brown, poorly sorted, calcareous sands. It is underlain by Peninsula Formation quartzites with minor green-to-grey shale bands. The often cross-bedded quartzites are white to light grey, fine to medium grained and poorly sorted (PRDW, 2001).

Peninsula formation quartzites form a rocky coastline. Extensively developed joint sets have caused the outcrop to have a very ragged appearance. Easterly striking faults and closely spaced joints have resulted in a number of parallel gullies. A 10 to 60 m wide grass covered flat strip occurs between the beach and the first dunes. Minor seepages occur sporadically along the contact between the grassy flats and bedrock, with a few fountains restricted to the faulted area on the northern portion of the site (PRDW, 2001).

A single dune with gentle easterly and westerly dipping slopes parallels the immediate coastline. The highest dune peaks vary from 10 to 15 m MSL. On the eastern side of the site, there is a gentle depression in the topography with a general decline in elevation to the south-east. Seabed slopes vary along the site. Between levels -5 m CD and +10m CD the average beach slope ranges from 1:42 to 1:37. Further offshore between -20 m CD and -5 m CD the average beach slope ranges from 1:150 to 1:24.

3. POSSIBLE CHANGES TO HYDROGRAPHIC CONDITIONS DUE TO CLIMATE CHANGE

3.1 Introduction

In the past, engineers relied on the assumption that the natural environment, although highly variable, remains statistically static and that probability distributions for prime environmental factors such as wind speed, wave height, flood frequency and sea level are unchanging with time. Efforts have therefore centred on the already difficult problem of estimating the underlying natural statistical variability of these phenomena through long-term measurement programs, sophisticated numerical modelling and statistical simulation. The proven rise in carbon dioxide levels and the possibility of the Earth being subject to an enhanced "greenhouse" effect has brought some aspects of this basis of design into question. Extrapolation of probability distributions to exposure times very much longer than the data base may be invalid in a changing environment unless some specific account can be taken of those changes. Scientific opinion suggests that changes to climate may occur within the design life of many coastal and ocean engineering activities. Consequently, consideration of the possible impacts of climate change should be included in the design process (Engineers Australia, 2004).

The oceanographic and coastal engineering parameters which may be influenced by climatic changes over the next 90 to 100 years are described in Appendix A. The adopted parameters for this site safety assessment are tabulated in Section 3.2. The 90 to 100 year horizon takes account of the likely life of the nuclear facility (60 years) and cognisance of the phasing in of facilities over the next 20 plus years.

3.2 Adopted Parameters for Long Term Climate Change

The adopted parameters for long term climate change for purposes of the SSR are summarized in the following table.

TABLE 3.1: ADOPTED PARAMETERS FOR CLIMATE CHANGE TO YEAR 2100

Parameter	Change
Sea level rise to 2100	+ 0.8 m
Sea temperature	+ 3°C
Wind speed	+ 10%
Wave height	+ 17%
Storm surge	+ 21%

These values are based on the information available at present, and need to be continually reassessed as new data and research results become available.

4. HYDROGRAPHIC CONDITIONS

Only details of hydrographic conditions required for the coastal engineering calculations are provided below. Details on other hydrographic conditions including waves, storm surge, tsunamis, currents and seawater temperature are described in PRDW (2009a).

4.1 Tides

The closest port to the Bantamsklip site for which long-term tidal data is available is Hermanus. The predicted tidal levels at Hermanus are as follows (South African Tide Tables, 2009):

TABLE 4.1: PREDICTED TIDAL LEVELS FOR HERMANUS

Parameter	Level [m CD]	Level [m MSL]
Lowest Astronomical Tide (LAT)	0.00	-0.79
Mean Low Water Springs (MLWS)	0.27	-0.52
Mean Low Water Neaps (MLWN)	0.75	-0.04
Mean Level (ML)	1.02	0.23
Mean High Water Neaps (MHWN)	1.29	0.50
Mean High Water Springs (MHWS)	1.78	0.99
Highest Astronomical Tide (HAT)	2.07	1.28

These levels are relative to Chart Datum, which is 0.788 m below Mean Sea Level or Land Levelling Datum (South African Tide Tables, 2009). The values for MSL are accurate to the precision as supplied in the South African Tide Tables.

HAT is the highest level which can be predicted to occur under average meteorological conditions and under any combination of astronomical conditions (South African Tide Tables, 2009). HAT is not the extreme upper level which can be reached, as storm surges and other meteorological or geological (e.g. tsunami) conditions may cause considerably higher levels to occur.

LAT is the lowest level which can be predicted to occur under average meteorological conditions and under any combination of astronomical conditions (South African Tide Tables, 2009). LAT is not the extreme lower level which can be reached, as negative storm surges and other meteorological or geological (e.g. tsunami) conditions may cause considerably lower levels to occur.

HAT and LAT will only be reached once every 18.6 years, although levels within approximately 0.10 m of HAT and 0.06 m of LAT will be reached annually.

4.2 Storm Surge

Storm surge is, for the purpose of this report, defined as the influence of meteorological effects such as winds and barometric pressure that result in actual sea level being above or below the predicted astronomical tide level.

For the calculations of extreme high and low water events, extreme values for positive and negative storm surge residuals (the difference between the actual water level and the predicted tide) have been calculated from long-term hourly tide gauge measurements. Refer to PRDW (2009a) for full details.

4.3 Long Waves

This section describes exclusively the maximum expected elevation due to long waves (refer to definition below), the analysis and run-up resulting from the Probable Maximum Tsunami is evaluated independently (PRDW, 2009a).

4.3.1 Definition

Long waves are, for the purpose of this report, defined as fluctuations in still water level with periods between 3 to 60 minutes. Long waves typically include: edge waves, shelf waves, bound waves and tsunami (both tectonically and meteorologically generated).

Meteo-tsunami are meteorologically initiated long waves which can subsequently propagate as an edge or shelf waves. Meteo-tsunami can also produce patterns in tide gauge records closely analogous to tectonic tsunami, with multiple waves impinging on the coast for a number of hours (PRDW, 2009a).

Bounded long waves are generated by gradients in radiation stress found in wave groups, causing a lowering of the mean water level under high waves and a raising under low waves (CEM, 2003). The bounded wave travels at the group speed of the wind waves, hence is bound to the wave group. The occurrences of bounded long waves are therefore expected to occur during a storm.

4.3.2 Analysis

High frequency (1 - 3 minute) measured data from tide gauges at Port Nolloth, Simon's Town, Cape Town, Mossel Bay and Port Elizabeth have been processed to determine the occurrence and severity of long waves (refer to Figure 4.1 for tide gauge locations). The data has been kindly provided by the Hydrographer of the South African Navy (who is not responsible for any transcription errors or errors due to calculations using the data). The data has been "cleaned" (by removing "spikes" and other errors), and the residuals (difference between the measured data and a 60 minute running mean) have been extracted. Details of the available data sets for each of the tide gauges are presented in Table 4.2 and illustrated in Figure 4.2.

TABLE 4.2: LONG WAVE DATA SET INFORMATION

Location	Start Date	End Date	Duration [years]
Port Nolloth	2006-01-01	2009-08-31	3.32
Cape Town	2008-03-31	2009-08-31	1.35
Simon's Town	2006-01-01	2009-08-31	3.45
Mossel Bay	2007-05-16	2009-08-31	1.96
Port Elizabeth	2005-06-09	2009-08-31	4.20

An extreme value analysis was completed on the residuals of the data using the MIKE EVA software package from DHI (refer to PRDW (2009a) for details regarding the EVA software). Extreme values for return periods of 1:1, 1:10, 1:100 and 1:10⁶ years have been calculated and are shown in Table 4.3 for all five tide gauge locations. As the measured datasets are only between 1.35 and 4.2 years in duration, results from extrapolation to return periods longer than 5 to 10 years should be interpreted with caution.

TABLE 4.3: EXTREME LONG-WAVE RESIDUALS AT FIVE SANHO TIDE GAUGE LOCATIONS AROUND SOUTH AFRICA

Return period [years]	Location	Positive Residuals [m]		Negative Residuals [m]	
		Best estimate	Upper 95% confidence	Best estimate	Upper 95% confidence
1	Port Nolloth	0.37	0.51	0.29	0.41
	Cape Town	0.37	0.45	0.40	0.51
	Simon's Town	0.18	0.21	0.18	0.21
	Mossel Bay	0.45	0.55	0.46	0.58
	Port Elizabeth	0.33	0.39	0.30	0.33
10	Port Nolloth	0.74	0.99	0.62	0.88
	Cape Town	0.52	0.64	0.59	0.74
	Simon's Town	0.26	0.31	0.26	0.30
	Mossel Bay	0.65	0.78	0.71	0.89
	Port Elizabeth	0.50	0.59	0.37	0.40
100	Port Nolloth	1.14	1.49	1.03	1.39
	Cape Town	0.67	0.82	0.77	0.94
	Simon's Town	0.33	0.39	0.32	0.38
	Mossel Bay	0.81	0.97	0.94	1.16
	Port Elizabeth	0.65	0.77	0.41	0.44
10 ⁶	Port Nolloth	2.91	3.64	3.16	3.77
	Cape Town	1.27	1.47	1.42	1.67
	Simon's Town	0.57	0.70	0.54	0.66
	Mossel Bay	1.34	1.62	1.83	2.21
	Port Elizabeth	1.15	1.44	0.51	0.59

4.3.3 General Discussion of Residuals

Figure 4.3 illustrates the typical residual values and periods associated with long-wave events. The figure shows recorded events at Port Nolloth, Mossel Bay and Port Elizabeth, with the events attributed to: a meteo-tsunami, bound long-waves and tectonic tsunami respectively. The tectonic tsunami is seen (NGDC, 2009) to have originated in Sumatra, Indonesia, from an 8.4 magnitude earthquake which occurred at approximately midday (GMT) on the 12th of August, 2007. As the tide gauges are located inside harbours, the measured data is likely to include localised effects such as resonance of the adjacent bay or harbour basin.

Figure 4.4 illustrates the progression of a meteo-tsunami from Port Nolloth to Port Elizabeth and demonstrates the typical travel times associated with these events and the relative magnitude of the residuals at each of the five SANHO tide gauge stations.

Figure 4.5 illustrates the progression of bound long-waves associated with a measured storm event and associated magnitude of the residuals at each of the five SANHO tide gauge stations.

Although Figure 4.4 indicates the initial location of the identified meteo-tsunami event as near Port Nolloth, there is currently insufficient information to suggest that the initiation mechanisms are specific to the coastal area around Port Nolloth. It is reasonable, and conservative, to assume that these initiating events could as readily occur at any location around the coast of South Africa. For this reason, the maximum predicted long-wave event tabulated in Section 4.3.4 and utilised in the calculation of combinations of maximum surface elevations expected at the proposed nuclear installation corridor, is the Port Nolloth 1:10⁶ year event.

4.3.4 Results for Bantamsklip

For the evaluation of the impact of long waves at Bantamsklip, three minute sampled data (2006-01-01 to 2009-08-31) from the Port Nolloth tide gauge have been used. This approach is considered to be conservative.

As only 3.45 years of continuous data are currently available, results from extrapolation to return periods longer than 10 years should be interpreted with caution. The upper 95% confidence level to the best estimate is calculated using the Monte Carlo method. The results of the extreme value analysis for Mossel Bay, not tabulated, are presented in Figures 4.6 and 4.7. The results for Port Nolloth are presented in Figures 4.8 and 4.9 and Table 4.4.

TABLE 4.4: EXTREME LONG WAVE RESIDUALS AT PORT NOLLOTH

Return Period [years]	Positive Residuals [m]		Negative Residuals [m]	
	Best estimate	Upper 95% confidence	Best estimate	Upper 95% confidence
1	0.37	0.51	0.29	0.41
10	0.74	0.99	0.62	0.88
100	1.14	1.49	1.03	1.39
10⁶	2.91	3.64	3.16	3.77

The large uncertainty in the EVA analysis for the longer return periods, particularly evident in the lower 5% confidence level plots in Figures 4.6 to 4.9, is indicative of the short period of data available compared to the extended return periods considered.

4.4 Extreme Waves

In this section sea and swell waves generated by wind and having periods between 4 and 25 s are described. The wave climate at the site was determined by refracting a 15 year offshore hindcast dataset to the -30 m CD depth contour opposite the site and then performing an extreme value analysis on the dataset. The modelling procedure and the results are described in PRDW (2009a). Wave data have also been recorded at two locations (15 m and 30 m water depths) at the site since March 2008. Full details are provided in PRDW (2009a).

4.5 Wave Transformation across the Surf-Zone

The cross-shore hydrodynamic engine of the LITPACK model (as described in PRDW, 2009a) was used to transfer each of the extreme wave conditions at the -30 m CD position inshore to the -5 m CD position, where the resulting wave conditions are required as input to the wave run-up computations.

The inputs for the LITPACK model are the beach profile and the wave conditions at -30 m CD. The water level is set to HAT plus any addition for storm surge and climate change where applicable. (Refer to Section 3.2 and Table 3.1). The calculations are performed using variable grid spacing with values between 1 m and 2 m. Note that the wave heights extracted at -5 m CD for calculations of run-up are broken wave heights and represent a depth-limited condition (refer to Table 4.5 for H_{m0} at -30 m CD and -5 m CD).

TABLE 4.5: SIGNIFICANT WAVE HEIGHT FROM DEEP WATER TO SHALLOW WATER LOCATION USED IN RUN-UP CALCULATIONS FOR PROFILE 04

Return period [years]	H_{m0} [m] at -30 m CD and -5 m CD							
	Excluding climate change				Including climate change			
	Best estimate		Upper 95% confidence		Best estimate		Upper 95% confidence	
	-30 m CD	-5 m CD	-30 m CD	-5 m CD	-30 m CD	-5 m CD	-30 m CD	-5 m CD
1	5.5	5.3	5.7	5.4	6.4	6.0	6.7	6.1
10	6.8	5.8	7.3	6.0	7.9	6.6	8.5	6.7
100	8.0	6.2	8.9	6.5	9.3	7.0	10.4	7.3
10⁶	12.6	7.4	15.6	8.1	14.8	8.4	18.2	9.1

4.6 Wave Set-up

The cross-shore wave model used (refer to Section 4.5) includes the effect of wave set-up. Although this result for wave set-up is not used explicitly, including this parameter takes into account the effect of a higher water level on the wave transformation in the surf zone in itself.

In the present study, wave run-up is calculated using empirical equations from laboratory investigations with irregular wave input (refer to Section 4.7). Total vertical run-up is correlated to a non-dimensional height based on physical measurements inclusive of the effect of set-up. Therefore, no separate analysis of wave set-up is required as it is implicit in the equations for wave run-up.

4.7 Wave Run-up

Wave run-up is calculated on the average beach slopes of five beach and coast profiles for the Bantamsklip site. The transformed wave conditions (refer to Section 4.5) are used in the run-up calculations. The plan view of the selected profiles is shown in Figure 4.10. The final value of vertical wave run-up is seen to be highly dependent on the chosen slope of the profile. In order to maintain consistency of approach for all of the profiles, the slope was taken as the average value between points at -5 m CD to +10 m CD.

4.7.1 Calculation of Run-up from Profile Data

Hughes (2004) re-examined existing wave run-up data for regular, irregular and solitary waves on smooth, impermeable plane slopes. A model is used to derive a new wave run-up equation in terms of a dimensionless wave parameter representing the maximum, depth-integrated momentum flux in a wave as it reaches the toe of the slope.

The approach by Hughes (2004) assumes a smooth impermeable slope. For an impermeable slope, the wave run-up will typically be more than for an equivalent permeable slope. This approach is considered conservative as these calculations for wave run-up will give values greater than for rough, permeable slopes.

For calculation of wave run-up for plunging/spilling waves refer to Equation 40 in Hughes (2004). In Hughes (2004), $R_{u,2\%}$ is the vertical elevation from sea water level exceeded by 2% of the run-ups.

4.7.2 Model Input Conditions

The above-mentioned method (Hughes, 2004), with modelled wave conditions at -5 m CD as input, is used for calculating design wave run-up $R_{u,2\%}$.

Run-up for each of the combined events (refer to Section 7.3) has been analysed for given wave and water-level input conditions for each profile. The values for H (local significant wave height) and h (water depth at -5 m CD) have been extracted from the LITPACK results files (refer to Section 4.5) and used to assess maximum wave run-up.

4.7.3 Analysis of Profile Slopes

Initial assessment of the results shows a high dependence on the average beach slope of the profile under consideration. Smoothing of profile features such as bars and naturally formed berms reduces the slope and tends to reduce the wave run-up, whereas using the maximum feature slope tends to greatly increase the levels of calculated run-up.

Since the intake structure details and terrace level structures are not yet defined, no coastline structures have been superimposed onto the profiles and considered in the calculations. The results will be subject to review once the design of the intake and terrace has advanced and any coastline structures can be incorporated into the assessment.

A number of cross-sections have been taken along the Bantamsklip site coastline. Beach slopes for each of the cross-sections have been assessed (refer to Figure 4.11 for profile details). Table 4.6 summarises slope information for all of the profiles. The mean values of the profile slopes between -5 m CD and +10 m CD are used in the run-up calculations.

TABLE 4.6: PROFILE SLOPES FOR RUN-UP CALCULATIONS

	-30 m CD to -20 m CD		-20 m CD to -5 m CD		-5 m CD to +10 m CD	
	Mean	Max	Mean	Max	Mean	Max
Profile 01⁽¹⁾	1:185	1:18	1:78	1:17	1:37	1:0.9
Profile 02	1:45	1:12	1:150	1:12	1:42	1:12
Profile 03	1:114	1:19	1:81	1:24	1:34	1:9
Profile 04	1:62	1:17	1:53	1:25	1:32	1:7
Profile 05	1:33	1:17	1:24	1:24	1:42	1:11

Notes:

- 1) Profile information extrapolated from + 5 m CD due to lack of topographic information

4.7.4 Results

Results are indicated in Figure 4.12 (excluding the effects of climate change) and Figure 4.13 (including the effects of climate change), and tabulated below (refer to Chapter 3 for details regarding increase water levels and wave conditions due to climate change).

TABLE 4.7: CALCULATED RUN-UP VALUES EXCLUDING CLIMATE CHANGE WAVE CONDITIONS

	Run-up [m above Still Water Level]							
	Best estimate				Upper 95% confidence			
	Return period [years]				Return period [years]			
	1	10	100	10 ⁶	1	10	100	10 ⁶
Profile 01	2.45	2.65	2.82	3.36	2.48	2.72	2.93	3.68
Profile 02	2.37	2.55	2.70	3.20	2.44	2.65	2.84	3.57
Profile 03	2.67	2.91	3.10	3.72	2.71	2.98	3.23	4.07
Profile 04	2.95	3.25	3.50	4.24	3.00	3.35	3.65	4.66
Profile 05	2.52	2.84	3.10	3.82	2.58	2.94	3.27	4.13

The run-up varies for each of the profiles due to wave refraction effects and most importantly the beach slope between -5 m CD to +10 m CD, (refer to Section 4.7.3).

TABLE 4.8: CALCULATED RUN-UP VALUES INCLUDING CLIMATE CHANGE WAVE CONDITIONS

	Run-up [m above Still Water Level]							
	Best estimate				Upper 95% confidence			
	Return period [years]				Return period [years]			
	1	10	100	10 ⁶	1	10	100	10 ⁶
Profile 01	2.77	3.00	3.19	3.81	2.81	3.07	3.31	4.18
Profile 02	2.62	2.81	2.98	3.53	2.65	2.87	3.09	3.86
Profile 03	3.02	3.28	3.51	4.21	3.07	3.37	3.65	4.63
Profile 04	3.34	3.67	3.95	4.80	3.40	3.78	4.12	5.29
Profile 05	2.88	3.24	3.53	4.34	2.95	3.35	3.73	4.70

Since the exact position of the nuclear terrace is unknown at present, the single maximum run-up from all of the profiles has been used to calculate the maximum water levels in Table 7.2. The maximum run-up occurs for Profile 04, due to increased profile slope.

4.8 Seiche

For the purpose of this report, a seiche has been defined as the collective term for long period 2 to 20 minute water surface fluctuations due to resonance, surf beat and water oscillation in a confined area. The effects of seiche combined with maximum instantaneous surface elevations due to wind wave propagation are modelled explicitly for the required return periods using a Boussinesq wave model. Results for seiche and maximum surface elevations have been calculated for three proposed basin layout conditions (refer to Chapter 6).

5. INTAKE AND OUTFALL DESIGN CONSIDERATIONS

5.1 Classification of Intake and Outfall Structures

Since no engineering feasibility studies on the intake and outfall structures have been completed by Eskom to date (October 2009), six conceptual layouts were developed which serve to illustrate the thermal plumes and recirculation that can be anticipated for typical combinations of intake and outfall types. The intakes considered are basins and offshore tunnels, while the outfalls considered are nearshore channels and offshore tunnels. Note that these conceptual layouts will need to be refined based on geotechnical and engineering considerations.

The six intake-outfall layouts assessed in this study are:

- Layout 1: Offshore tunnel intake (45 m depth) and offshore tunnel outfall (25 m depth)
- Layout 2: Basin intake and offshore tunnel outfall (40 m depth)
- Layout 3: Offshore tunnel intake (45 m depth) and nearshore channel outfall (2 m depth)
- Layout 4: Basin intake and nearshore channel outfall (2 m depth)
- Layout 5: Offshore tunnel intake (30 m depth) and nearshore channel outfall (5 m depth)
- Layout 6: Basin intake and nearshore channel outfall (5 m depth)

Further details of these layouts, along with the thermal plume, recirculation and sediment transport modelling results for these layouts are provided in PRDW (2009a).

5.2 General Requirements

5.2.1 Quantity of Intake Water

For a new installed power output of 10 000 MWe, the anticipated seawater cooling flow rate is 456 m³/s (refer to PRDW (2009a) for details).

In the case of intake and outfall tunnels, the diameter of the tunnels is designed to avoid the risk of sediments settling in the tunnel (minimum velocity of 2.5 to 3 m/s). On the other hand, the velocity in the tunnels need to be limited in order to reduce head losses in the tunnels. For the purposes of maintenance redundancy, it is assumed each reactor unit will be provided with an intake and/or outfall tunnel to allow the reactor and tunnel to go into maintenance outage independently of the other units. All intake and outfall configurations have been based on a layout with 6 nuclear units, each having a capacity of 1650 MWe. This results in an intake/outfall discharge of 76 m³/s per unit and a tunnel diameter of between 5.5 to 6.5 m to meet the above mentioned requirements. Other configurations (with different capacity of nuclear units) are possible, but no significant differences in modelling output are expected.

5.2.2 Quality of Intake Water

5.2.2.1 Clean Water

Most nuclear power plants obtain condenser cooling water from the open sea, in which case pre-screening of the intake water using travelling screens, mechanically cleaned bar screens, or passive well screens is necessary. In many instances, the screening chamber is located on or near shore and the intake pipe may extend out hundreds of meters into the sea.

It is recommended (Bosman and Wijnberg, 1987) to:

- Remove sediment particles larger than 0.15 mm (by dredged stilling basin or settling pond)
- Remove marine organisms larger than 5 mm
- Prevent marine fouling in pressure ducts

The intake design will have to respond to the maximum allowable sediment concentrations for the pumps. The pumps of the existing Koeberg nuclear power station can cope with sediment concentrations up to 50 ppm (Eskom, 2006). No information on the maximum allowable sediment concentrations for the planned installation is available.

A dredged stilling basin or an onshore settling pond will be required to enable capture of sediment particles by settlement. Offshore intake systems will take in water of better quality and will require less pre-treatment than a nearshore intake system. The conventional method of intake is the open intake of seawater by active or passive screens of different kind. These are subject to marine biological activity and suspended matter, which needs to be removed or reduced by pre-treatment. Impingement of marine life in offshore intakes can be reduced by proper design of the velocity cap. The velocity cap, the cover placed over the vertical terminal of an offshore intake pipe, converts vertical flow into horizontal flow at the intake entrance to reduce fish entrainment. This velocity ranges from 0.15 to 0.45m/s (ASCE, 1982). The velocity cap is sized to ensure a maximum horizontal velocity of 0.3 m/s or less is achieved.

Chlorine, produced by electrolysis, is typically used to keep the cooling system free of marine growth. Maintenance of the pipelines can add a significant factor to the overall costs. The offshore tunnel intake option should include adequate redundancy to allow for periodic maintenance/cleaning of the tunnel and intake system.

In case of a basin intake, the settling basin needs to be designed to capture fine suspended sediments. The basin layout needs to fulfil the following requirements (Bosman and Wijnberg, 1987):

- Sand larger than 0.15 mm should be removed
- Currents in the entrance channel $U > 0.6$ m/s
- Currents in the settling basin $U < 0.1$ m/s
- Required space for installation of the pumphouses

For the purposes of developing a basin concept, the main characteristics of the existing Koeberg basin have been rescaled to meet the above requirements. Table 5.1 summarizes the design criteria and compares the criteria with the actual conditions of the existing intake basin at Koeberg. The minimum current in the entrance channel is significantly lower than the recommended 0.6 m/s. This results in accretion of sediments at the entrance of the basin and will carry on until a natural equilibrium is reached. These shallow entrance conditions don't impact on the proper functioning of the intake basin.

TABLE 5.1: DESIGN CRITERIA INTAKE BASIN

Parameter	Design criteria	Actual conditions existing basin	New basin
Cooling water intake	---	76 m ³ /s	380 m ³ /s
Basin entrance width	---	145 m	145 m
Basin entrance depth	---	-5 m CD	-12 m CD
Width of the settling basin	---	380 m	530 m
Length of the settling basin	---	385 m	750 m
Dredge depth	---	-3 m CD (actual depth)	-7.5 m CD (dredge design depth)
Current in entrance channel	> 0.6 m/s	0.1 m/s	0.2 m/s
Current in settling basin	< 0.1 m/s	0.06 m/s	0.09 m/s
Min. particle diameter able to settle	150 microns	60 microns	60 microns

Although the cooling water intake volume for the new basin is much higher, the entrance width of the basin is fixed to 145 m, increasing the minimum velocity at the entrance. All other dimensions of the new basin are rescaled in order to meet the same sediment settling capacity of the existing Koeberg basin. This results in a settling basin of 530 m x 750 m (width x length) with a dredged depth of -7.5 m CD. The sediment settling capacities of the existing and new basin are calculated based on the retention time for individual grains according to USACE (1987). The retention time is a function of the hydraulic efficiency of the settling basin which is dependant on the length to width ratio of the settling basin.

5.2.2.2 Recirculation Risk

Six different configurations of intake and outfall structures have been considered for the Bantamsklip site and are dealt with in more detail in the Numerical Modelling Report (PRDW, 2009a). For each of these configurations, the thermal plume dispersion has been modelled for a typical winter, summer and calm weather conditions in order to evaluate the recirculation risk of heated cooling water to the cooling water intake point of the new nuclear power installation.

5.3 Damage to Cooling Water Intakes and Outfall Structures

In the case of offshore intake or outfall structures, the structures need to be positioned in a depth where extreme wave conditions will have no damaging impact on the structure or any of its components which might jeopardize the intake or discharge of cooling water. In the case of nearshore basin or channel type structures (rock structures), the structure will be designed to a “no-damage” criteria (less than 5% damage). The damage is defined as a percentage of the eroded volume (CEM, 2006).

5.4 Sedimentation Risk

The sediment transport rates around and into the proposed basin intakes, as well as the suspended sediment concentrations and sand volumes drawn into the proposed offshore tunnel intakes has been modelled in PRDW (2009a).

Bottom shear by a strong tsunami current may be significant in shallow water. The deposition of a large amount of sediment could affect the safety features of the plant. In particular, the deposition of sediment around cooling water structures or the water inlet and outlet might disrupt the operation of the plant.

5.4.1 Tsunami Deposition

As part of the investigation into sedimentation risk from tsunami waves a literature study has been completed. Historic cases of deposition from tsunami events from the 1998 Papua New Guinea Tsunami, 2001 Peru Tsunami and the most recent 2004 Indonesian Tsunami have been researched and a summary of the relevant results presented. The events associated with these tsunamis are described in Table 5.2.

TABLE 5.2: TSUNAMI DEPOSITION STUDY: EVENT IDENTIFICATION

Tsunami event	Ocean	Earthquake Magnitude	Maximum water level relative to Mean Sea Level (m)
1998 - Papua New Guinea	Pacific	7.0 + landslide	15
2001- Peru	Pacific	8.4	7
2004 - Indonesia	Indian	9.2	10

5.4.1.1 Papua New Guinea, 1998, Peru, 2001

Details of the maximum and minimum deposition vary between resources examined for the study. The maximum values measured have recorded values of up to 1 m, with average historic values of approximately 0.25 m (Morten *et al.*, 2007).

5.4.1.2 *Indonesia, 2004*

After the 2004 Indonesian Tsunami, field data of tsunami inundation and sediment deposits along the west Sumatra coast were collected (USGS, 2005).

At Kuala Mersi, approximately 100 km south of Banda Aceh, a 15 m high tsunami wave inundated a distance of nearly 2 km across a coastal plain that was only 3 - 4 m above sea level. The tsunami eroded the beach face and left a deposit that varied in thickness from less than 0.01 m to 0.34 m across the coastal plain.

At Lhoknga and Leupueung, the maximum thickness of the tsunami deposits of sediment observed along surveyed lines was about 0.7 m. Most of them were composed of beach-sand including shells and corals. At the village of Lampuuk, 0.73 m of sediment was deposited over soil.

In Sri Lanka, run-up elevation measured varied from less than 3 m to more than 12 m (increasing on the East Coast of Sri Lanka towards the south). Measured water levels near the coastline varied from less than 3 m to more than 10 m (increasing on the East Coast of Sri Lanka towards the south, and on the south coast toward the East). Erosion was often concentrated in a relatively narrow zone near the coast.

At Mankerni (Sri Lanka), a grassy area was eroded about 1 m in the vertical in a zone about 20 to 30 m wide near the coast. Tsunami sediment deposits started about 50 m inland, and decreased in thickness from about 0.10 m total thickness to about 0.02 m thickness at about 150 m inland.

5.4.1.3 *Discussion of Results*

According to the sediment surveys undertaken for different modern tsunamis events, a maximum value of 1 m for tsunami sediment deposition is verified. The table below summarises deposition patterns from the study.

TABLE 5.3: SUMMARY OF DEPOSITION THICKNESS

Tsunami Event	Location	Deposition thickness [m]
Papa New Guinea, 1998		0.25
Peru, 2001		1.00
Indonesia, 2004	Kuala Mersi, Sumatra	0.01 to 0.34
	Lhoknga and Leupueung, Sumatra	0.70
	Lampuuk, Sumatra	0.73
	Mankerni, Sri Lanka	0.02 to 0.10

5.4.2 Tsunami Erosion

5.4.2.1 *Inundation Scour*

Scour comparisons were undertaken for Banda Aceh and Lhoknga, Sumatra. These two adjacent coastal communities are located very near the tsunami source which bore the brunt of severe

inundation flow and suffered large areas of complete destruction from the 2004 Indonesian Tsunami (FEMA, 2006).

The Lhoknga coast experienced the highest run-up elevations recorded in the event (>20 m).

All observed scour depths appear to be less than 3 m, at both Banda Aceh and Lhoknga. The scour patterns were in areas of relief, near structures, and with vast areas of eroded coastlines.

A scour evaluation was performed for 20 sites selected to represent a range of locations, inundation conditions and scour depth measured after the 2004 Indonesian Tsunami in India, Andaman/Nicobar, Thailand and Sumatra (FEMA, 2006).

The selected site parameters provided a broad range of run-up heights (up to 20 m) and inundation distances (up to several kilometers). However, all evaluated scour features were located within 200 m of the coastline, except at the Lhoknga mosque in Sumatra which was approximately 600 m from the coastline. Soil conditions included various gradations of silty sands, sand and gravels typical of coastal environments. Table 5.4 provides a summary of the water levels and inundation distances observed (FEMA, 2006):

TABLE 5.4: SUMMARY OF INUNDATION

Location	Run-up height	Overland flow depth	Inundation distance
India	2 to 5 m	0.2 to 2 m	Up to 800 m
Andaman/Nicobar	3 to 15 m	Not available	Not available
Thailand	5 to 10 m	2 to 5 m	Up to 5000 m
Sumatra	5 to 20 m	2 to 15 m	Up to 10,000 m

Topography generally consisted of low (1 to 2 m) fore-dunes, some areas of slightly raised profiles on higher more stabilized dunes, associated with relatively flat beach plains. Vegetation adjoining beaches varied from mostly agricultural fields and coconut plantations, with some areas of more dense tropical forests or shrubbery. Some areas of steep or rocky coastlines also produced damaging scour, though not as predominant as in the broad low lying inundation (refer to Table 5.5).

TABLE 5.5: SUMMARY OF EROSION CHARACTERISTICS

Run-up Height (m)	Dist. to Coastline (m)	Scoured Soil Type	Surface Cover	Observed Scour (m)	Scour Feature
4 to 5	30 to 100	Med to Fine Sand	Beach / very large beach	0.5 to 1.5	Road / Railway scour
5 to 12	5 to 180	Coarse/Med to Med/Fine Sand	Beachfront	0.5 to 2	Footing / Bridge scour
15	50 to 75	Coarse/Med to Med/Fine Sand	Beachfront with spit	1.5 to 2.5	Abutment washout/sinkhole
4	5	Med to fine sand w/gravel	Beachfront w/seawall	1	Seawall road scour
11	5	Silty gravel base & boulders	Jungle slope, rocky coast	4	Road scour

5.4.2.2 *Sub-aerial Scour*

Though not measured or assessed in the case studies referenced, sub-aerial scour due to tsunami are likely to be destructive to coastal structures (Yim, 2006). Offshore tsunami scour differs from ordinary coastal structure scour, which occurs gradually caused by periodic waves and steady current loads. In a tsunami or storm surge, the leading wave may scour away much of the supporting materials around the base of the structure such that catastrophic failure occurs with following waves due to hydrodynamic drag forces. Deposition usually occurs within sub-aerial scour holes shortly after initially scouring, thus making measurements and investigations of sub-aerial scour difficult.

Sub-aerial scour is particularly site specific (Yeh *et. al.*, 2003). Yeh *et. al.* (2003) make reference to the 1960 Chilean Tsunami where a 10 m deep scour hole occurred in the mouth of the Kesen-numa port in Japan, but little other scour damage for the site was observed.

Currently, no simple formula exists for scour prediction. Much experimental work needs to be conducted to provide data for empirical prediction and analysis (Yim, 2006).

5.4.2.3 *Discussion of Results*

Inundation scour depth observations appear to be largely limited to less than 2.5 m for run-up values of maximum 15 m. These are seen to occur within 200 m of the coastline and at less than half the maximum inundation distance.

Sub-aerial scour is currently poorly understood and information is scarce due to the inherent difficulties in measuring offshore scour information.

5.5 **Blockage of Cooling Water Intake**

Measures to prevent the complete blockage of the cooling water intake will depend on the type of intake structure. A brief overview of the measures to be considered in the intake design development to mitigate blockage risks is provided below.

5.5.1 General Considerations

In case of an offshore intake structure, cooling water is taken from much larger depths (25 m to 30 m water depth). This reduces the risk of blockage of the intake structure significantly. Suspended sediment concentrations at these levels are much lower, reducing the amount of sediment drawn in by the pumps and thus reducing the dimensions of the required settlement basins. The cover placed over the vertical terminal of an offshore intake tunnel/pipe is called a “velocity cap”. The cover converts vertical flow into horizontal flow at the intake entrance to reduce fish entrainment. It has been noted that fish will avoid rapid changes in horizontal flow and velocity cap intakes have been shown to provide 80-90% reduction in fish impingement.

In case of a nearshore intake structure (basin or channel type structure), the pumphouse will be designed to limit the possibility of blockage of the intakes. The front wall of the pumphouse is such that water is drawn at a suitable level to limit risk of blockage by flotsam, fuel oil and marine flora and fauna. Nevertheless suitable coarse and fine screens are provided to prevent a sudden complete blockage. The layout and position of the basin will be designed in such a way to reduce the siltation rate of the basin. The depth of the basin will be maintained by maintenance dredging.

Chlorine produced through electrolysis, is typically used to keep the cooling system free of marine growth.

5.5.2 Marine Debris

Consideration of potential blockages due to marine debris needs to be included in the design of the intake.

A study by the World Association of Nuclear Operators (WANO) in 2006 found that in the period 2004 to 2006, there were 44 occurrences of blockages at nuclear power plants (EPRI, 2008). Of the 44 events, 37 of these were attributed to aquatic life, including algae, seaweed and other grasses, mussels, jellyfish, crustaceans (shrimps and crabs) and fish. The remaining blockage events were caused by depositions of sand and silt and ingress of crude oil.

An environmental impact assessment for the proposed Bantamsklip site indicated that the following ecological species are to be found at Bantamsklip (Eskom, 2008b):

- Inter-tidal Zone - Small gastropods, algae, giant winkles and polychaete worms
- Benthic environment - Kelp, gastropod, rock lobster and abalone
- Open Water - Kob, White steenbras, Musselcracker, Galjoen, Cape salmon, Yellowtail, Great white shark, Southern right whale, Bottlenosed dolphin, Common dolphin and African fur seal.

WANO has identified four main categories for tackling the problem of blockages (EPRI, 2008), namely:

- Implementing proactive methods, including prediction tools and low level event trending, to understand potential threats and to take pre-emptive actions to mitigate their effects;
- Confirming plant system and equipment design are sufficient to address potential events;
- Verifying that maintenance strategies maintain and enhance equipment performance and
- Establishing operational criteria, procedure guidance and personnel training to address potential events and to incorporate industry operating experience.

The Electric Power Research Institute (EPRI, 2008) is in the process of carrying out a project which is aiming at identifying best management practices for preventing cooling water intake blockages. The draft report, though due to be complete by June 2009, is at present still unavailable. The recommendations put forward by WANO and the outcome of the EPRI project will form an important and valuable input to the intake design and prevention of cooling water intake blockages through the plant life.

There is no extra-ordinary marine debris identified at the site which the intakes could not be designed to cope with and which would be expected to cause a complete blockage of the intake.

5.5.3 Biofouling

Biofouling has been measured at the Bantamsklip site by mooring 20 cm x 20 cm asbestos plates 3 m and 8 m below the water surface in 10 m water depth (Eskom, 2008). These plates are periodically removed, photographed and the thickness of marine growth measured. The biofouling organisms are then scraped off the plates and then stored in sample bottles with formaldehyde and seawater for further analysis if required. Further details are provided in PRDW (2009a).

Results are currently available for plates deployed in October 2008 and recovered on 3 April 2009, i.e. approximately 6 month in the sea. However, due to suspected human interference, the buoy line holding the plates at the required depth had been severed. Only the PVC backing plates were recovered from the sea bed covered with a thin layer of sand and negligible evidence of fauna or flora. The plates are shown in Figure 5.1. Due to this interference the observed biofouling is not considered to be representative.

Further to the continued vandalism and loss of the biofouling plates, the plates were mounted directly onto a seabed positioned frame. The plates and frame was deployed on 23 May 2009 and will be retrieved in November 2009.

5.6 Sea Temperatures

The following data have been provided for the seawater intakes temperatures of a typical Pressurised Water Reactor (PWR) (Eskom, 2007):

- maximum cooling water temperature: 30°C
- minimum cooling water temperature: -0.4°C
- extreme conditions for safety assessment: 34.5°C

The two factors influencing the intake temperature are the ambient temperature at the intake depth and possible recirculation from the outfall back to the intake, refer to PRDW (2009a) for details.

6. MODELLING OF WAVE PENETRATION AND SEICHE IN BASIN LAYOUTS

6.1 Introduction

The existing Koeberg installation relies on a protected basin to provide access to seawater for the condenser and essential cooling water systems (Eskom, 2006). The basin layout is designed to provide a calm inner basin area free of excessive water level variations at the pump house intakes and to permit suspended sediments to settle out (refer to Figure 6.1 for a plan view of the basin).

The layout provides for an overlap of the breakwaters to limit wave penetration into the basin. The lateral arm provides a further cut-off of energy, thereby using wave diffraction around the south breakwater as well as the end of the lateral arm to provide the required conditions in the inner basin (refer to Figure 6.2). The basin was not required to be designed for navigation. As a result the entrance could be narrow and storm waves breaking seaward of the entrance were acceptable.

Three similar basin layouts have been proposed for the Bantamsklip site to provide for cooling water. In order to provide design criteria for the proposed layouts at the Bantamsklip site it is necessary to estimate the wave heights and maximum and minimum water levels inside the basins for specified return periods.

This is achieved by using a numerical model developed for modelling non-linear wave interactions and wave propagation into harbours.

6.2 Description of Two Dimensional Boussinesq Wave Model

The two dimensional version of the MIKE 21 Boussinesq Wave (BW) model is used. The BW model is ideally suited for modelling wave trains from deep to shallow water and harbour and marina hydrodynamics (DHI, 2009).

MIKE 21 BW 2D includes numerical solutions for the following physical phenomena:

- Shoaling
- Refraction
- Diffraction
- Wave breaking
- Bottom friction
- Moving shoreline
- Partial reflection and transmission
- Non-linear wave-wave interaction
- Frequency spreading

- Directional spreading.

The MIKE 21 BW model is based on the numerical solution of time domain formulations of Boussinesq type equations. The Boussinesq equations include nonlinearity as well as frequency dispersion. The equations are solved using a flux-formulation with improved linear dispersion characteristics.

These enhanced Boussinesq type equations make the modules suitable for simulation of the propagation of directional wave trains traveling from deep to shallow water. The model has been extended into the surf zone by inclusion of wave breaking and moving shoreline.

6.3 Model Calibration

6.3.1 Model Setup

The model was calibrated using water surface elevation data obtained from a LIDAR survey conducted on the 7th September 2007 (SMC, 2007). Due to the high turbidity of the water, the survey was able to obtain a snapshot of the water surface elevation in the Koeberg cooling water basin and some distance offshore. The data was then interpolated onto a calibration grid used in the numerical model. The water surface elevation was calculated from the LIDAR data and used to specify the still water level.

Wave data assessed from the offshore area of the LIDAR survey is used to specify the offshore wave boundary condition in the model. A JONSWAP wave spectrum was used. A directional spreading (\cos^m) of $m = 12$ was applied for swell ($T_p > 9.2$ s). The remaining model parameters were set to default values. The JONSWAP spectrum is truncated at a period, T_{min} , of 9.2 seconds in order to facilitate a minimum grid size of 2 m. T_{min} is defined (DHI, 2009) as the minimum wave period that can be resolved in a BW model simulation. The value of T_{min} is governed by the maximum water depth in the model area and by whether deep water terms are included (DHI, 2009). The wave input conditions for the calibrated model are tabulated below.

TABLE 6.1: CALIBRATION MODEL INPUT PARAMETERS

Wave Direction	232.5 °
H_{m0}	2.2 m
T_p	12.5 s
Still water level	1.04 m CD
Water depth at model boundary	16.3 m

The model time step was 0.1 s, which ensured a Courant Number of less than 1.0. The grid spacings were selected to ensure at least 20 to 30 grid points per wavelength. The moving shoreline option has been excluded in order to increase numerical stability and reduce run-time. The beach around the Koeberg basin has been modelled with a sponge layer in order to limit wave reflection. Refer to Figure 6.2 for bathymetry and layout details. Wave breaking is included in the model.

Reflection coefficients for the pump house sea wall have been taken as unity, a fully reflective boundary. Similarly the reflection in the internal breakwater walls of the basin has been set at 0.95, representing a highly reflective boundary. This is considered a conservative approach as standing waves near the walls will be accentuated.

The BW manual (DHI, 2009) suggests a range of breakwater reflection coefficients for different surface coverings and gradients for impermeable breakwater structures and land boundaries. The values for a 1:1.5 rubble covered breakwater are suggested in the range of 0.2 to 0.6. These values are then used as inputs into a MIKE 21 sub-programme used to calculate porosity coefficients used in the numerical model, representing the amount of energy removed from the wave as a function of H_{m0} , T_p , water depth at the toe of the structure and specified thickness of the porosity layer within the model.

For calibration of the model, H_{m0} and T_p were obtained from the LIDAR survey profiles at the offshore wave boundary (see Section 6.3.2), a thickness of 8 grid cells was used with a recommended reflection coefficient of 0.4 to give a porosity coefficient of 0.49.

The model was calibrated to confirm capabilities for wave transformation from the offshore model boundary into the basin and obtain viable quantitative values for reflection coefficients from the breakwaters, internal basin revetments and pump house sea wall.

The model was run for a total simulation time of 30 minutes, allowing enough time for wave propagation into the basin from the open water boundary and sufficient time for extraction of surface elevation data within the basin.

6.3.2 Calibration Results

Figure 6.3 shows a plan view comparison of the surface elevation contours at a moment in time. The reflected wave train from the south breakwater can be clearly seen and compares well with the measured LIDAR data. The wave heights, wave lengths and wave directions inside the basin are also well represented in the model.

Further, Figure 6.4 shows a cross-section of surface elevation from the offshore wave boundary of the model (line output 01), entrance to basin (line output 02) and wave progression to the land side of the basin (line output 03). Refer to Figure 6.2 for locations of the line outputs.

The model is seen to accurately predict wave transformation processes of shoaling and refraction (line output 01), wave diffraction around the south breakwater (line output 02) and additional diffraction inside the basin (line output 03).

6.4 Basin Layouts Modelled

6.4.1 Model Setup

Generally model parameters chosen in the production runs are consistent with the values used for the calibration model. Modifications in the input parameters are discussed below.

- The model time step was 0.2 s, which ensured a Courant Number of less than 1.0.
- The grid spacing, 5 m x 5 m, was selected to ensure at least 20 to 30 grid points per wavelength at T_p and between 12 to 20 grid points per wavelength at T_{min} .
- Bed resistance has been included and specified by a Manning number of $32 \text{ m}^{1/3}/\text{s}$. The larger H_{m0} in the production runs increases the effect of bed resistance on the energy loss in the waves due to bottom surface effects on the orbital velocities for shallow water waves.
- Porosity coefficients have been recalculated for input conditions based on the 1:10 and 1:10⁶ year return period waves with a suggested reflection coefficient of 0.6. This gives a more conservative (higher) value for wave heights within the basin, though still within the range of expected reflection coefficients for the structure.
- Simulation time has been increased to 40 minutes to allow wave propagation through the larger numerical model.
- Sensitivity to increased model simulation time is addressed in PRDW (2009b)

As the Courant number is maintained at less than 1.0 and the grid spacing is still between 20 to 30 grid points per wavelength, the production model is expected to maintain consistency and grid independence with the calibration model.

The water level modelled and input significant wave height has been obtained for each of the run cases directly from the results of the wave transformation calculations (refer to Section 4.5) at a depth of approximately 30 m CD. Input conditions have been extracted from Profile 03 (refer to Figure 4.10). Only the upper 95% confidence values for still water level, H_{m0} and T_p have been used for input conditions.

6.4.2 Bathymetry and Breakwater Plan

The intake and outfall configurations listed in Section 5.1 include three possible configurations where a basin intake is used. For all three of the configurations the location and dimensions of the basin are the same (PRDW, 2009a). The entrance width, position and length of the breakwaters has been detailed in the numerical modelling report (PRDW, 2009a) and has been analysed with respect to the modelling of the thermal plume and long shore sediment transport. For the purposes of the wave heights and surface elevation within the basin, three possible modifications to the length of the internal lateral arm have been tested. These modifications are briefly discussed below.

For consistency with the naming convention in Section 5.1, the modified basin layouts are referenced to Layout 2. The results, however, will be equally applicable to Layouts 4 and 6.

- Layout 02a: The geometry and dimensions are consistent with those used in the numerical modelling report (PRDW, 2009a).
- Layout 02b: Equivalent to Layout 02a, with the inclusion of a second lateral arm. The length of the second lateral arm is equal to the width between the primary lateral arm and the eastern breakwater (refer to Figure 6.5).
- Layout 02d: Equivalent to Layout 02b. The length of the second lateral arm has been doubled to increase the effect of diffraction to reduce wave heights within the basin (refer to Figure 6.5).

Figure 6.5 shows details of the model bathymetry and plan views of the modelled layout configurations. The bathymetry within the basin is specified at -7.5 m CD.

6.5 Results

For all models the following output values have been extracted:

- Instantaneous surface elevations for the last 10 minutes of solution time for the entire domain (refer to Figures 6.6 to 6.8).
- Statistical values of the maximum surface elevation, minimum surface elevation, significant wave height and mean surface elevations within the entire domain (refer to Figures 6.6 to 6.8).
- Instantaneous surface elevation for three control points along the pump house sea wall over the entire simulation period.
- Statistical values of the maximum surface elevation, minimum surface elevation, significant wave height and mean surface elevations for the same three control points and along the total length of the pump house sea wall.

As only the upper 95% confidence wave and water level conditions have been modelled, it is necessary to interpolate the best estimate values from the model results. To this end the results obtained from the BW model can be seen as a representative sample from which to interpolate, using the H_{m0} values for the best estimate and upper 95% confidence level as the independent parameter in the interpolation for all return periods. A partial logarithmic interpolation is seen to best represent the curve through this representative sample.

Results for the above values have been used to interpolate logarithmic curves using the input H_{m0} as the dependant variable. Final results have then been obtained from the interpolated logarithmic functions for: maximum negative and positive surface elevations and H_{m0} for given input H_{m0} for all of

the return periods and both the upper 95% confidence and best estimate level. Refer to Figure 6.9 showing maximum H_{m0} within the basins. Refer to Figures 6.10 to 6.11 for a comparison of the extreme high and low water conditions for all return periods.

Final results for each of the modelled layouts, obtained from the interpolated logarithmic function for the best estimate and upper 95% confidence level input H_{m0} for the required return periods, are tabulated in Table 6.2 to Table 6.4.

**TABLE 6.2: BW MODEL RESULTS RELATIVE TO STILL WATER LEVEL:
PROPOSED LAYOUT 02A**

Return Period [years]	Results [m]	Excluding climate change		Including climate change	
		Best estimate	Upper 95% confidence	Best estimate	Upper 95% confidence
1:1	H_{m0}^1	1.12	1.20	1.45	1.53
	Min. Elevation	-1.01	-1.05	-1.16	-1.20
	Max. Elevation	0.75	0.86	1.21	1.33
	Mean Elevation	0.00	0.01	0.02	0.02
1:10	H_{m0}^1	1.55	1.69	1.87	2.01
	Min. Elevation	-1.21	-1.28	-1.37	-1.43
	Max. Elevation	1.36	1.56	1.82	2.02
	Mean Elevation	0.02	0.03	0.04	0.05
1:100	H_{m0}^1	1.89	2.10	2.21	2.42
	Min. Elevation	-1.38	-1.48	-1.53	-1.63
	Max. Elevation	1.84	2.15	2.31	2.61
	Mean Elevation	0.04	0.05	0.05	0.06
1:10 ⁶	H_{m0}^1	2.83	3.26	3.15	3.59
	Min. Elevation	-1.94	-2.20	-2.13	-2.39
	Max. Elevation	3.24	3.90	3.73	4.39
	Mean Elevation	0.08	0.10	0.10	0.12

Notes:

- 1) Calculated as 4 times the standard deviation (σ) of surface elevation above still water level

**TABLE 6.3: BW MODEL RESULTS RELATIVE TO STILL WATER LEVEL:
PROPOSED LAYOUT 02B**

Return Period [years]	Results [m]	Excluding climate change		Including climate change	
		Best estimate	Upper 95% confidence	Best estimate	Upper 95% confidence
1:1	H_{m0}^1	0.76	0.83	1.04	1.11
	Min. Elevation	-0.75	-0.79	-0.89	-0.92
	Max. Elevation	0.69	0.75	0.93	0.99
	Mean Elevation	0.00	0.01	0.02	0.02
1:10	H_{m0}^1	1.13	1.26	1.41	1.54
	Min. Elevation	-0.93	-0.99	-1.06	-1.12
	Max. Elevation	1.00	1.11	1.24	1.35
	Mean Elevation	0.02	0.03	0.04	0.05
1:100	H_{m0}^1	1.43	1.62	1.71	1.90
	Min. Elevation	-1.07	-1.16	-1.20	-1.29
	Max. Elevation	1.26	1.41	1.50	1.65
	Mean Elevation	0.04	0.05	0.05	0.06
1:10 ⁶	H_{m0}^1	2.26	2.64	2.54	2.92
	Min. Elevation	-1.53	-1.73	-1.68	-1.89
	Max. Elevation	2.16	2.54	2.44	2.82
	Mean Elevation	0.08	0.10	0.10	0.12

Notes:

- 1) Calculated as 4 times the standard deviation (σ) of surface elevation above still water level

**TABLE 6.4: BW MODEL RESULTS RELATIVE TO STILL WATER LEVEL:
PROPOSED LAYOUT 02D**

Return Period [years]	Results [m]	Excluding climate change		Including climate change	
		Best estimate	Upper 95% confidence	Best estimate	Upper 95% confidence
1:1	H_{m0}^1	0.62	0.68	0.87	0.93
	Min. Elevation	-0.57	-0.61	-0.74	-0.79
	Max. Elevation	0.49	0.55	0.74	0.81
	Mean Elevation	0.00	0.01	0.02	0.02
1:10	H_{m0}^1	0.94	1.05	1.19	1.30
	Min. Elevation	-0.80	-0.87	-0.97	-1.05
	Max. Elevation	0.83	0.94	1.09	1.20
	Mean Elevation	0.02	0.03	0.04	0.05
1:100	H_{m0}^1	1.20	1.37	1.45	1.61
	Min. Elevation	-0.98	-1.09	-1.15	-1.27
	Max. Elevation	1.10	1.27	1.36	1.53
	Mean Elevation	0.04	0.05	0.05	0.06
1:10 ⁶	H_{m0}^1	1.92	2.26	2.17	2.50
	Min. Elevation	-1.52	-1.78	-1.71	-1.97
	Max. Elevation	1.87	2.23	2.14	2.49
	Mean Elevation	0.08	0.10	0.10	0.12

Notes:

- 1) Calculated as 4 times the standard deviation (σ) of surface elevation above still water level

6.6 Discussion of Results

The maximum positive and negative surface elevation is seen to occur during the 1:10⁶ year return period storm event for Layout 02a. The combination of breakwater overlap and lateral arm in Layouts 02a and 02d are seen to be very effective in reducing the H_{m0} within the basin in front of the cooling water intakes. The values for maximum and minimum surface elevation and H_{m0} are seen to be further reduced with the inclusion of the secondary lateral arm within the basins and the extension of this lateral arm.

The final layout and configuration of the intake basin will likely be based on a multi criteria assessment including the effectiveness of the thermal plume dispersion (refer to PRDW (2009a), long shore sediment transport implications and design constraints of the cooling water intake pumps. However, the current study and options provided for reducing the H_{m0} and surface elevations, give an initial estimate of the efficacy of possible modifications to the basin internal layout.

A comparison of the Layout 02a and Layout 02d is given in Chapter 7 with respect to the extreme high and low water levels expected and the design basis.

7. COMBINATIONS OF MAXIMUM AND MINIMUM WATER LEVELS

7.1 Introduction

The IAEA (2003) safety guide on 'Flood Hazard for Nuclear Power Plants on Coastal and River Sites' gives some general guidelines concerning combined events to be considered in deriving the design basis flood for a nuclear installation. These guidelines have been used in deriving the design basis for extreme high water levels.

7.2 Design Basis for Extreme Events

In deriving the design basis flood for a nuclear installation, combined events should be considered as well as single events. Combinations of events should be carefully analysed with account taken of the stochastic and nonlinear nature of the phenomena (IAEA, 2003).

For evaluating combined flooding events on coastal, estuary and river sites, distinctions may be made between (IAEA, 2003):

1. Extreme events (such as storm surges, river floods and tsunamis)
2. Wind waves related or unrelated to the extreme events
3. Maximum seiche (in the case of an enclosed or semi-enclosed body of water)
4. Reference water levels (including tides if significant).

Appropriate combinations of extreme events with wind waves and reference water levels should be taken into consideration. The probability range of each combination should be estimated (IAEA, 2003).

The design basis flood for a given site may result not from the occurrence of one extreme event but from the simultaneous occurrences of more than one severe event each of which is in itself less than the extreme event. The interdependence or independence of the potential flood causing phenomena should be examined according to the site specific features (IAEA, 2003).

For independent events, the probability that they will occur in such conditions that their effects will be additive is related to the duration of the severity level of each event. The events to be combined should be selected appropriately with account taken not only of the resultant probability but also of the relative effect of each secondary event on the resultant severity of the flood. For example for estuary sites, combinations that should be examined should include both maritime and river conditions. If the consequences of these combinations are significant and the combined probability of the results is not very low, they should be taken into account (IAEA, 2003).

Wind wave activity should be considered in association with all the flood events. For surge, wind waves are dependent events and the waves that are generated by the storm producing the surge should be considered (IAEA, 2003).

In this report both Tsunami and long waves are considered independent events. Long waves are categorised as independent events because the generation mechanisms (atmospheric pressure fluctuations, propagation of edge waves and shelf waves) are independent on the atmospheric and ocean conditions leading to storm induced surges and associated maximum wind wave. Only wind waves with a shorter recurrence interval should thus be considered in the combination. Independent events are combined with the 1:10 year return period of dependant events.

The potential for instability of the coastline should be evaluated and if the occurrence of these events affects the flood at the site they should be combined with other primary flood causing events (IAEA, 2003).

Considerable engineering judgement is necessary in selecting the appropriate combinations (IAEA, 2003).

7.3 Combination of Events

From all of the above-mentioned potential flooding hazards the most severe and relevant hazards for the nuclear installation at the Bantamsklip site are combined to obtain the maximum water levels at the site required for flooding risk assessment and the minimum levels for loss of cooling water assessment.

The following hydrographic conditions contribute to the combined water level:

- Sea level rise: Refer to Section 3.2
- Tidal levels: Refer to Section 4.1
- Storm surge: Refer to Section 4.2
- Wave set-up and run-up: Refer to Sections 4.6 and 4.7
- Positive and negative basin seiche: Refer to Section 6.5
- Long wave: Refer to Section 4.3
- Tsunami: Refer to Section 7.3.3

7.3.1 Reference Water Level and Return Periods

Following international recommendations (IAEA, 2003) a conservatively high reference water level should be considered for each combination of dependant events. In this case the Highest Astronomical Tide (HAT) is added to obtain the extreme high water level (see Table 4.1). Similarly Lowest

Astronomical Tide (LAT) has been used as a conservative low water level for combinations leading to loss of cooling water.

Independent events should be considered in combination with waves having a shorter recurrence interval (IAEA, 2003). USNRC (2007) recommends that the 90th percentile of high tides be used as the initial water surface elevation when evaluating tsunami run-up, which for Bantamsklip is +1.04 m MSL. Based on these recommendations, for extreme high water levels, independent events are combined with a tide of +1.04 m MSL and a 1:10 year combination of dependant events (see Table 7.4). For extreme low water, independent event water levels are combined with the 90th percentile of low tides (-0.54 MSL) and the 1:10 combination of dependent events.

7.3.2 Dependant Events

Storm surge is for the purpose of this report defined as the effective term for the meteorological effects such as winds and barometric pressure that results in actual sea level being above (positive) or below (negative) the predicted astronomical tide level.

Storm surge, wave set-up and wave run-up are considered to be dependent events since they are all associated with the passage of frontal weather systems (Refer to Chapter 4). For this reason, storm surge is combined with wave set-up and wave run-up having the same return period when calculating maximum water levels on exposed beaches. In the case of the extreme low water condition on an exposed beach, the individual effects of wave draw-down are not included, as the set-up (a positive elevation) would negate the effects of the draw down.

For the case of the basin layouts, wave set-up and run-up (refer to in Section 4.6 and Section 4.7) would be virtually the same at the basin entrance. The effects of set-up due to breaking in the basin is implicitly calculated in the BW Model (refer to Section 6.5). Positive storm surge is therefore combined with the calculated mean and maximum surface elevations due to seiche.

Further, as the effects due to seiche on surface elevations are comparable in magnitude for both positive and negative elevations, and the set-up within the basin is negligible, the minimum surface elevation is combined with negative storm surge for extreme low water calculations within the basin. As the layout for the proposed basin has not been finalised, a number of different basin configurations have been modelled (refer to Chapter 6). In ascertaining the maximum possible flood levels within the basin, the results from the best case (Layout 02d) and the worst case (Layout 02a) are given. These can be seen as representing a range of possible maximum flood level within the basin for different configurations.

All dependant events have been calculated for 1, 10, 100 and 10^6 year return periods. As long waves are considered independent events (refer to Section 7.2) they are not included in the results of Table 7.2 and Table 7.3

7.3.3 Independent Events

As both tsunami and long waves are considered independent events, the maximum value obtained from either: the run-up from the maximum probable tsunami or the positive elevation associated with the $1:10^6$ year return period long wave is used in obtaining design flood levels. Similarly the minimum of either: the run-down from the maximum probable tsunami or the negative elevation associated with the $1:10^6$ year return period long wave is used to ascertain the lowest water levels.

PRDW (2009a) investigated the tsunami risk at the site based on local and distant tsunamigenic sources provided by the Council for Geoscience. Values for the maximum predicted tsunami run-up level from a distant tsunamigenic source are available in PRDW (2009a). As discussed in PRDW (2009a), there is presently insufficient data to assess the risk from local tsunamigenic sources, e.g. submarine slumps. The maximum predicted tsunami run-up level from a distant tsunamigenic source is +2.0 m (PRDW, 2009a).

The tsunami run-up level used in the combination of events is the maximum of the estimated long wave positive water level (refer to Section 4.3), and the maximum credible earthquake induced tsunami run-up (+2.0 m, above). For the inclusion of climate change parameters, the adopted increase for long waves is consistent with that used for storm surge (refer to Section 3.2 and Appendix A). Refer to Table 7.4 for values used.

The maximum predicted tsunami draw down level from a distant tsunamigenic source is -2.0 m (PRDW, 2009a). As discussed in PRDW (2009a), there is presently insufficient data to assess the risk from local tsunamigenic sources, e.g. submarine slumps.

The tsunami draw down level used in the combination of events is the maximum of the estimated long wave negative water level (refer to Section 4.3), and the maximum credible earthquake induced tsunami draw down (-2.0 m, above). For the inclusion of climate change parameters, the adopted increase for long waves is consistent with that used for storm surge (refer to Section 3.2 and Appendix A). Refer to Table 7.4 for values used.

As long wave are inclusive of tsunami and meteo-tsunami, all references to tsunami in the following section regarding combination of events will imply the above mentioned maximum of the independent events. Refer to Section 7.3.1 for combination of tsunami event and storm events

7.3.4 Long Term Sea Level Rise and Climate Change Parameters

All combinations have also been evaluated for climate change conditions. An additional component is added for sea level rise and the effect of higher waves and winds on wave set-up, wave run-up and storm surge was taken into consideration (refer to Chapter 3).

In the analysis of extreme low water level, no component for long term sea level rise has been added to the still water level in order to have the design values for the worst case scenario. Other components of climate change having an impact on the extreme low water level are taken into consideration, like increase on wind speeds increasing the negative storm surge (winds blowing from the land).

7.3.5 Confidence Levels

Extreme values for wave height and storm surge have been obtained by fitting a Weibull distribution to the available data sets (refer to PRDW (2009a) for details). The output of the procedure is the best estimate value as well as the upper 95% confidence value. This means that 4 different values are calculated for each component in the extreme water level:

1. Best estimate – Excluding climate change
2. Upper 95% confidence level – Excluding climate change
3. Best estimate – Including climate change
4. Upper 95% confidence level – Including climate change

The combinations of events are schematically tabulated in Table 7.1.

TABLE 7.1: SCHEMATIC OF COMBINATION OF EVENTS

	Beach Layout		Basin Layout		Tsunami ⁴	
	Low water	High water	Low water	High water	Low Water	High Water
Tide	LAT	HAT	LAT	HAT	P ₉₀ low tides	P ₉₀ high tides
Sea level rise		YES		YES		YES
Storm surge	YES	YES	YES	YES	YES ¹	YES ¹
Set-up/run-up²		YES				YES ¹
Seiche³			YES	YES	YES ¹	YES ¹

Notes:

- 1) Calculated for the 1:10 year return period
- 2) Only used in calculations for open beaches
- 3) Only used in calculations for enclosed basins
- 4) P₉₀ is the 90th percentile, the value of a variable below which a certain percent of observation fall, of a specific data set

7.4 Results

Reference is made to Table 7.2 summarizing results for extreme high water levels for the design return periods for beach Profile 04 and the current and proposed basins.

TABLE 7.2: EXTREME HIGH WATER LEVEL RESULTS

Return Period [years]	Individual component of extreme water level calculations	Units	Excluding climate change		Including climate change		
			Best estimate	Upper 95% confidence	Best estimate	Upper 95% confidence	
1	HAT ^(Hermanus)	m MSL	1.28	1.28	1.28	1.28	
	Sea level rise	m	0.00	0.00	0.80	0.80	
	Positive storm surge	m	0.61	0.63	0.74	0.76	
	Set-up and run-up ¹	Beach	m	2.95	3.00	3.34	3.40
	Positive seiche ²	Basin 02a	m	0.75	0.86	1.21	1.33
		Basin 02d	m	0.49	0.55	0.74	0.81
	Extreme high water level	Beach	m MSL	4.84	4.91	6.16	6.24
		Basin 02a	m MSL	2.64	2.77	4.03	4.17
		Basin 02d	m MSL	2.38	2.46	3.56	3.65
10	HAT ^(Hermanus)	m MSL	1.28	1.28	1.28	1.28	
	Sea level rise	m	0.00	0.00	0.80	0.80	
	Positive storm surge	m	0.78	0.83	0.94	1.00	
	Set-up and run-up ¹	Beach	m	3.25	3.35	3.67	3.78
	Positive seiche ²	Basin 02a	m	1.36	1.56	1.82	2.02
		Basin 02d	m	0.83	0.94	1.09	1.20
	Extreme high water level	Beach	m MSL	5.31	5.46	6.70	6.87
		Basin 02a	m MSL	3.42	3.67	4.84	5.11
		Basin 02d	m MSL	2.89	3.05	4.11	4.28
100	HAT ^(Hermanus)	m MSL	1.28	1.28	1.28	1.28	
	Sea level rise	m	0.00	0.00	0.80	0.80	
	Positive storm surge	m	0.94	1.04	1.14	1.26	
	Set-up and run-up ¹	Beach	m	3.50	3.65	3.95	4.12
	Positive seiche ²	Basin 02a	m	1.84	2.15	2.31	2.61
		Basin 02d	m	1.10	1.27	1.36	1.53
	Extreme high water level	Beach	m MSL	5.72	5.97	7.16	7.46
		Basin 02a	m MSL	4.06	4.47	5.52	5.95
		Basin 02d	m MSL	3.32	3.59	4.58	4.87
10 ⁶	HAT ^(Hermanus)	m MSL	1.28	1.28	1.28	1.28	
	Sea level rise	m	0.00	0.00	0.80	0.80	
	Positive storm surge	m	1.51	1.86	1.83	2.25	
	Set-up and run-up ¹	Beach	m	4.24	4.66	4.80	5.29
	Positive seiche ²	Basin 02a	m	3.24	3.90	3.73	4.39
		Basin 02d	m	1.87	2.23	2.14	2.49
	Extreme high water level	Beach	m MSL	7.03	7.80	8.71	9.62
		Basin 02a	m MSL	6.03	7.04	7.64	8.72
		Basin 02d	m MSL	4.66	5.37	6.04	6.82

Notes:

- 1) Used in calculations for maximum water levels for flood conditions on beaches
- 2) Used in calculations for maximum water levels in basin layout configurations

Reference is made to Table 7.3 summarizing results for extreme low water levels for the design return periods.

TABLE 7.3: EXTREME LOW WATER LEVEL RESULTS

Return Period [years]	Individual component of extreme water level calculations	Units	Excluding climate change		Including climate change		
			Best estimate	Upper 95% confidence	Best estimate	Upper 95% confidence	
1	LAT ^(Herманus)	m MSL	-0.79	-0.79	-0.79	-0.79	
	Negative storm surge	m	-0.62	-0.65	-0.75	-0.79	
	Negative seiche ¹	Basin 02a	m	-1.01	-1.05	-1.16	-1.20
		Basin 02d	m	-0.57	-0.61	-0.74	-0.79
	Extreme low water level	Basin 02a	m MSL	-2.42	-2.49	-2.70	-2.78
Basin 02d		m MSL	-1.98	-2.05	-2.28	-2.36	
10	LAT ^(Herманus)	m MSL	-0.79	-0.79	-0.79	-0.79	
	Negative storm surge	m	-0.84	-0.92	-1.02	-1.11	
	Negative seiche ¹	Basin 02a	m	-1.21	-1.28	-1.37	-1.43
		Basin 02d	m	-0.80	-0.87	-0.97	-1.05
	Extreme low water level	Basin 02a	m MSL	-2.84	-2.99	-3.17	-3.34
Basin 02d		m MSL	-2.43	-2.58	-2.78	-2.95	
100	LAT ^(Herманus)	m MSL	-0.79	-0.79	-0.79	-0.79	
	Negative storm surge	m	-1.07	-1.21	-1.29	-1.46	
	Negative seiche ¹	Basin 02a	m	-1.38	-1.48	-1.53	-1.63
		Basin 02d	m	-0.98	-1.09	-1.15	-1.27
	Extreme low water level	Basin 02a	m MSL	-3.23	-3.47	-3.61	-3.88
Basin 02d		m MSL	-2.84	-3.09	-3.24	-3.52	
10 ⁶	LAT ^(Herманus)	m MSL	-0.79	-0.79	-0.79	-0.79	
	Negative storm surge	m	-1.93	-2.46	-2.34	-2.98	
	Negative seiche ¹	Basin 02a	m	-1.94	-2.20	-2.13	-2.39
		Basin 02d	m	-1.52	-1.78	-1.71	-1.97
	Extreme low water level	Basin 02a	m MSL	-4.66	-5.45	-5.25	-6.15
Basin 02d		m MSL	-4.24	-5.03	-4.84	-5.74	

Notes:

- 1) Used in calculations for maximum water levels in basin layout configurations

For calculations of combined extreme high and low water level for the beach, wave run-up calculations for Profile 04 (refer to Section 4.7) are used. In calculating the extreme water levels for the basin layout configurations, wave inputs consistent with Profile 03 (refer to Section 4.7) are used.

Refer to Table 7.4 for maximum high and low water levels during a tsunami event.

TABLE 7.4: MAXIMUM HIGH AND LOW WATER DURING TSUNAMI EVENT

Individual component of extreme water level calculations	Units	Excluding climate change		Including climate change		
		Best estimate	Upper 95% confidence	Best estimate	Upper 95% confidence	
90 th percentile high tides	m MSL	1.04	1.04	1.04	1.04	
Sea level rise	m	0.00	0.00	0.80	0.80	
Positive storm surge ¹	m	0.78	0.83	0.94	1.00	
Tsunami ²	m	2.91	3.64	3.52	4.40	
Set-up and run-up ³	Beach	m	3.25	3.35	3.67	3.78
Positive seiche ⁴	Basin 02a	m	1.36	1.56	1.82	2.02
	Basin 02d	m	0.83	0.94	1.09	1.20
Extreme high water level	Beach	m MSL	7.98	8.86	9.98	11.03
	Basin 02a	m MSL	6.09	7.07	8.13	9.27
	Basin 02d	m MSL	5.56	6.45	7.39	8.44
90 th percentile low tides	m MSL	-0.54	-0.54	-0.54	-0.54	
Negative storm surge ¹	m	-0.84	-0.92	-1.02	-1.11	
Tsunami ²	m	-3.16	-3.77	-3.82	-4.56	
Negative seiche ⁴	Basin 02a	m	-1.21	-1.28	-1.37	-1.43
	Basin 02d	m	-0.80	-0.87	-0.97	-1.05
Extreme low water level	Basin 02a	m MSL	-5.75	-6.50	-6.74	-7.64
	Basin 02d	m MSL	-5.33	-6.10	-6.34	-7.26

Notes:

- 1) Based on a 1:10 year return period
- 2) Maximum value of 1:10⁶ year return period long wave and maximum probable tsunami run-up and run-down values
- 3) Based on the 1:10 year return period, used in calculations for maximum water levels on beaches or offshore intake layout configurations
- 4) Based on the 1:10 year return period, used in calculations for maximum water levels in basin layout configurations

7.5 Discussion of Results

Maximum extreme high water level is seen to occur during a meteo-tsunami event (refer to Table 7.4 and Section 4.3) for flooding from the beach and in the case of a basin intake.

One approach to deal with the uncertainties associated with future climate change is adaptive design, for example provision can be made for a seawall in front of the terrace which can be raised in future as necessary. The phased development of the site also allows for the design of the second and third phases to respond to the more accurate climate change predictions that will be available in future.

Comparison of the extreme low water levels calculated for two of the basin configuration model runs, Layout 02a and Layout02d, completed for this coastal engineering report (refer to Section 6.4 are shown graphically in Figure 7.1.

Maximum water levels calculated for the best case (Layout 02d), the worst case (Layout 02a) and beach run-up levels are shown in Figure 7.2. The final layout and configuration of the intake basin will likely be based on a multi criteria assessment including the effectiveness of the thermal plume dispersion (refer to PRDW (2009a), long shore sediment transport implications and design constraints of the cooling water intake pumps. The range of values tabulated above, and shown graphically in

Figures 7.1 and 7.2, give an indication of the efficacy of basin modifications to limiting the maximum and minimum surface elevations within the intake basin.

For the inclusion of climate change in the calculations of extreme flood levels, values are based on the information available at present, and need to be continually reassessed as new data and research results become available. Refer to Chapter 3 for the climate change parameters used in the assessment of the extreme flood levels. Though incorporated implicitly within the calculations for run-up, storm surge and wave heights, any new data regarding sea level rise can for preliminary estimates be added to the calculated levels in Table 7.2 and Table 7.4.

Climate change is described in detail in Appendix A. For this SSR the upper end projection from the IPCC (2007) of 0.8 m sea level rise to 2100 is used to estimate the maximum wave run-up levels at the site (see Table 7.2 and Table 7.4). These run-up levels do not take into account the presence of the nuclear power installation, since this has not yet been designed.

The design of the nuclear power installation will need to consider the following:

- The extent to which the infrastructure will modify the topography of the site and thus modify the run-up levels, e.g. excavations or revetments.
- The type and position of intake and outfall structures.
- The volume rate of wave overtopping of the specific structures (in addition to wave run-up levels).
- An evaluation of the risk to the specific design of an extreme upper limit sea level rise of 2 m by 2100. Depending on the specific design, it may be cost effective to design for this extreme level from the start, or to plan future design adaptations or make specific contingency plans.

As discussed in Appendix A, it is highly unlikely that sea level rise will occur suddenly and there will thus be many years warning should the sea level start to rise faster than the predicted rates.

8. COASTLINE STABILITY AND CROSS-SHORE SEDIMENT TRANSPORT

8.1 Introduction

The morphology of the coastline is a result of many individual sediment transport events caused by a succession of waves. In this sense, the shape of the beach and nearshore region may be thought of as representing a form of averaging over time (Reeve *et al.*, 2004). The stability of a length of coastline will depend on the difference between the volumes of sediment entering and leaving this section owing to the net cross-shore and longshore sediment transport due to waves, currents and wind. The coastline will be eroding, accreting or remaining in equilibrium. If equilibrium exists, it is most likely to be a dynamically stable equilibrium, whereby the coastline is evolving continuously in response to varying winds, waves and currents (Reeve *et al.*, 2004). Nevertheless, the typical coastline is relatively constant over a period of months or years, although the position of the coastline at any particular point will vary about this average.

In order to assess the impacts of the driving mechanisms of coastline stability, the following physical processes of erosion/accretion are considered:

- Long-term coastline trends
- Seasonal variation in the coastline
- Storm event erosion
- Effects on coastline movement due to long term sea level rise.

Of the above, the storm events and sea level rise trends can be effectively modelled. Due to the nature of long-term coastline trends and seasonal variation, the most feasible approach to a quantitative estimation of stability related from these processes requires detailed measurements from historic profiles spanning many years.

Recent profile measurements for the months of January, April, July and October (all from 2008) and January, April and July of 2009, have been processed and analysed for a number of beacon locations. These include 40 beacons for the Bantamsklip site spanning from north at Castle Beach to south at Jessie se Baai (see Figures 8.1 to 8.15 for profile locations). These profiles are the first available from the ongoing profile surveys being conducted as part of the oceanographic data collection programme. The data collection programme commenced in January 2008 and is scheduled to run until August 2010 (31 months of data). This data is used to ascertain seasonal variations in erosion/accretion for specific profiles.

Further to the physical monitoring of beach profiles along the Bantamsklip site, a number of aerial photographs have been utilised in qualitatively assessing the long term erosional/accretional processes for: Castle Beach, Pearly Beach, Shell Point beaches, Plaatjieskraalbaai and Jessie se Baai.

8.2 Long-term Coastline Trends from Aerial Photographs

8.2.1 Physical Process

Long-term coastline trends are typically processes which are likely to persist over a number of years, and which result in erosion and accretion rates in the order of a few meters per year. Reeve *et al.*, (2004) suggest that records as long as 20 years are sometimes required to establish an average longshore transport rate with reasonable accuracy. Due to the long time scales and complex process interaction associated with long-term coastal changes, numerical modelling is problematic and has a limited reliability of results. Statistical analysis of past records for historically collected data is considered to be the most accurate method for establishing coastline trends due to long-term processes (Coastal CRC, 2006).

8.2.2 Methodology

Three contour lines, namely: the vegetation line, the high water mark and the +5 m MSL contour line, were digitised on each of the available geo-referenced aerial photographs. Profile comparison lines, positioned on each beach at approximately 200 m intervals, were superimposed onto the available images for comparison between consecutive aerial photographs.

The position of the vegetation line, 5 m contour and the high water mark were compared at each profile comparison line in each photo taking into account the beach slope variation, tidal ranges and seasonal variations in order to deduce any accretion or erosion trend.

By comparing the vegetation line and the high water mark (based on wetted area) with the profile comparison lines in each photo, an assessment was made of long term coastline processes within the time difference of the photographs. Based on this methodology a general overview of the stability of the coastline was made and specific areas of interest categorised as having: eroded, accreted or remained dynamically stable.

8.2.3 Accuracy

The accuracy of the comparison of the high water mark is dependent on available information regarding tidal data and storm information at the time of the respective photographs. As this information is not generally available, the accuracy is limited by the maximum possible horizontal movement of the high water mark between MHWS and MHWN (refer to Section 4.1) and possible variations in storm surge, wave set-up and wave run-up. For the beaches at Bantamsklip with a maximum tidal variation (MHWS to MHWN) of approximately 0.5 m, an approximate vertical variation due to storm surge, set-up and run-up of 2 m, and considering an average slope of 1:34, the maximum error is approximately 85 m horizontal. Additional sources of error include rectification and

image resolution. The combined magnitude of imaging errors is found to be in the order of an 8 m horizontal residual (Crowell *et al.*, 1991).

8.2.4 Coastline Trends

The coastline evolution was assessed on this basis for the following beaches located around the Bantamsklip site:

1. Castle Beach
2. Pearly Beach
3. Shell Point
4. Plaatjieskraalbaai
5. Jessie se Baai

8.2.4.1 *Castle Beach*

Castle Beach is a 2 km long beach located 7 km north-west of the Bantamsklip site. Photos available for this area are dated from 1981 and 2004. As insufficient information regarding the 5 m contour line is available, only the vegetation and high water lines have been used to ascertain coastline trends. Generally, the vegetation line is seen to have eroded over the observation period (refer to Figure 8.3). Some accretion of the vegetation line is noticeable on the northern extent (refer to Figure 8.2). The high water line is seen to have remained dynamically stable (refer to Figures 8.2 and 8.3).

8.2.4.2 *Pearly Beach*

Pearly Beach is a 2.8 km long beach located 2.5 km north-west of the Bantamsklip site. Photos available for this area are dated from 1981, 2004 and 2007. As insufficient information regarding the 5 m contour line is available, only the vegetation and high water lines have been used to ascertain coastline trends. The vegetation line is seen to have accreted over the entire observation period (refer to Figures 8.4, 8.5 and 8.6). The high water mark, initially showing accretion between 1981 and 2004, appears to be dynamically stable between the periods of 2004 to 2007. Generally the beach can be said to have accreted between 1981 and 2007.

8.2.4.3 *Shell Point*

Shell Point is a 1.4 km long beach located 0.5 km south-east of the Bantamsklip site. Photos available for this area are dated from 1981, 2004 and 2007. The area around shell point (refer to Figures 8.7, 8.8 and 8.9) is characterised by a generally rocky coast with small pocket beaches. The vegetation line for the entire observation period is seen to be dynamically stable. The movement of the high water line, though seen to have accreted between 1981 and 2004, appears to have remained dynamically stable till the period 2007.

8.2.4.4 *Plaatjieskraalbaai*

Plaatjieskraalbaai a 2 km long beach located 3.5 km south-east of the Bantamsklip site. Photos available for this area are dated from 1981, 2004 and 2007. As insufficient information regarding the 5 m contour line is available, only the vegetation and high water lines have been used to ascertain coastline trends. The vegetation line, though seen to be dynamically stable in the north western corner of the bay (refer to Figure 8.10), shows sign of having eroded in the south eastern corner (refer to Figure 8.11). Evidence from the interrogation of the high water line suggests significant accretion between the 1981 and 2004 aerial photographs, with the beach showing erosion to the 2007 date.

8.2.4.5 *Jessie se Baai*

Jessie se Baai a 2 km long beach located 8 km south-east of the Bantamsklip site. Photos available for this area are dated from 1981 and 2004. As insufficient information regarding the 5 m contour line is available, only the vegetation and high water lines have been used to ascertain coastline trends. Both the vegetation line and the high water line are seen to have accreted over the observation period (refer to Figures 8.12 to 8.14).

8.2.5 Discussion

By comparing the vegetation line and the high water mark (based on wetted area) on each set of photos, an assessment was made of whether the beach eroded, accreted or remained dynamically stable.

Although a rigorous method has been followed in the assessment of coastline trends using aerial photographs, the method is subjective. The above observations of coastline trends are qualitative and must be interpreted as such.

Though signs of both erosion and accretion are noticed in the analysis of the aerial photographs, these are believed to be indications of long term variations about dynamically stable beach shapes (refer to Section 8.1)..

8.3 Seasonal Variation in Coastline

8.3.1 Physical Process

Seasonal variations can be seen as coastline modification events with averaging periods typically in the order of months. These are generally due to seasonal variations in wave conditions and the occurrence of erosional storms separated by periods of low wave accretion events. In South Africa the majority of erosion related storms occur in the winter months, with summer months predominated by accretionary periods of low wave height conditions (Rossouw, 1989). As in long-term coastline trends, a statistical analysis based on measured profile data is the primary method of determining seasonal variations.

With the limited profile data currently available only a preliminary quantitative assessment of seasonal variation for the Bantamsklip coastal sites is possible. For coasts that do exhibit a seasonal signature, the large perturbations caused by storm events require repetitive surveys over many years to extract this seasonal signature (CEM, 2002).

8.3.2 Methodology

As mentioned in Section 8.1, recent profile measurements for the months of January, April, July and October of 2008, and January, April and July 2009 have been processed and analysed for a number of beacon locations along the beaches for the Bantamsklip site. Refer to Figure 8.15 for an overview of profile locations at the Bantamsklip site and Figures 8.16 to 8.20 for plots of the measured profiles.

Distances from the respective beacon locations have been calculated from interpolated values obtained at 0 m MSL, +1 m MSL, +2 m MSL and +3 m MSL for each of the available measurements. An average distance has then been calculated from these interpolated values. The difference between this calculated average and the measured distance, for each survey date, has been used in order to calculate seasonal variations.

8.3.3 Coastline Trends

Figures 8.21 and 8.22 shows the variations for horizontal displacements for beach profiles along the coast to the north, south and in front of the proposed nuclear installation corridor. Figure 8.21 specifically show variations for Pearly Beach and a profile to the north of the proposed installation corridor. Generally these beaches exhibit a typical winter storm erosion pattern, with erosion of the majority of profiles between April and October, winter storm months, and accretion from October to April.

Generally the erosion (refer to Figure 8.22) in front of the proposed nuclear installation corridor (refer to Figure 8.15) and that for Plaatjieskraalbaai (refer to Figures 8.10 and 8.11) is less than the erosion noticed for the beaches further north. This is believed to be due to the steep beach and cliff slopes (refer to Figures 4.10 and 4.11) in front of the installation corridor.

8.3.4 Quantification of Seasonal Variations

Maximum (+ve: accretional), and minimum (-ve: erosional) deviations from the calculated average, refer to Section 8.3.2, for each of the profiles over the survey periods of 2008 and 2009 are provided in Figures 8.21 and 8.22 and Table 8.1.

TABLE 8.1: MAXIMUM SEASONAL VARIATIONS IN HORIZONTAL DISPLACEMENTS OF THE MEASURED BEACH PROFILES

Profile no.	0 m MSL		+1 m MSL		+2 m MSL		+3 m MSL	
	Erosion [m]	Accretion [m]	Erosion [m]	Accretion [m]	Erosion [m]	Accretion [m]	Erosion [m]	Accretion [m]
02	-26.91	23.84	-12.88	17.00	-6.99	7.18	-3.30	5.95
03	-27.87	27.68	-19.03	19.11	-12.93	6.05	-1.11	2.15
04	-25.02	8.74	-11.13	8.08	-34.60	21.54	-14.55	9.40
05	-6.65	10.04	-8.15	10.43	-14.24	18.30	-13.32	12.64
06	-23.54	16.63	-12.88	11.70	-6.71	4.65	-7.57	5.32
07	-23.50	15.78	-18.99	14.83	-6.23	8.46	-13.62	14.32
14	-3.93	3.92	-5.38	5.24	-3.19	2.69	-4.49	10.63
24	-13.82	17.17	-10.86	12.01	-9.52	9.29	-6.02	3.84
25	-11.22	19.84	-11.16	13.17	-7.22	12.18	-4.83	3.50
26	-4.38	11.65	-5.04	9.28	-5.09	7.95	-4.79	3.50
27	-5.00	12.01	-4.14	9.81	-8.23	10.00	-2.46	2.02
28	-6.89	6.54	-2.63	6.10	-8.40	7.98	-2.82	3.16
32	-7.30	5.84	-4.45	4.29	-6.70	3.27	-1.10	1.02
34	-2.05	2.05	-2.02	1.46	-7.67	4.12	-5.32	5.50
35	-14.46	8.83	-7.36	3.37	-2.75	4.58	-5.39	5.69
36	-9.82	10.02	-5.22	7.09	-6.91	7.37	-3.58	7.93

Notes (refer to Figure 8.15):

1. Profiles 02 to 07 refer to profiles on Pearly beach
2. Profile 14 is to the north of the proposed nuclear installation corridor
3. Profiles 24 to 28 are in front of the proposed nuclear installation corridor
4. Profiles 32 to 36 refer to profiles from Plaatjieskraalbaai

The available profile data indicates that the maximum seasonal erosion from the *average* of the survey data occurring on the beaches in front of the proposed nuclear site is approximately -14 m (at 0 m MSL level for Profile 24).

Profile measurements for Bantamsklip are on-going and will provide additional data in future, (refer to Section 8.1), however the data utilised on the profile analysis above can be seen as the first complete season of measured data.

8.4 Storm Event Erosion

8.4.1 Physical Process

Severe storms can cause significant modifications of the littoral zone, particularly to the profile of the beach (IAEA, 2003). Sediment transport at a point in the nearshore zone is a vector with both longshore and cross-shore components. Although the long-term beach profile might be stable, severe storm conditions can cause cross-shore sediment transport resulting in a 'storm profile' (see Figure 8.23). The evolution of the beach profile can have an impact on the nearshore waves. An increase of nearshore waves has a direct impact on wave run-up.

8.4.2 Methodology

Continual longshore and cross-shore sediment transport processes are expected with the beaches not deviating exceptionally from a dynamic equilibrium. Only during episodic events would back of coast dunes possibly be vulnerable.

SBEACH, a beach response model for storm events (CERC, 1993), has been used to model storm erosion for the combined storm events (refer to Chapter 7) for 1:1 year, 1:10 year, 1:100 and 1:10⁶ year return periods at a specific profile at the Bantamsklip site.

As SBEACH is fundamentally a cross-shore storm erosion model it is necessary to calibrate the model with profile information from a relatively straight beach where profile changes are predominantly due to cross-shore transport and unlikely to be caused by long-shore sediment gradients. The Duynefontein site exhibits such characteristics and has thus been used to calibrate the SBEACH model. Based on the profiles obtained from historic measurements for the Duynefontein site (PRDW, 2009c) a representative beach profile has been chosen for calibration of SBEACH (refer to Figure 8.24 for a plan view of the location of the profile (PRDW, 2009c) used for model calibration).

8.4.2.1 Calibration: Beach Profile and Sediment Properties

In order to calibrate the model, historic information of beach profiles is needed. Measured profiles from April 2008 and July 2008 have been used (PRDW, 2009c). The profiles have then been interpolated onto existing bathymetric and topographic data to obtain a full profile for modelling.

Since SBEACH requires a constant grain size across the profile a representative D_{50} grain size has been used in the calibration of the model. From measured sediment sample data for the profile considered, a D_{50} of 0.3 mm is considered as representative. This grain size has been used consistently in the calibration process.

8.4.2.2 Calibration: Wave Conditions

Wave conditions for the period from April 2008 to July 2008 have been extracted from a previous wave refraction study, described in the modelling report for Duynefontein (PRDW, 2009b). For initial calibration of the model a complete time series of significant wave heights and peak wave periods for every 6 hours has been used. Figure 8.25 shows a plot of the significant wave heights and peak wave periods used over the modelling period.

8.4.2.3 Calibration: Water Levels

SBEACH models the wave setup and run-up internally, whilst the combined tidal, wind setup and pressure setup are specified as a time-varying boundary condition. For input water level conditions measured tidal data from Cape Town has been interpolated as hourly boundary data for the period

coinciding with the calibrated wave data. Figure 8.25 shows a plot of the tidal data used over the modelling period.

8.4.2.4 Calibration: Model Parameters

The primary model parameters for SBEACH are the transport rate coefficient, K , the coefficient for slope dependence, ϵ , and the transport rate decay coefficient multiplier, λ . A sensitivity test was performed using values corresponding to the minimum recommended value, the default value and the maximum recommended value for each of the model parameters with the other parameters set to default. For the transport rate decay coefficient multiplier, λ , an intermediate value between the minimum and maximum recommended values was modelled, as the default value is equal to the maximum recommended value (CERC, 1993).

TABLE 8.2: SBEACH CALIBRATION PARAMETERS

Calibration Parameter	Minimum Value	Intermediate Value	Maximum Value
K [m^4/N]	0.50E-06	1.75E-06 ⁽¹⁾	2.5E-06
ϵ [m^2/s]	0.001	0.002 ⁽¹⁾	0.003
λ [-]	0.1	0.3	0.5 ⁽¹⁾

Notes:

- 1) Model default values

8.4.2.5 Calibration: Sensitivity of Model Parameters

The model has been tested, using different calibration parameters and beach profiles, for 1:100 year storm in order to ascertain the sensitivity of the calibration parameters. Using the maximum values of the calibration parameters, an increase in erosion of approximately 10% of the value obtained for the calibrated parameters was obtained. This range is consistent with the accuracy expected from the model.

8.4.2.6 Calibration: Discussion of Results

Results show:

- High dependence on K
- Marginal dependence of ϵ
- Little dependence on λ

Refer to Figure 8.26 for results of the calibration analysis. The default values (refer to Table 8.2) for all calibration parameters show sufficient correlation for modelling purposes. For the further modelling of storm induced erosion, these values are used.

8.4.3 Storm Events

Further calibration of the model input conditions is achieved using shorter time scales with actual storm and water levels, obtained from the wave refraction model (PRDW, 2009b), and measured tidal data for Cape Town.

As knowledge of storm progression, i.e. duration, increase in H_{m0} and T_p , is not known before hand for the design storm conditions, a method is utilised whereby a measured storm is compared to a modelled storm using the equivalent wave energy for the measured storm (MacHutchson, 2006).

8.4.3.1 Measured Storm Conditions

Individual storm events extracted from the data set for April to July 2008 (refer to Section 8.4.2.2) have been used for more detailed calibration and verification of final model storm parameters. The four highest energy storms, as calculated with the equivalent wave energy calculations, have been isolated and applied to the SBEACH model (refer to Figure 8.27).

8.4.3.2 Modelled Storm Conditions

Equivalent design storms are modelled using an equivalent wave energy storm progression, with the maximum H_{m0} for the measured storm events, and the $H_{m0} - T_p$ relationship obtained from PRDW (2009b). Further to the maximum H_{m0} and T_p , a representative storm duration, and storm threshold value for H_{m0} are required. Storm threshold is defined as being equal to the annual average H_{m0} for the area (MacHutchson, 2008). For the calibration of storm data from the Dufnefontein site the storm threshold has been extracted from existing measured data and corresponds to an H_{m0} of 1.8 m.

Furthermore, MacHutchson (2006), categorised South African storm events with respect to a defined steepness ratio, difference in maximum H_{m0} and storm threshold H_{m0} over duration, for specific individual coastal regions in South Africa based on historical data. The steepness ratio used in calculations for both the modelled calibration storm events and design modelled storm events corresponds to that determined for the south coast region. Using this steepness ratio, typical storm durations based on storm maximum H_{m0} , T_p and mean H_{m0} are calculated (refer to Figure 8.27).

8.4.3.3 Results

The SBEACH modelled erosion patterns for the *modelled storm progressions* show close agreement with the SBEACH modelled erosion patterns for the *measured storm events* (refer to Figure 8.28). Good agreement is seen with erosion of the dune and set-back at high water levels. Based on these results from initial tests, the assumption of a linear equivalent wave energy storm progression for individual storm events appears justifiable. Using the method described, storm progressions for extreme design wave conditions are modelled.

8.4.4 Storm Analysis

8.4.4.1 Beach Profile and Sediment Properties

Model runs have been completed with an interpolated profile based on detailed topographic measurements of the dunes and surveyed data of the coast seaward of the beach (refer to PRDW, 2009a). Profile 03 (refer to Figures 4.10 and 4.11) has been used for storm analysis.

From sediment grading data for Bantamsklip, (PRDW, 2009a) representative samples show D_{50} values of 0.2 to 0.4 mm. D_{50} values of 0.2, 0.3 and 0.4 mm have been specified in three SBEACH models for the profile.

8.4.4.2 Wave Conditions and Water Levels

Values of the maximum H_{m0} and T_p for the 1:1, 1:10, 1:100 and 1:10⁶ year storm conditions have been used in determining the modelled storm profiles for Bantamsklip. Refer to Section 4.4 and PRDW (2009a) for wave conditions. Storm threshold values are specified as the local mean H_{m0} for Bantamsklip as 2.2 m (PRDW, 2009a).

A sinusoidal tidal variation has been modelled for each of the storm conditions, with a period of 12 hours and maximum amplitude of half of HAT - LAT. The peak of the storm, the maximum H_{m0} and T_p values, correspond to HAT for the water levels with an inclusion due to maximum storm surge (refer to Section 4.1).

8.4.4.3 Discussion of Results

Figure 8.29 shows erosion patterns for the surf zone for Profile 03 and the three D_{50} values. Maximum horizontal erosion at any level for all model runs are tabulated below:

TABLE 8.3: MAXIMUM STORM EROSION HORIZONTAL DISPLACEMENTS - EXCLUDING CLIMATE CHANGE

D_{50}	Units	Return Period [years]			
		1:1	1:10	1:100	1:10 ⁶
0.2 mm	[m]	-32	-38	-45	-74
0.3 mm	[m]	-25	-30	-36	-58
0.4 mm	[m]	-18	-20	-25	-44

As can be seen in Table 8.3, the maximum absolute value of shoreline recession due to a single storm event occurs during the 1:10⁶ year.

As SBEACH assumes a standard grain size, and the model is calibrated for measured profiles in the surf zone, no vertical position of the tabulated horizontal change is given. Similarly, and considering avalanching of the dune during storm erosion, the maximum horizontal values should conservatively be seen as occurring from the foredune crest.

8.5 Long-term Sea level Rise

8.5.1 Physical Process

The effect of increased water levels due to climate change (see Section 3.2) needs to be accounted for. These effects are shown to be highly complex and inclusive of local geomorphological and sedimentological characteristics (Cooper and Pilkey, 2004). However, the majority of coastline response studies to sea level change are based on the simplified fundamental assumption that a beach will maintain an equilibrium profile dependent on the dominant wave climate. As such, provided that the rate of sea level rise is small, the beach profile will translate vertically and horizontally landward such that this equilibrium profile is maintained.

8.5.2 Methodology

One of the best known shore response models to climate induced sea level change was proposed by Bruun in 1962 (CEM, 2002). This model, though noted as omitting factors other than wave action affecting sediment transport (CEM, 2002), has nonetheless been widely used in predicting long-term sea level change tendencies.

It remains the “only practical way of yielding a rapid, semi-quantitative assessment of shore response to a rise in sea level” (Cooper and Pilkey, 2004). Based on the complexity of long-term sea level rise due to climate change and the unknowns regarding rates of change, and effects on wave and climate conditions it is suggested that Bruun-type calculations give, at best, order of magnitude estimates of shoreline retreat (CEM, 2002).

8.5.2.1 Bruun’s Rule

The use of Bruun’s rule is based on the following assumptions:

- The upper beach erodes because of a landward translation of the profile
- Sediment eroded from the upper beach is deposited immediately offshore; the eroded and deposited volumes are equal (i.e. longshore transport is not a factor).
- The rise in the seafloor offshore is equal to the rise in sea level. Thus, offshore, the water depth stays constant.

$$R = \frac{L_*}{B + H_*} S \quad \text{Equation 1}$$

Where:

R is the horizontal coastline retreat [m]

S is the increase in sea level [m]

L_* is the cross-shore distance to the water depth H_* [m]

B is the berm height of the eroded area [m]

8.5.2.2 Applied Modification to Bruun's Rule

Reformatting the Bruun Rule in a simplified form (CEM, 2002) gives:

$$x = \frac{zX}{Z} \quad \text{Equation 2}$$

Where:

z is the change in water level [m]

x is the ultimate profile retreat [m]

X is the corresponding distance determined from the depth of closure to the upper point of profile adjustment (refer to Figure 8.30). [m]

Z is the vertical distance from the depth of closure to the upper point of profile adjustment (refer to Figure 8.30). [m]

The upper point of profile adjustment is taken to be the crest of the foredune. The modified Bruun Rule, shown above, is a simple geometric rule to account for sea level changes and related beach response profiles. From the depth of closure, the minimum depth at which no measurable or significant changes in the bottom depth occurs, the profile is relocated such that sediment is conserved and the profile is assumed to reach an equilibrium profile at the new water level. The following equation is used to calculate the depth of closure (CEM, 2002):

$$d_l = 2.28H_e - 68.5 \left(\frac{H_e^2}{gT_e^2} \right) \quad \text{Equation 3}$$

Where:

d_l is the annual depth of closure below the mean water level [m]

H_e the non-breaking significant wave height that is exceeded 12 hours per year (0.137 %) [m]

T_e the associated wave period [s]

g gravitation acceleration [m.s⁻²]

For calculations of modified profile changes based on Bruun's Rule for sea level change, H_e is predicted from the 1:1 year return period wave (refer to Section 4.4). The parameters and solution for the calculation of long term horizontal displacement due to sea level rise are given in Table 8.4.

**TABLE 8.4: PARAMETERS FOR LONG-TERM HORIZONTAL EROSION
DUE TO SEA LEVEL RISE**

Parameter	Value
H_e	5.5 m
T_e	14.7 s
g	9.81 m.s ⁻²
d_l	12.8 m MSL
Z	22 m
z	0.8 m
X	880 m
x	35 m

Figure 8.31 shows the horizontal and vertical translation of Profile 03. For the assumed sea level rise of **0.8 m** (Section 3.2), the maximum horizontal change is calculated to be approximately **35 m** (refer to Table 8.4).

8.5.3 Storm Erosion Including Climate Change

Extreme wave conditions exacerbated by climate change events (refer to Section 3.2) have been used to model the storm erosion patterns for Profile 03 and the climate changed beach profile. Refer to Figure 8.32 for details of erosion patterns for the representative D_{50} values as specified in Section 8.4.4.1. As the equilibrium profile is assumed to translate vertically and horizontally due to climate induced sea level rise, the maximum horizontal values should conservatively be seen as occurring from the foredune crest.

Maximum horizontal erosion for all model runs is tabulated below:

**TABLE 8.5: MAXIMUM STORM EROSION HORIZONTAL DISPLACEMENTS -
INCLUDING CLIMATE CHANGE**

D_{50}	Units	Return Period [years]			
		1:1	1:10	1:100	1:10 ⁶
0.2 mm	[m]	-35	-44	-52	-85
0.3 mm	[m]	-28	-34	-41	-66
0.4 mm	[m]	-20	-25	-31	-48

The maximum absolute value for erosion is seen to occur during the 1:10⁶ year return period storm for a D_{50} of 0.2 mm.

8.6 Discussion of Results

Results for the following physical processes of erosion/accretion events considered in the section above are tabulated:

- Long-term coastline trends (Section 8.2)
- Seasonal variation in the coastline position (Section 8.3)
- Storm event erosion based on 1:10⁶ year with grain size 0.2 mm (Section 8.4)
- Effects on coastline movement due to long-term sea level rise (Section 0)

TABLE 8.6: MAXIMUM EXPECTED HORIZONTAL COASTLINE EROSION AT BANTAMSKLIP BEACH FOR THE EXPECTED INSTALLATION LIFE

	Long-term Trend	Seasonal Erosion	Storm Event Erosion	Long Term Sea level rise	Total Coastline Erosion
Excluding climate change	Dynamically stable	14 m	74 m	N/A	88 m
Including climate change	*Dynamically stable	**14 m	85 m	35 m	≥ 134 m

Notes:

* Future changes in wave direction could modify the long-term trend (no information available at present);

** Likely to exceed 14 m based on future increase in wave height (see Section 3.2 and Appendix A);

Coastline recession data and models due to climate induced sea level change are based on the information available at present, and need to be continually reassessed as new data and research results become available.

9. CONCLUSIONS

The following conditions for the Bantamsklip site have been addressed in this report and where applicable numerical models have been used to generate results:

- Physiography and marine/coastal geology
- Possible changes to hydrographic conditions due to climate changes
- Hydrographic conditions
- Intake and outfall design considerations
- Calculation of maximum and minimum seiche in basin layouts
- Combinations of maximum and minimum water levels
- Coastline stability and cross-shore sediment transport

Hydrographic conditions for the proposed Bantamsklip site have been analysed as well as the impact of climate change on these conditions within the lifetime of the planned nuclear installation. The risk of flooding assessment and availability of cooling water have been undertaken according to internationally specified standards as documented in the IAEA (2003).

The results of these investigations, along with the Numerical Modelling of Coastal Processes Report (PRDW, 2009a) provide inputs to the SSR Chapter on Oceanography and Coastal Engineering.

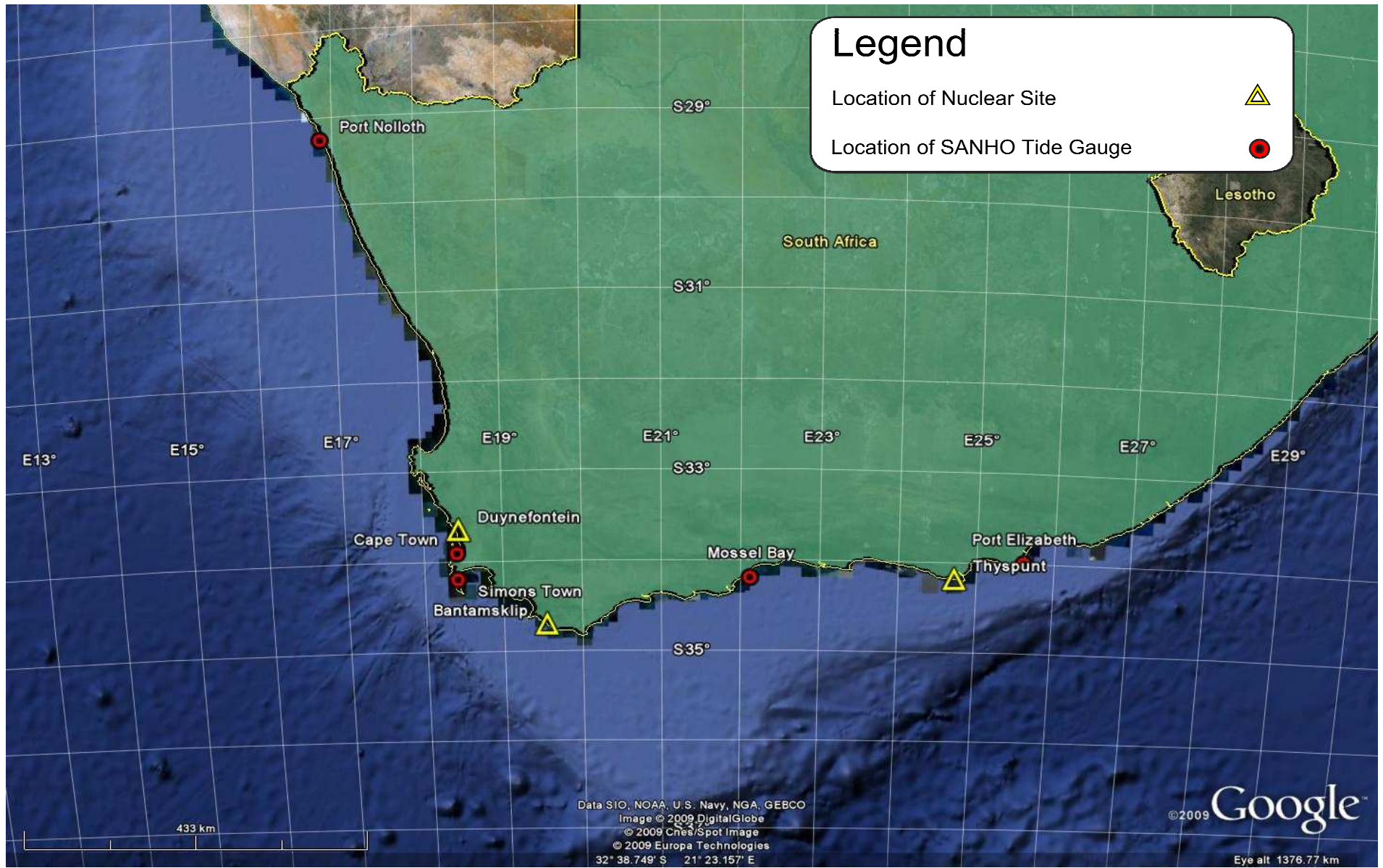
REFERENCES

1. ASCE (1982) Design of Water Intakes for Fish Protection, American Society of Civil Engineers, 1998
2. Bosman, D. E. and Wijnberg, A. R (1987) Gouriqua Marine Reports, Volume V. Nuclear Coastal Engineering NSE – 1 Project. Cost model for marine Cooling Systems for S.A. Nuclear Sites, November 1987
3. CEM (2002) CEM Part IV Chapter 3 - Coastal Morphodynamics, US Army Corps of Engineers, April 2002
4. CEM (2003) CEM Part II Chapter 4 - Surf Zone Hydrodynamics, US Army Corps of Engineers, July 2003
5. CEM (2006) CEM Part VI Chapter 5 - Fundamentals of Design, US Army Corps of Engineers, June 2006
6. CERC (1993) SBEACH: Numerical Model for Simulating Storm-Induced Beach Change, Report 3, User's Manual, US Army Corps of Engineers, 1993.
7. Coastal CRC (2006) The evolution of Jumpinpin Inlet, McCaully, E. and Tomlinson, R. Cooperative Research Centre for Coastal Zone, Estuary and Waterway Management, 2006.
8. Cooper and Pilkey (2004) Sea-level rise and shoreline retreat: time to abandon the Bruun Rule, Cooper J. A. G and Pilkey O. H, *Global and Planetary Change*, 43 (2004) 157-171
9. Crowell M, Leatherman S.P and Buckley M.K, 1991. Historical Shoreline Change: Error Analysis and Mapping Accuracy. *Journal of Coastal Research*, Vol. 7, No. 3, pp. 839-852.
10. DHI (2009) MIKE 21 BW, Boussinesq Waves Module, User Guid, Danish Hydraulics Software, 2009
11. Engineers Australia (2004) Guidelines for Responding to the Effects of Climate Change in Coastal and Ocean Engineering, The National Committee on Coastal and Ocean Engineering, Engineers Australia.
12. EPRI (2008) Best Management Practice for Preventing Cooling Water Intake Blockage, Electric Power Research Institute, Palo Alto, California, January 2008
13. Eskom (2006) Koeberg Site Safety Report, Chapter 8, Oceanography and Cooling Supply, Rev 3.
14. Eskom (2007) Areva, EPR Technical Description, Rev A, Received from Eskom, August 2007.
15. Eskom (2008) ESKOM Holdings Limited; Environmental Impact Assessment for the Proposed Nuclear Power Station ('Nuclear-1') and Associated Infrastructure; Marine Ecology Study; September 2008.

16. FEMA (2006) “Tsunami Inundation Scour of Roadways, Bridges and Foundations Observations and Technical Guidance from the Great Sumatra Andaman Tsunami”, EERI Earthquake Engineering Research Institute / FEMA [Federal Emergency Management Agency](#), 2006
17. FUGRO Survey (2007) Marine Geophysical Survey BANTAMSKLIP Seabed Features, FUGRO SURVEY AFRICA (PTY) LTD, Commissioned for ESKOM HOLDINGS LTD., January 2007
18. Hughes (2004) Estimation of wave run-up on smooth, impermeable slopes using the wave momentum flux parameter, S. A. Hughes, 2004, *Coastal Engineering*, 51, 1085-1104
19. IAEA (2003) Flood Hazard for Nuclear Power Plants on Coastal and River Sites. International Atomic Energy Agency. IAEA Safety Standards Series No. NS-G-3.5.
20. IPCC (2007) Climate Change 2007 - The Physical Science Basis, Contribution of Working Group I to the Fourth Assessment Report of the IPCC
21. MacHutchson (2006) The Characterisation of South African Storms, K. R MacHutchson, MSc. Thesis, University of Stellenbosch, 2006
22. Morton, R. A, Gelfenbaum, G, Jaffe, B. E, Physical criteria for distinguishing sandy tsunami and storm deposits using modern examples, *Sedimentary Geology*, 2007.
23. NGDC (2009) National Geophysical Data Centre (NGDC), NOAA Satellite and Information Service, The Significant Earthquake Database, Available from <http://www.ngdc.noaa.gov/nndc/>
24. PRDW (2001) ESKOM Nuclear Power Stations - Site Investigation Program NSIP Coastal Engineering - Bantamsklip Site, Prestedge Retief Dresner Wijnberg (Pty) Ltd, Report 345/02 October 2001.
25. PRDW (2009a) Eskom, Nuclear Sites, Numerical Modelling of Coastal Processes - Bantamsklip, Prestedge Retief Dresner Wijnberg (Pty) Ltd, Report 1010/3/101.
26. PRDW (2009b) Eskom, Nuclear Sites, Numerical Modelling of Coastal Processes - Duynfontein, Prestedge Retief Dresner Wijnberg (Pty) Ltd, Report 1010/4/101 Rev 03.
27. PRDW (2009c) Eskom, Nuclear Sites, Coastal Engineering Investigations - Duynfontein, Prestedge Retief Dresner Wijnberg (Pty) Ltd, Report 1010/4/102 Rev 03.
28. Reeve D, Chadwick A and Flemming C ,2004. Coastal Engineering, Processes, Theory and Design Paractice, D Reeve, A Chadwick and C Fleming. SPON Press, 2004
29. Rossouw (1989) Rossouw, J. Design Waves for the South African Coastline. Dissertation approved for the degree Doctor of Philosophy at the University of Stellenbosch, March 1989.

-
30. SMC(2007) Southern Mapping Company. "LIDAR Survey Report, Eskom Nuclear Site: Koeberg", Report submitted to Argus Gibb Consulting Engineers, September 2007.
 31. South African Tide Tables (2009) SAN HO-2, Published by the Hydrographer, South African Navy, ISBN 0-97809584817-4-8.
 32. USACE (1987) "Confined Disposal of Dredged Material". US Army Corps of Engineers. Engineer Manual, 30 September 1987
 33. USGS (2005) The 26 December 2004 Indian Ocean Tsunami: Initial Findings from Sumatra, Based on Survey Conducted January 20-29, 2005, USGS U.S. Geological Survey, 2005, Available from: <http://walrus.wr.usgs.gov/Tsunami/sumatra05/>
 34. USNRC (2007) US Nuclear Regulatory Commission (2007) NUREG-0800, Part 2.4.6, Probable Maximum Tsunami Hazards, Washington.
 35. Yeh, H, Tonkin S, Kato, F and Sato, S, Tsunami Scour Mechanisms Around a Cylinder, Journal of Fluid Mechanics (2003), 496 : 165-192
 36. Yim (2006) Modelling and Simulation of Tsunami and Storm Surge Hydrodynamic Loads on Coastal Bridge Structures, Yim, S., 2006, Technical Memorandum of Public Works Research Institute.

FIGURES

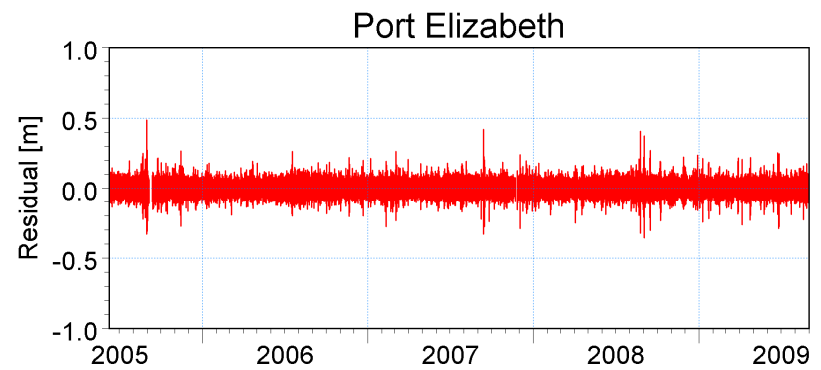
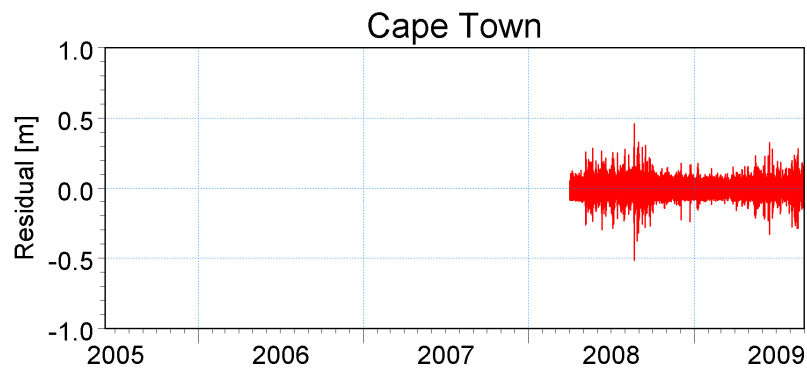
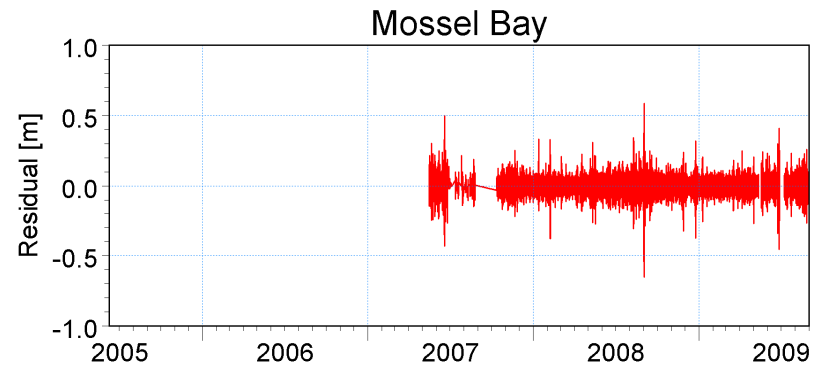
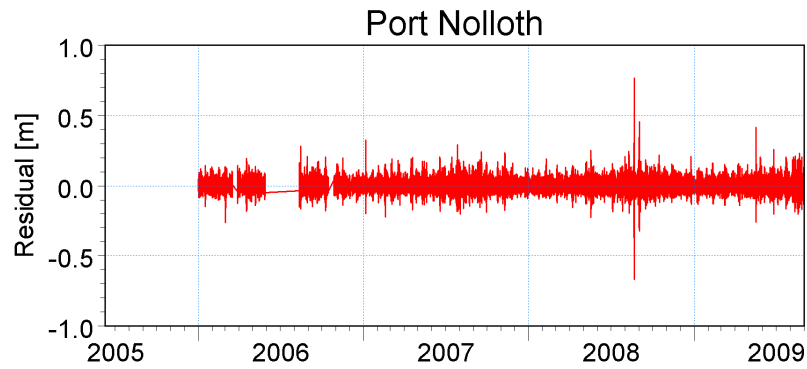


Title:

Locations of SANHO tide gauges used in the extraction of long wave extreme values

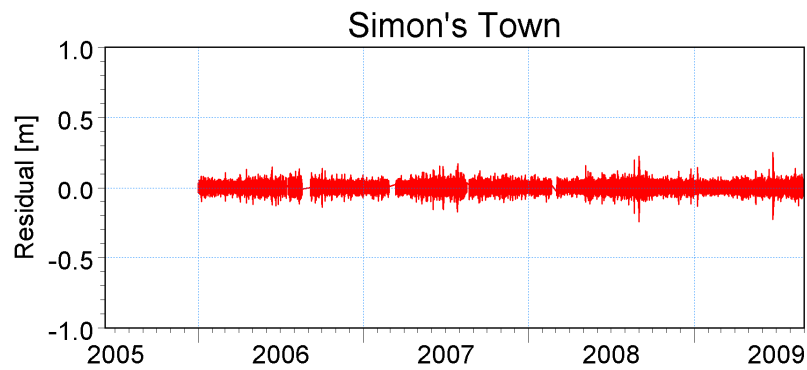
Figure No.

4.1



X:\PRDW Projects\Current\SA (1010) Nuclear Sites
SSRs\Working\Engineers\RLH\Meteotsunami\Data\Sites\ResidualComparisonAll1t.png

X:\PRDW Projects\Current\SA (1010) Nuclear Sites
SSRs\Working\Engineers\RLH\Meteotsunami\Data\Sites\ResidualComparisonAll1t.png

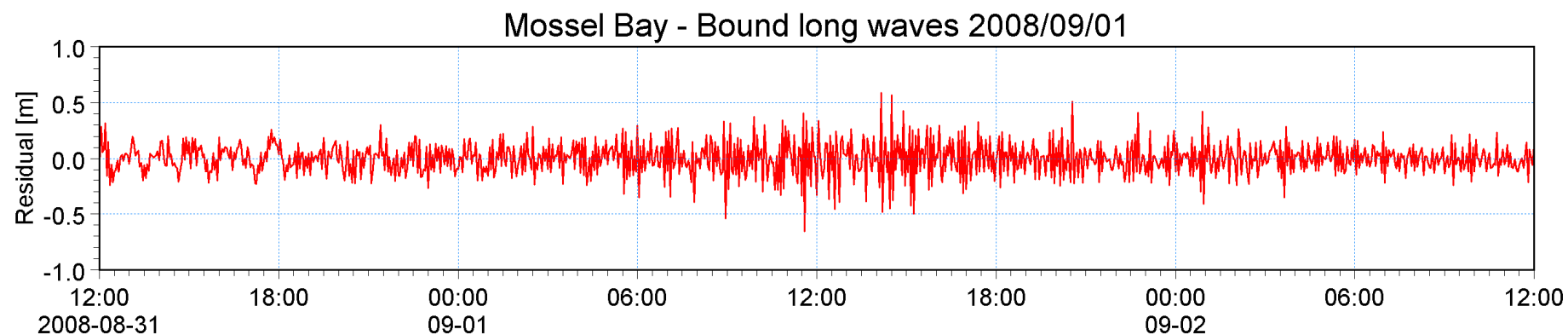
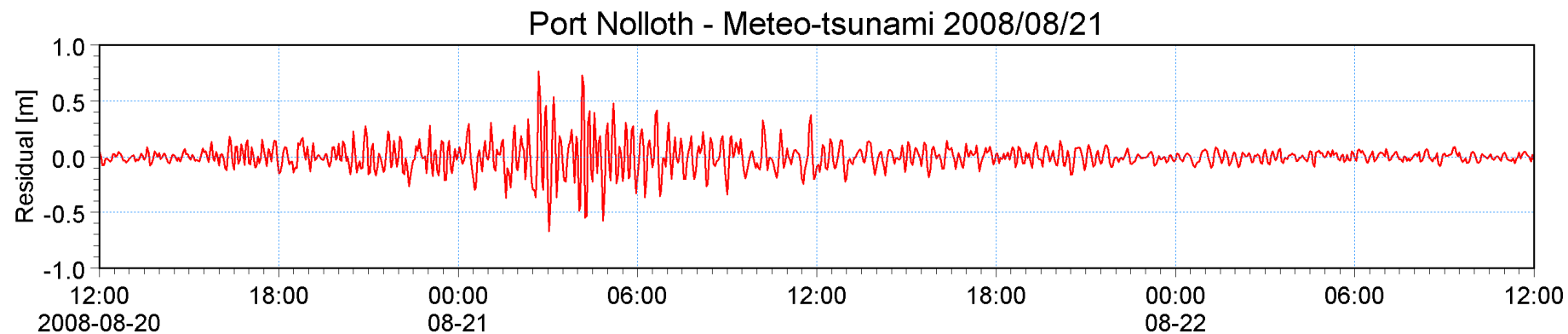


Title:

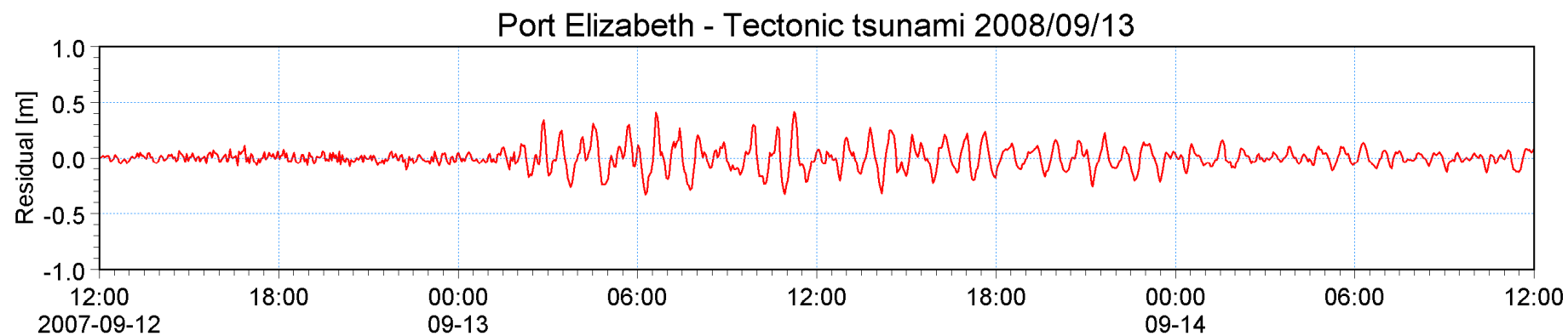
**Complete residual of three min data for 5 SANHO
tide gauge locations around South Africa**

Figure No.

4.2



X:\PRDW Projects\Current\SA (1010) Nuclear Sites SSRs\Working\Engineers\RLH\Meteotsunami\Data\Sites\ResidualComparisonEvents.png

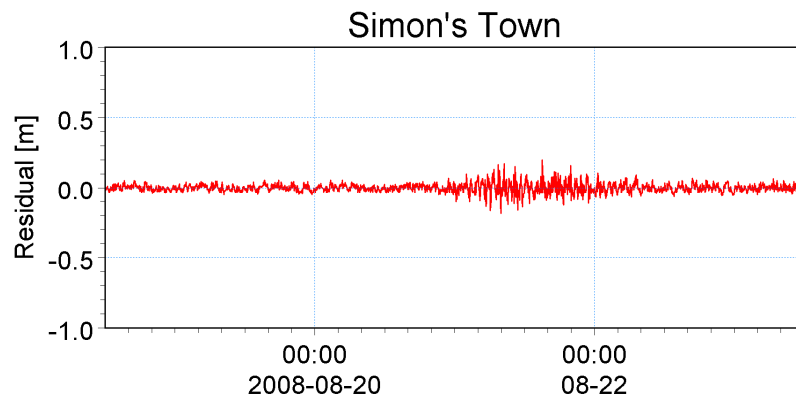
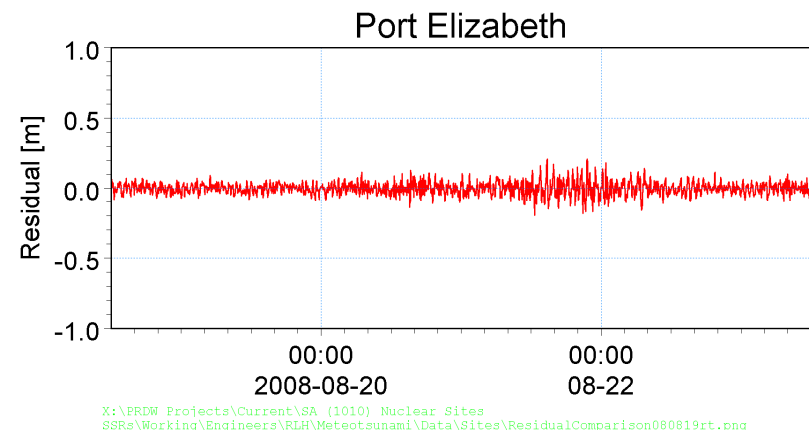
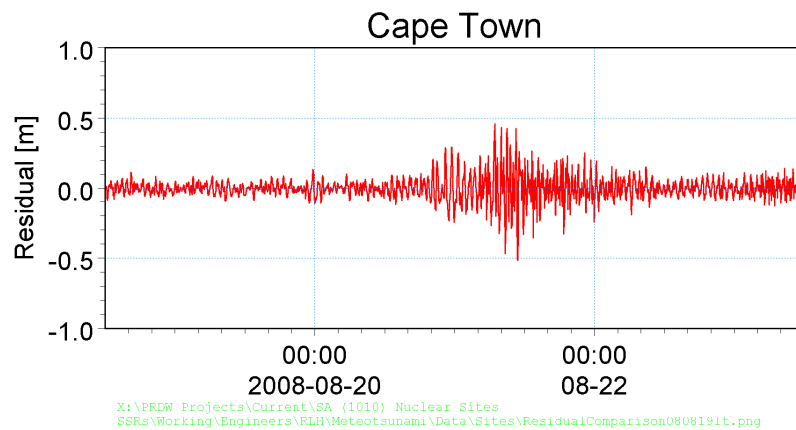
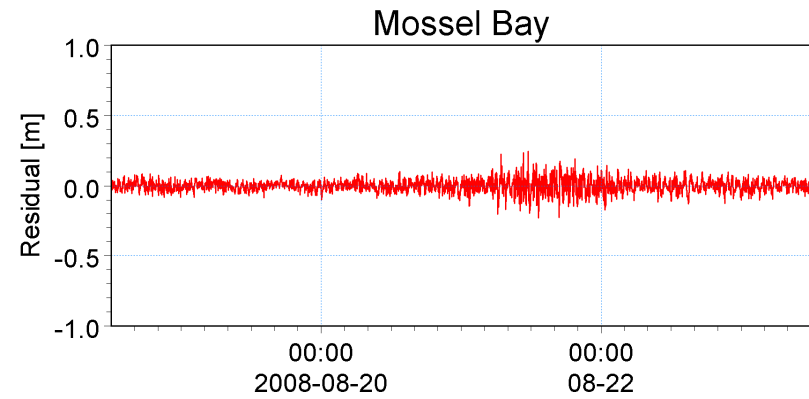
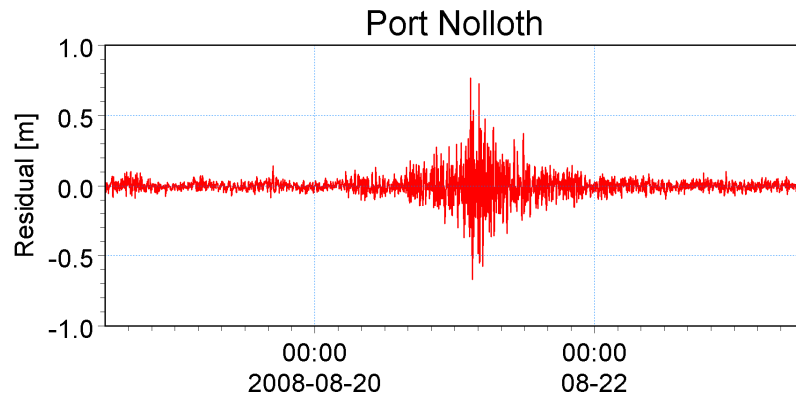


Title:

**Comparison of residual values for three long wave events
for 3 SANHO tide gauge sites around South Africa**

Figure No.

4.3

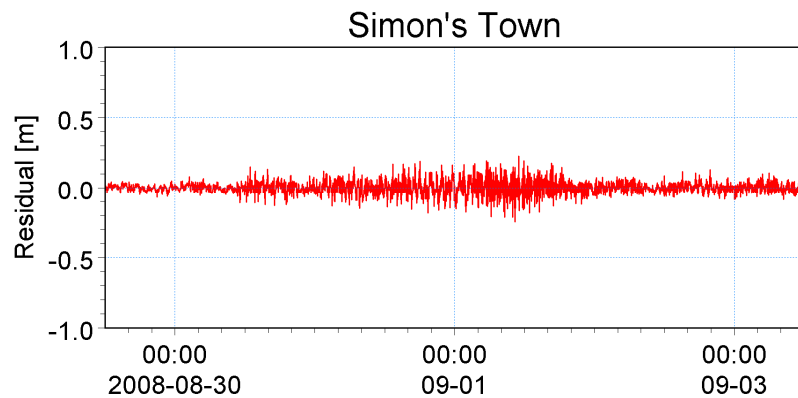
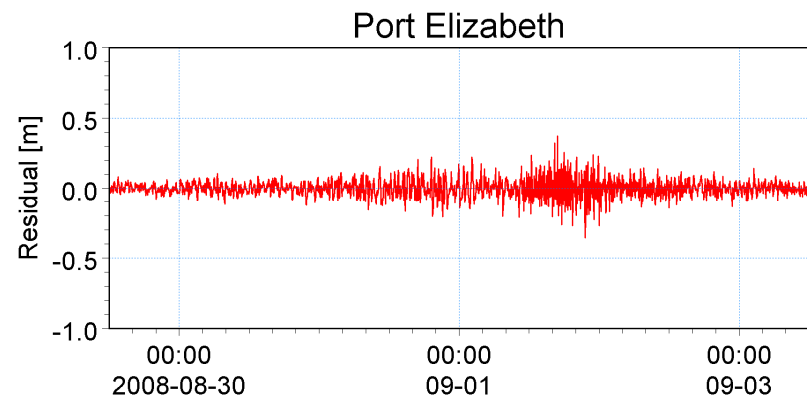
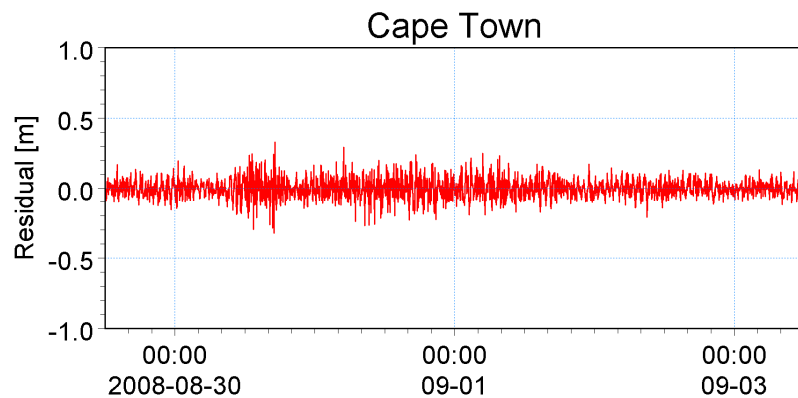
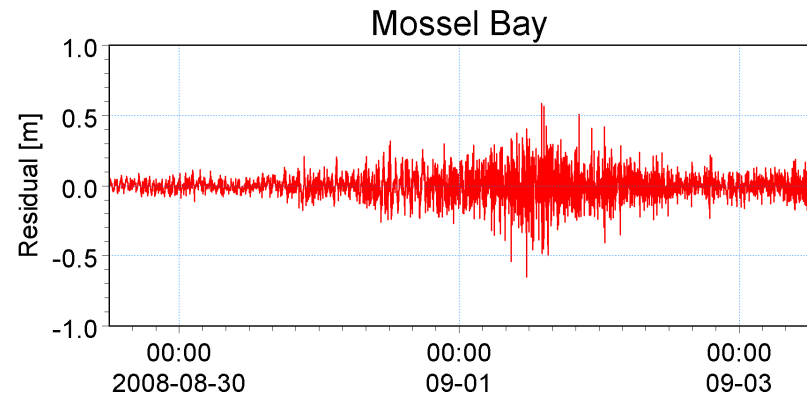
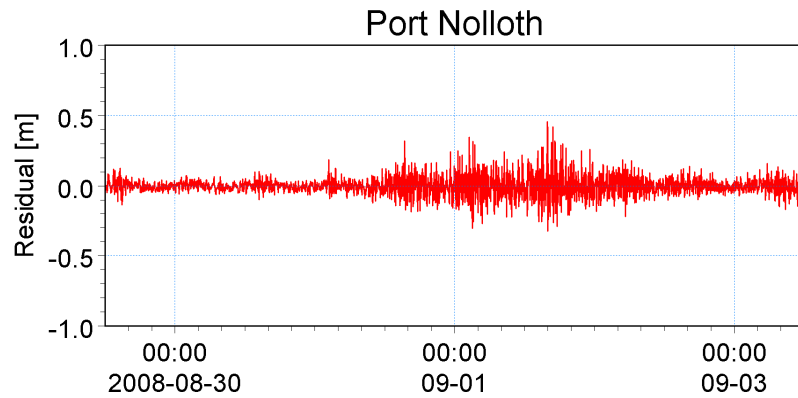


Title:

**Comparison of residual values for a meteo-tsunami event
for 5 SANHO tide gauge sites around South Africa**

Figure No.

4.4



X:\PRDW Projects\Current\SA (1010) Nuclear Sites
SSRs\Working\Engineers\RLH\Meteotsunami\Data\Sites\ResidualComparison080831t.png

X:\PRDW Projects\Current\SA (1010) Nuclear Sites
SSRs\Working\Engineers\RLH\Meteotsunami\Data\Sites\ResidualComparison080831rt.png

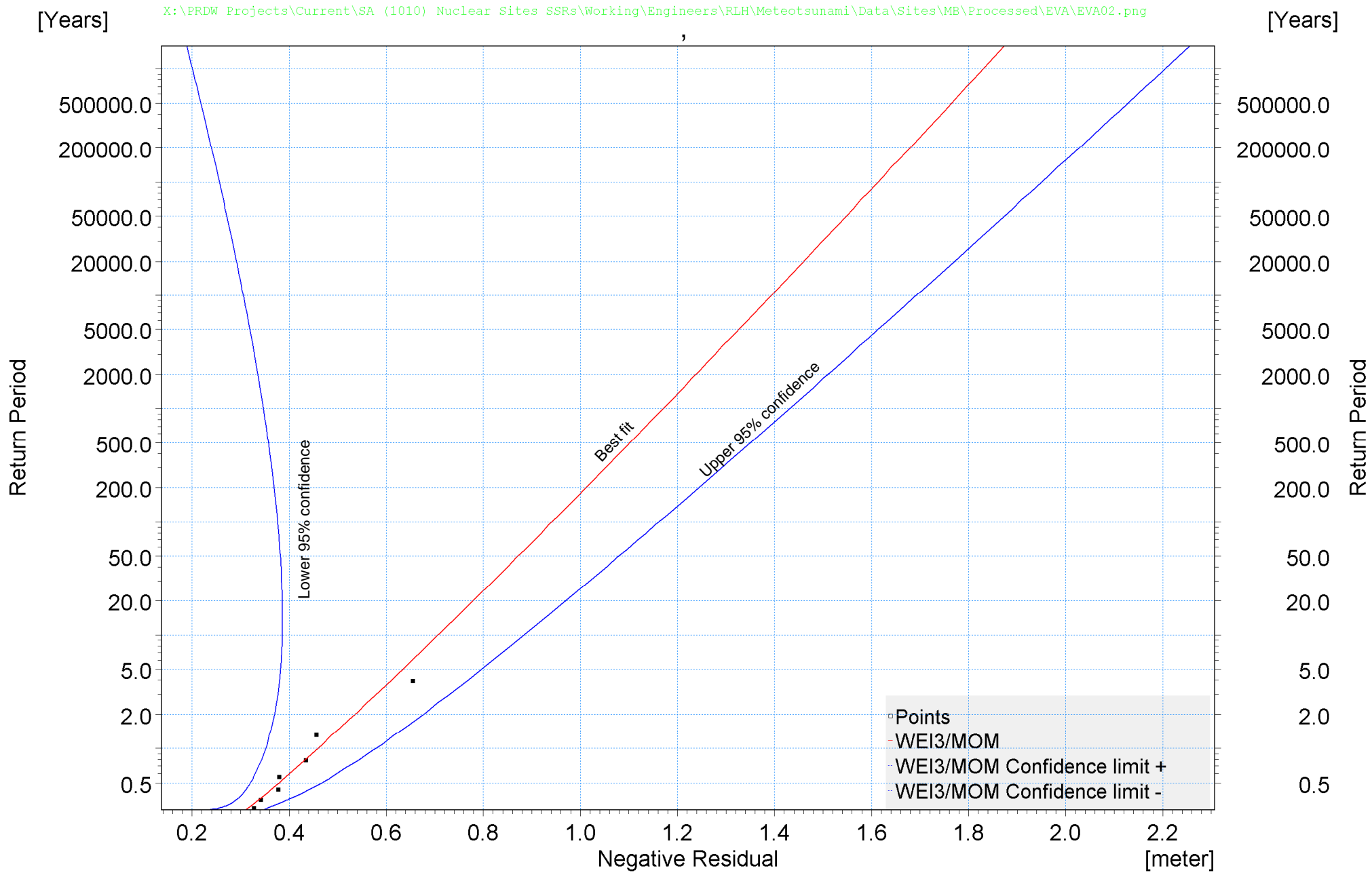


Title:

**Comparison of residual values for a bound long wave event
for 5 SANHO tide gauge sites around South Africa**

Figure No.

4.5

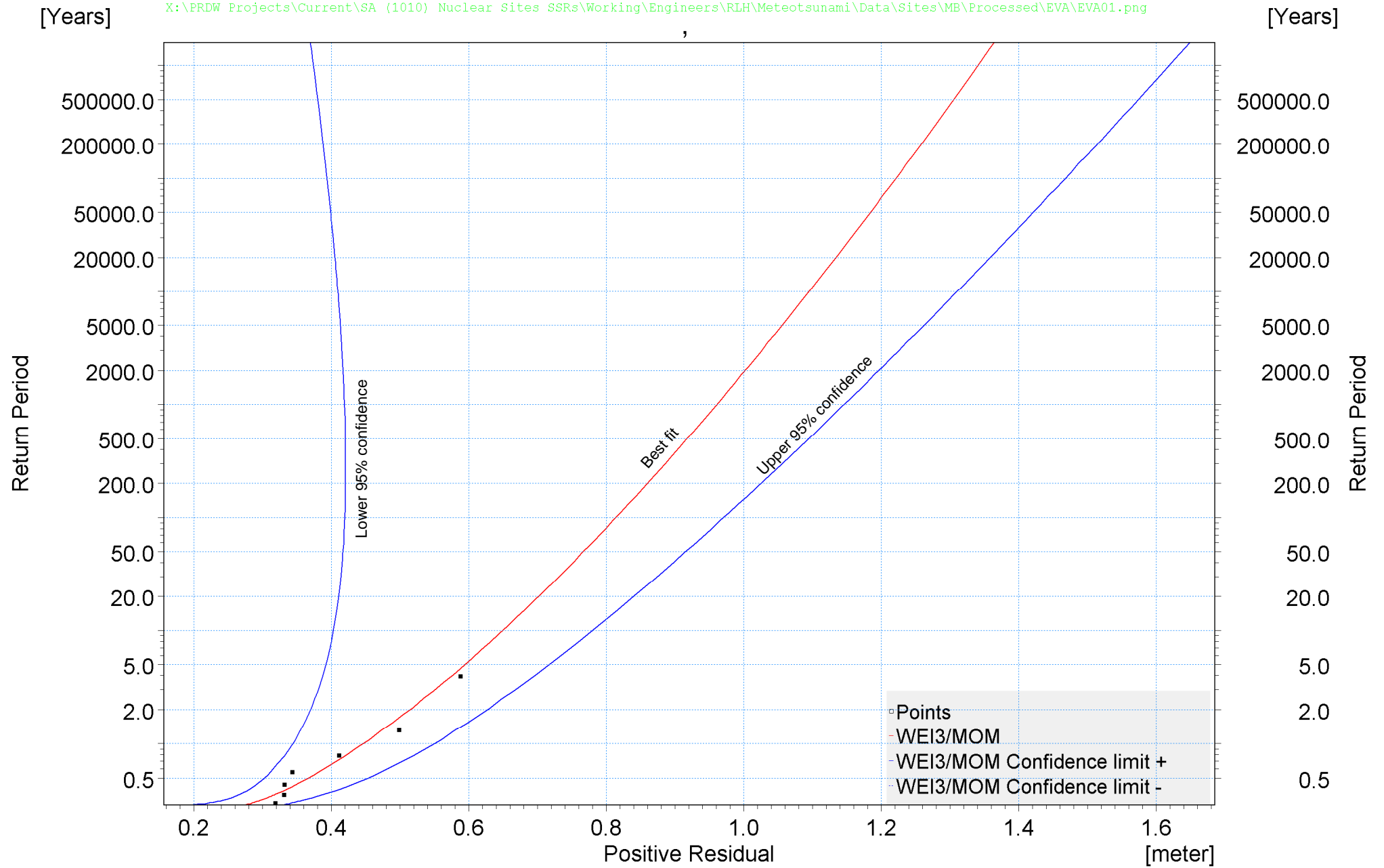


Title:

Extreme value analysis of negative long wave residuals at Mossel Bay

Figure No.

4.6

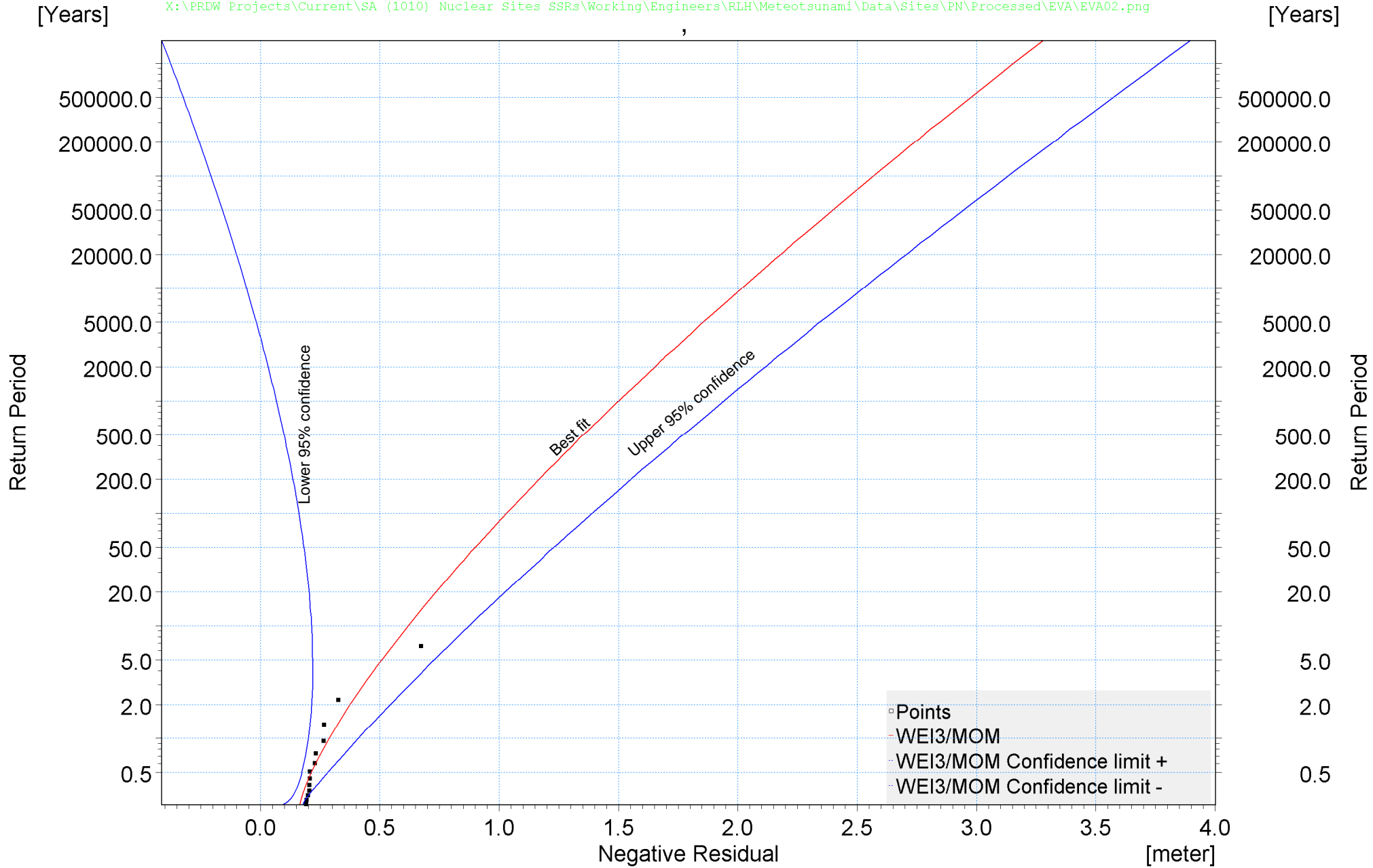


Title:

Extreme value analysis of positive long wave residuals at Mossel Bay

Figure No.

4.7

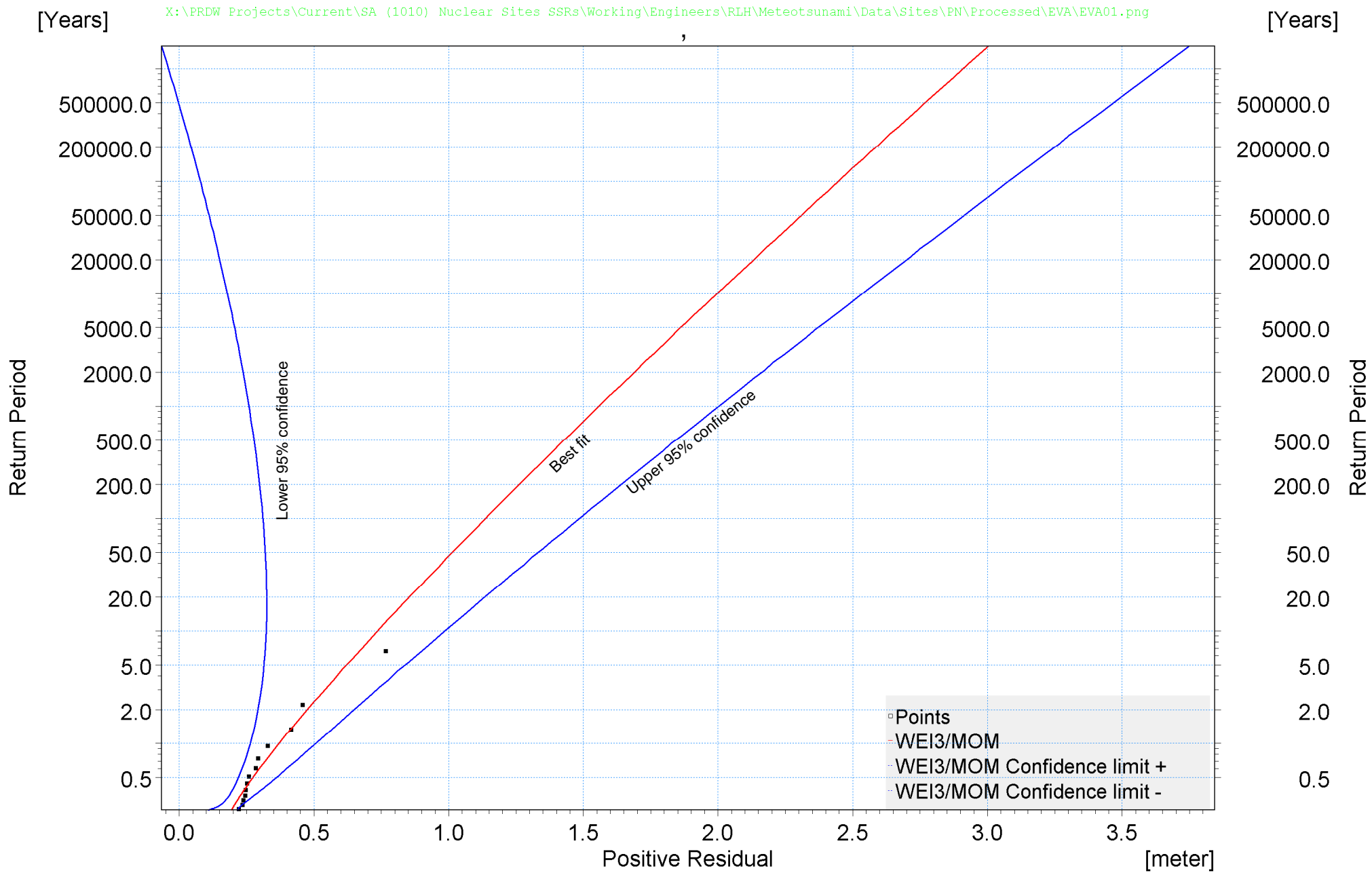


Title:

Extreme value analysis of negative long wave residuals at Port Nolloth

Figure No.

4.8

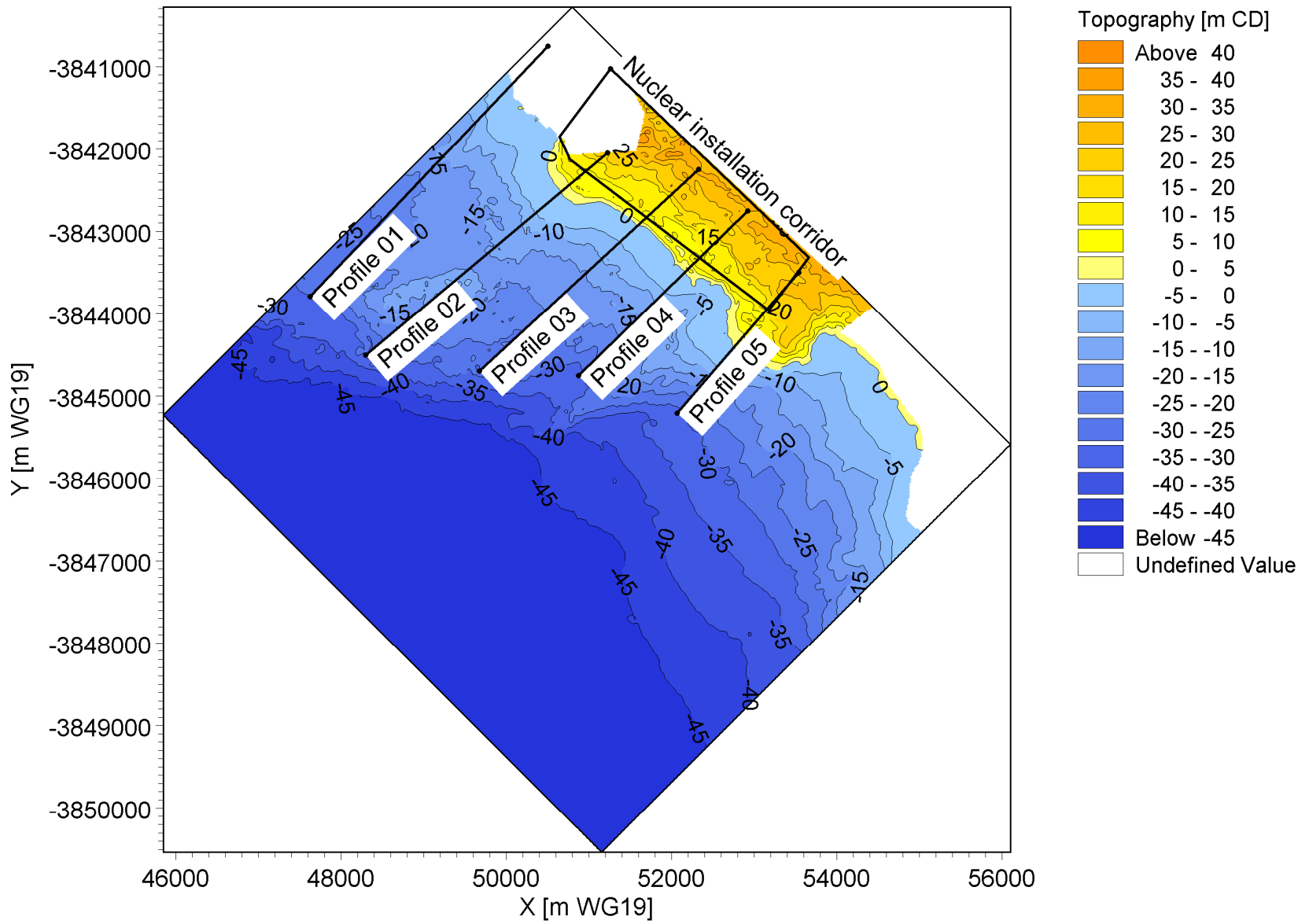


Title:

Extreme value analysis of positive long wave residuals at Port Nolloth

Figure No.

4.9



X:\PRDW Projects\Current\SA (1010) Nuclear Sites
 SSRs\Working\Engineers\RLH\CoastalEngineeringModelling\Bantamsklip\Data\Bathy\Bantamsklip_WG19_CD_AutoCad_Blanked.png



Title:

Run-up calculations: Plan view of profiles used

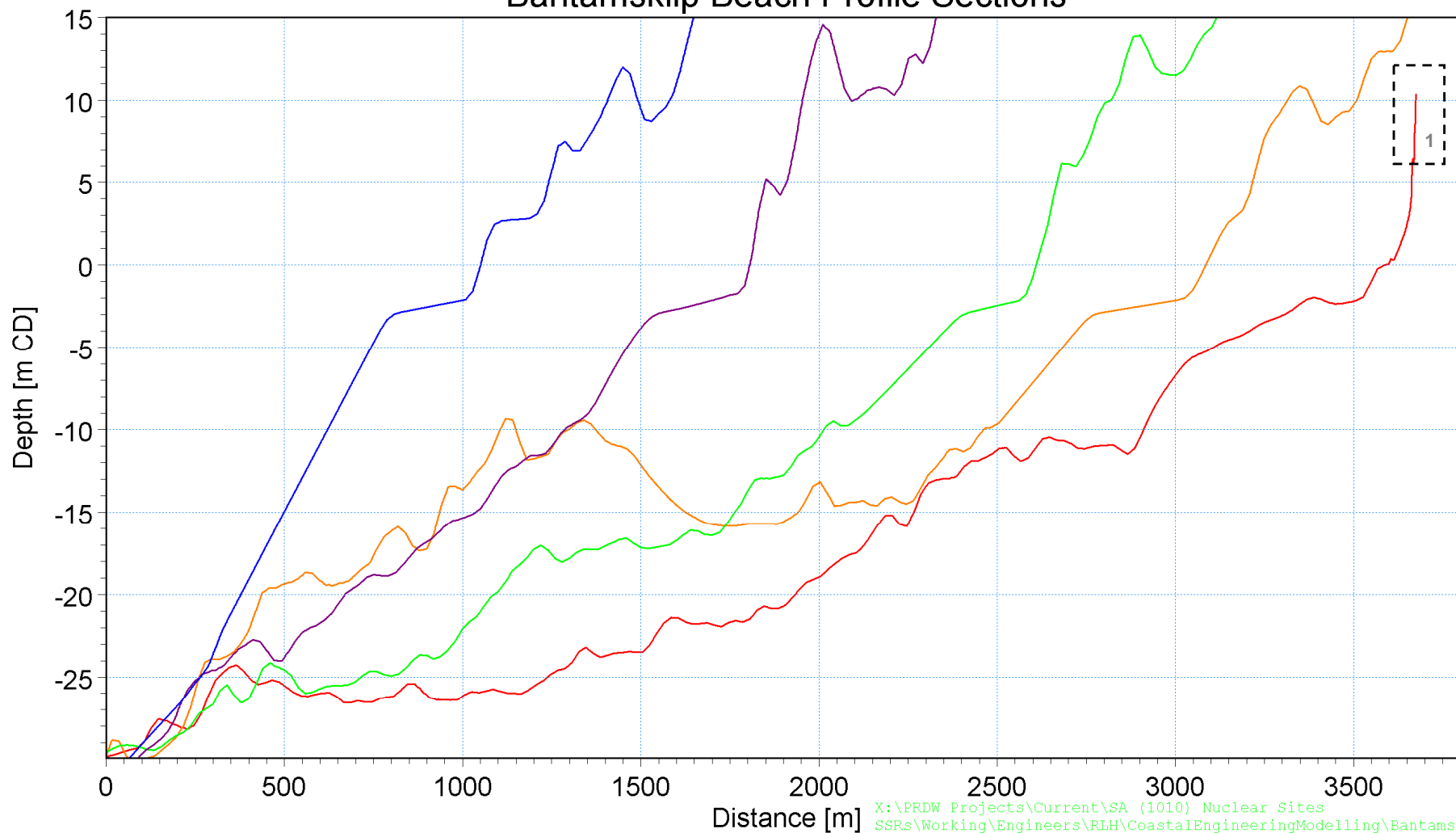
Figure No.

4.10

Profile01 [m] —
 Profile02 [m] —
 Profile03 [m] —
 Profile04 [m] —
 Profile05 [m] —

Notes: 1. Profile01 extrapolated from 5 m CD due to lack of survey data

Bantamsklip Beach Profile Sections



01/01/00 00:00:00:000

X:\PRDW Projects\Current\SA (1010) Nuclear Sites
 SSRs\Working\Engineers\RLH\CoastalEngineeringModelling\Bantamskl
 ip\Data\RunUpProfiles\Profiles.png

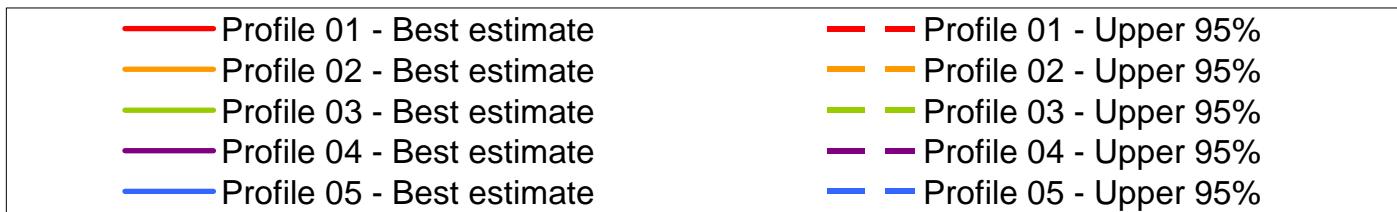
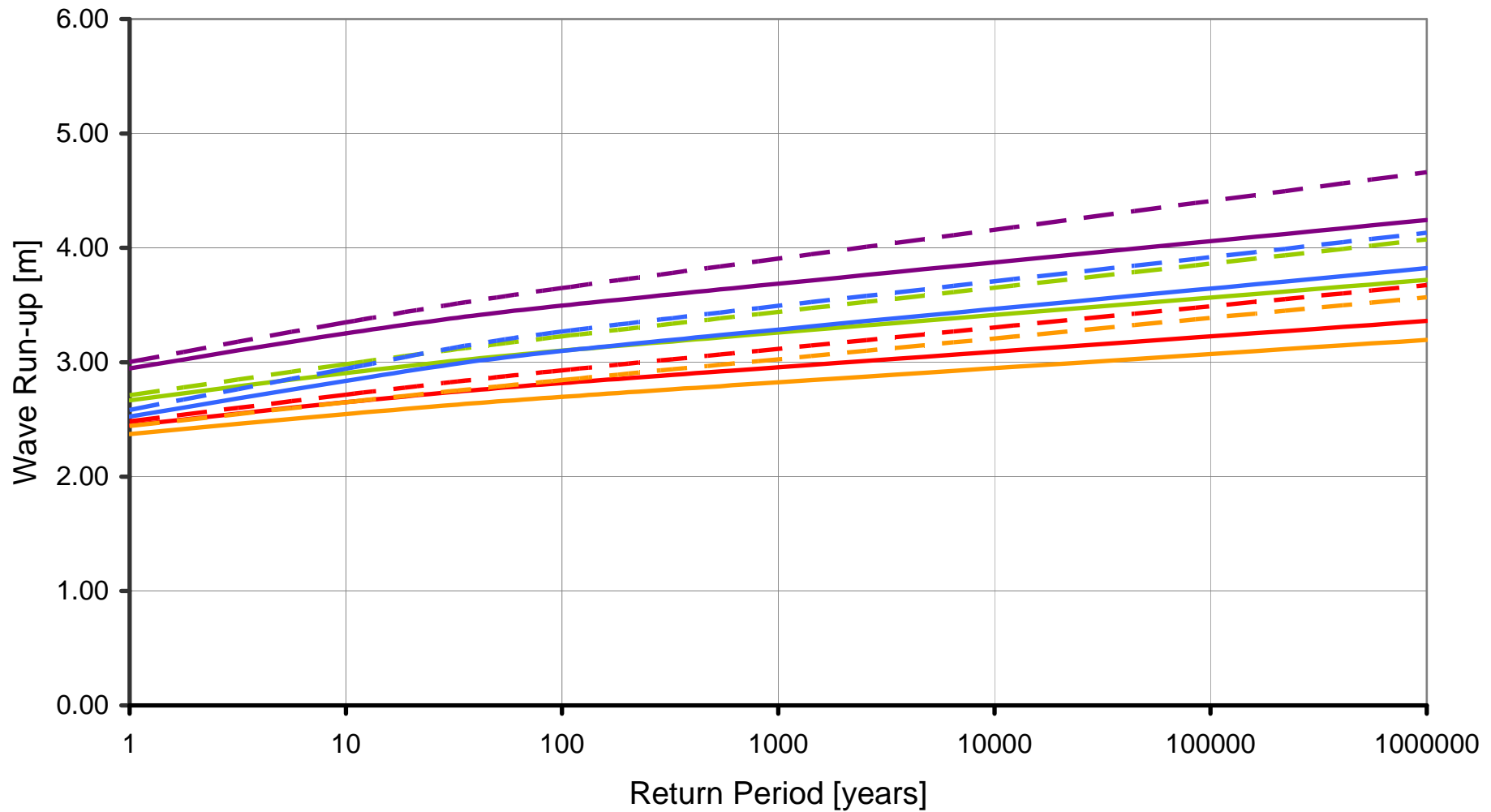


Title:

Selected coastline profiles for run-up calculations

Figure No.

4.11

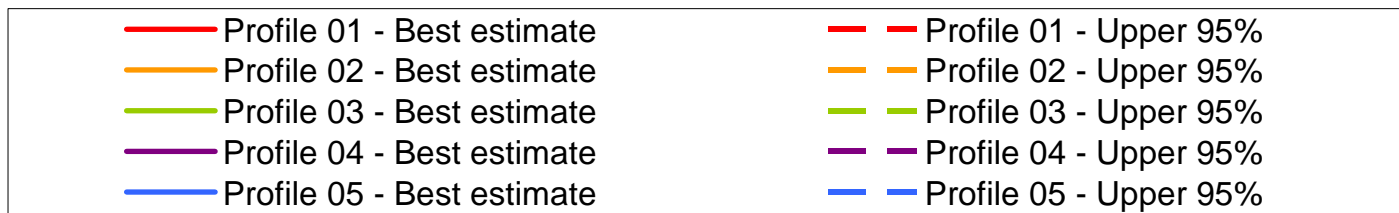
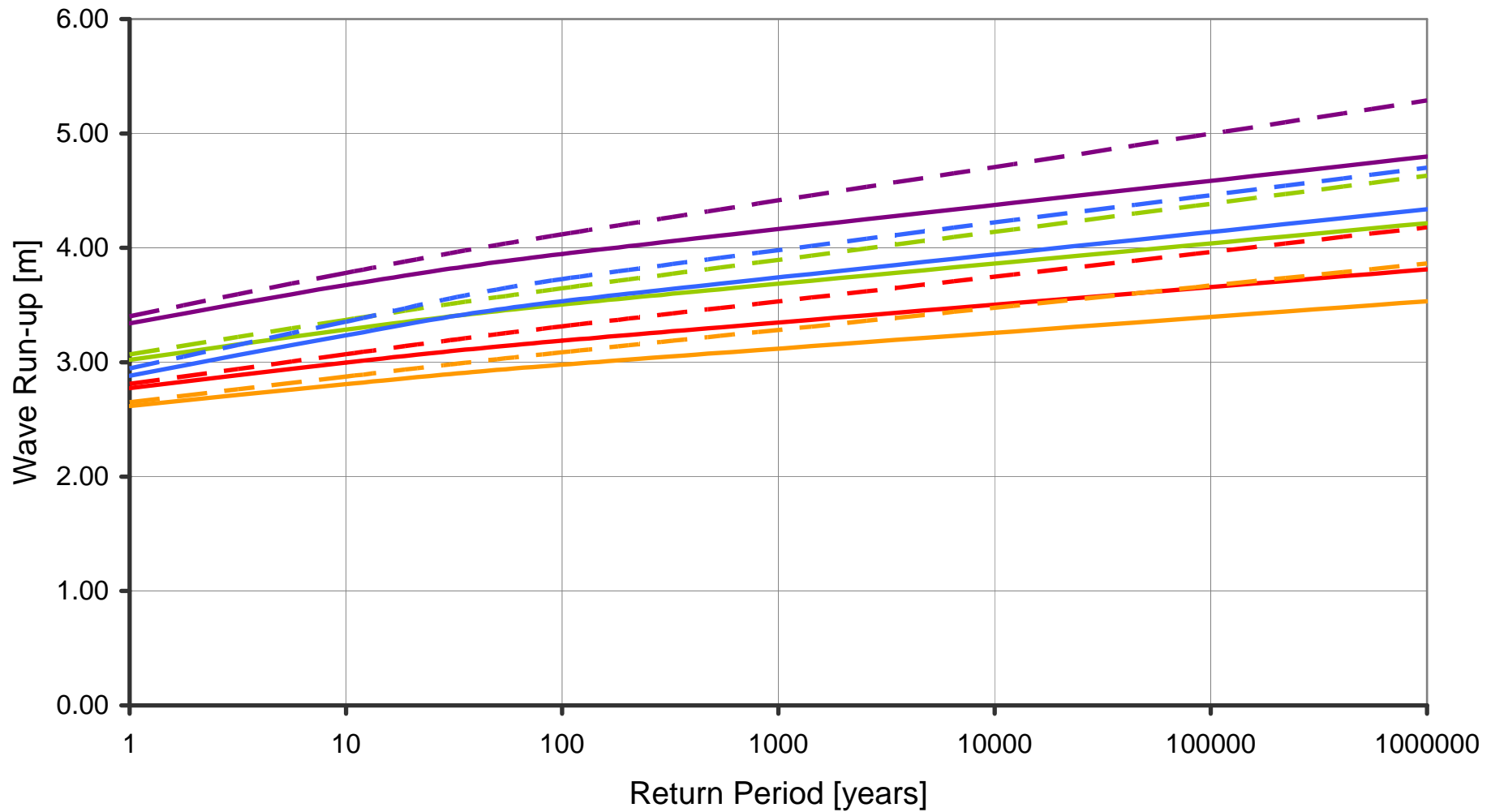


Title:

**Extreme high water level beach run-up -
Excluding climate change**

Figure No.

4.12



Title:

**Extreme high water level beach run-up -
Including climate change**

Figure No.

4.13



Due to damage to buoy lines holding the plates, limited information available as plates were recovered from the sea bed.

Backing plates are PVC with dimensions approximately 20 cm x 50 cm. Water depth is 10 m.

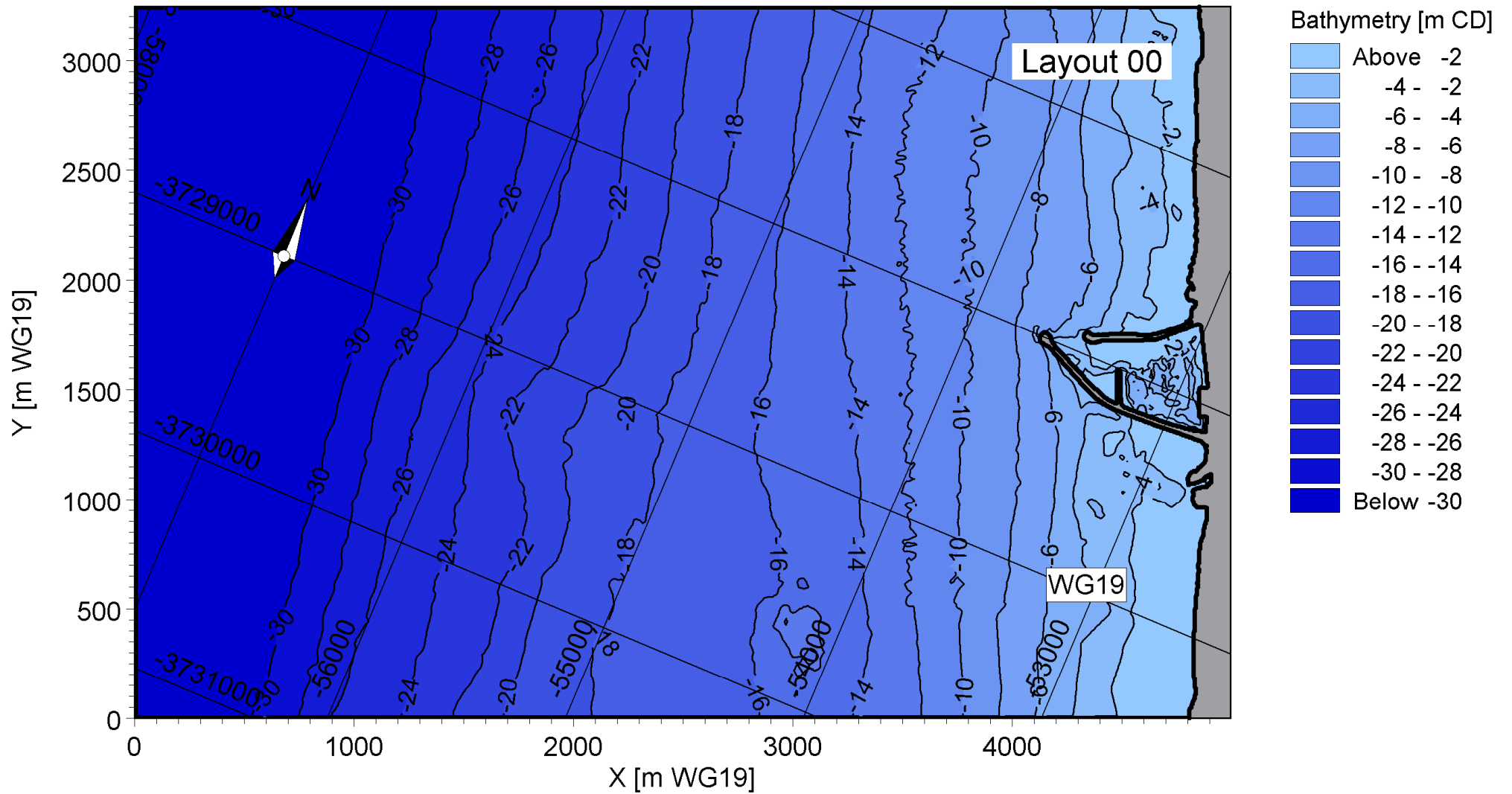


Title:

Biofouling plates recovered from Bantamsklip

Figure No.

5.1

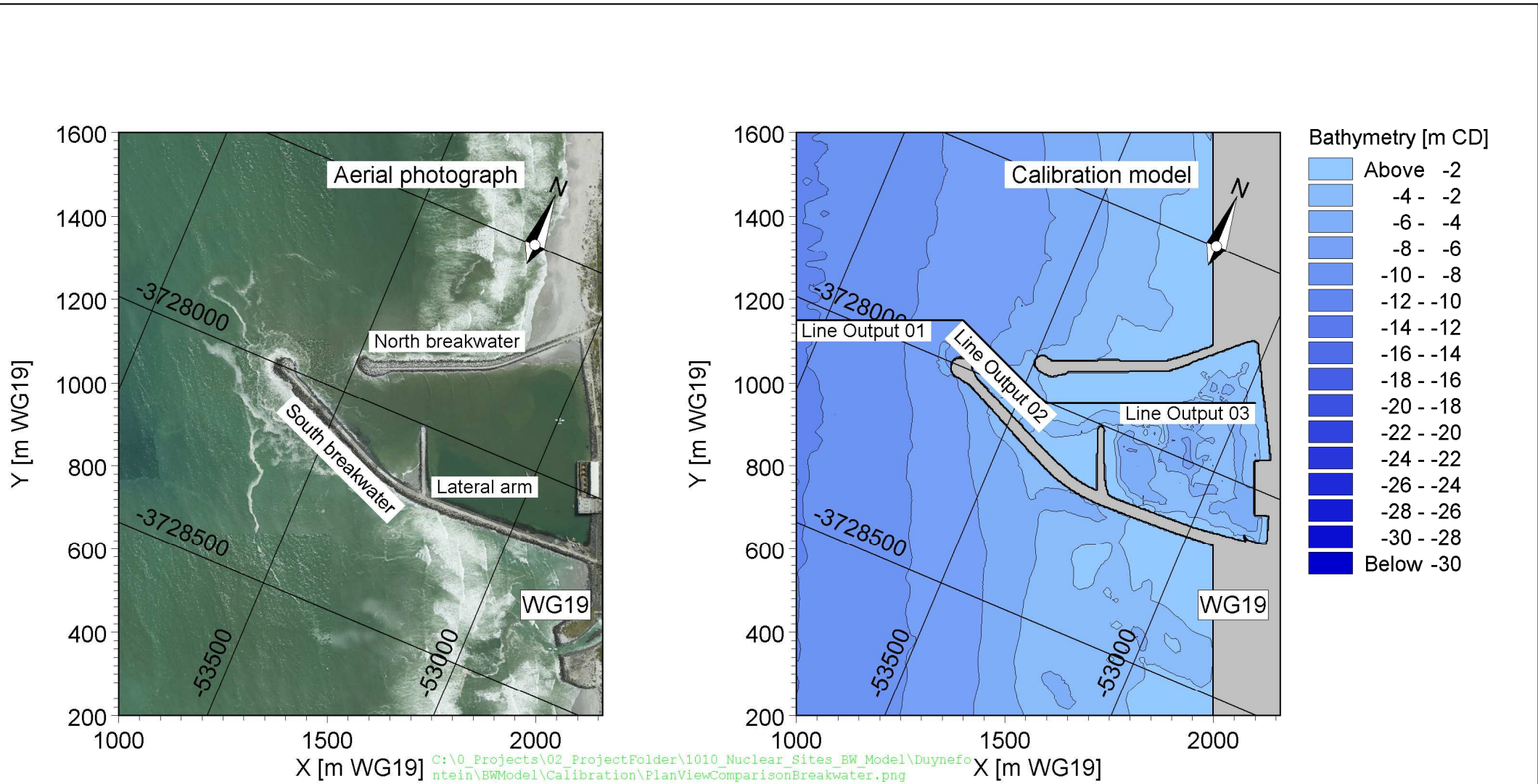


C:\0_Projects\02_ProjectFolder\1010_Nuclear_Sites_BW_Model\Duynefontein\BWModel\ProductionRuns\Layout00\Data\Bathy\00_hd_PR.png



Title: Calibration of Boussinesq Wave modelling using existing Koeberg installation:
Bathymetry and model layout

Figure No.
6.1

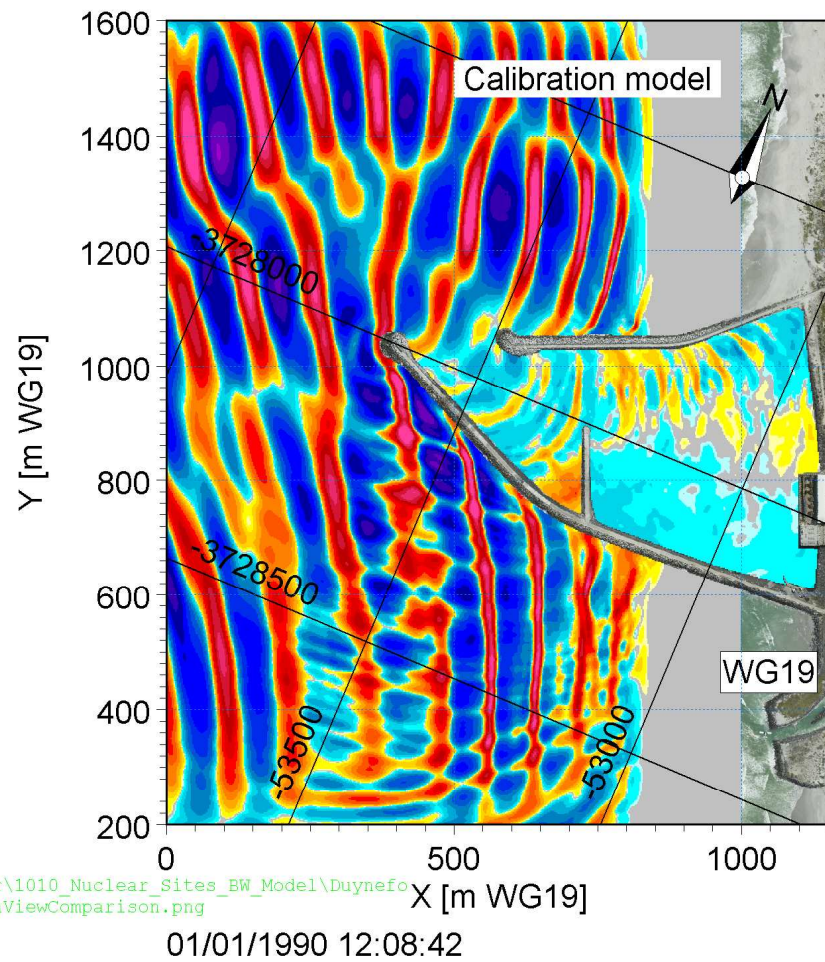
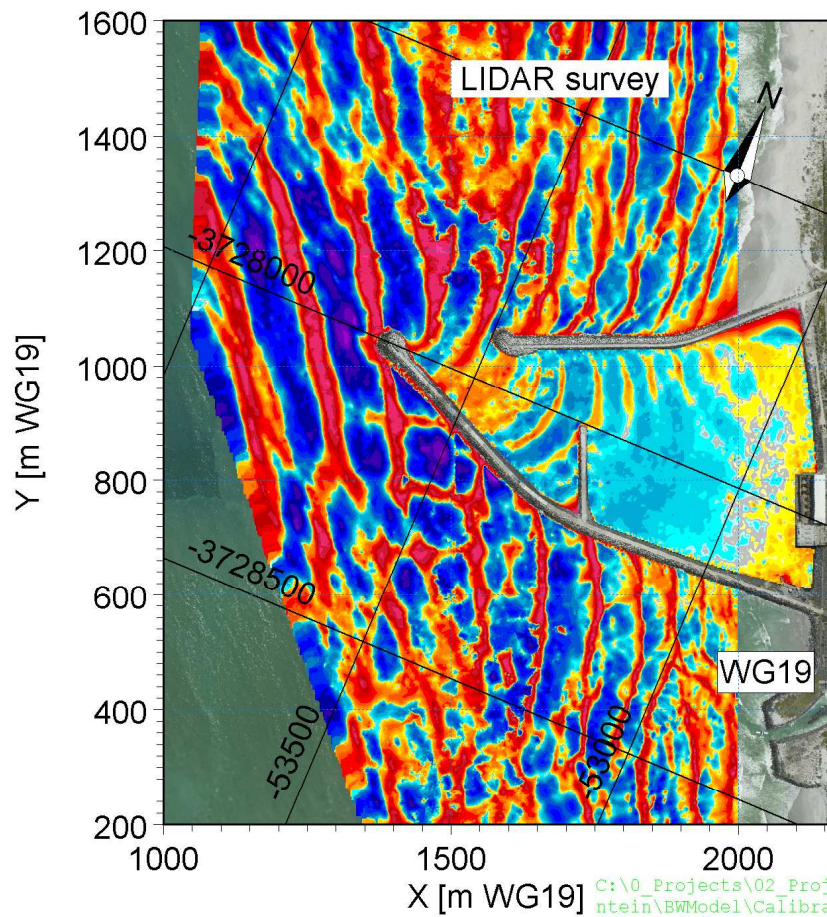


Title:

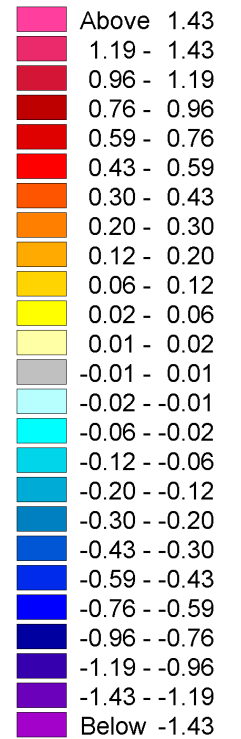
**Calibration of Boussinesq Wave modelling using existing Koeberg installation:
Settling basin main components (left) and position of calibration outputs (right)**

Figure No.

6.2



Water Surface (SWL)
(meter)

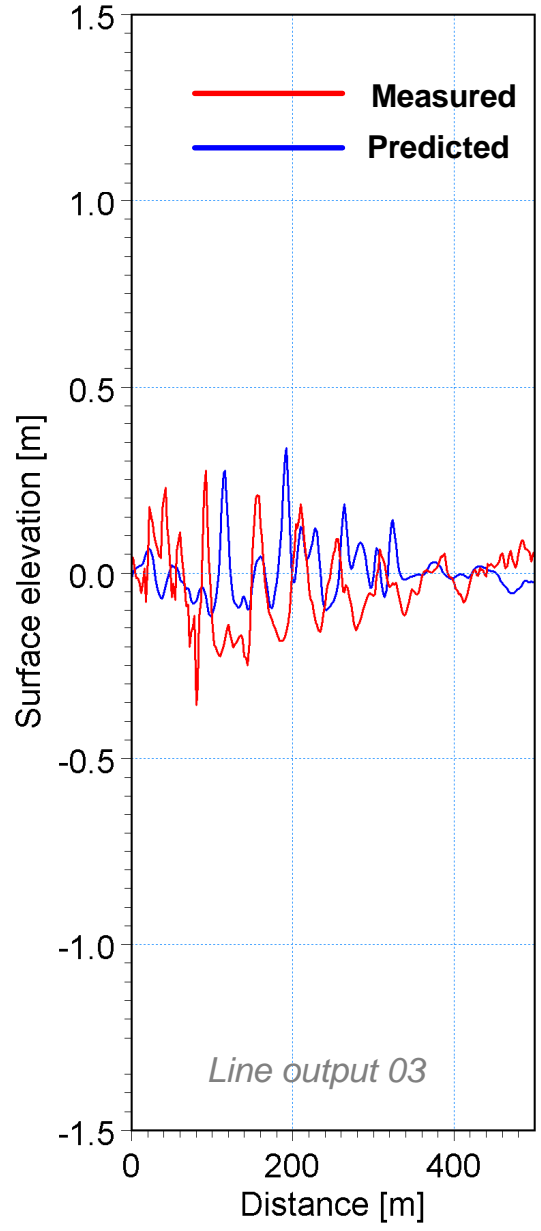
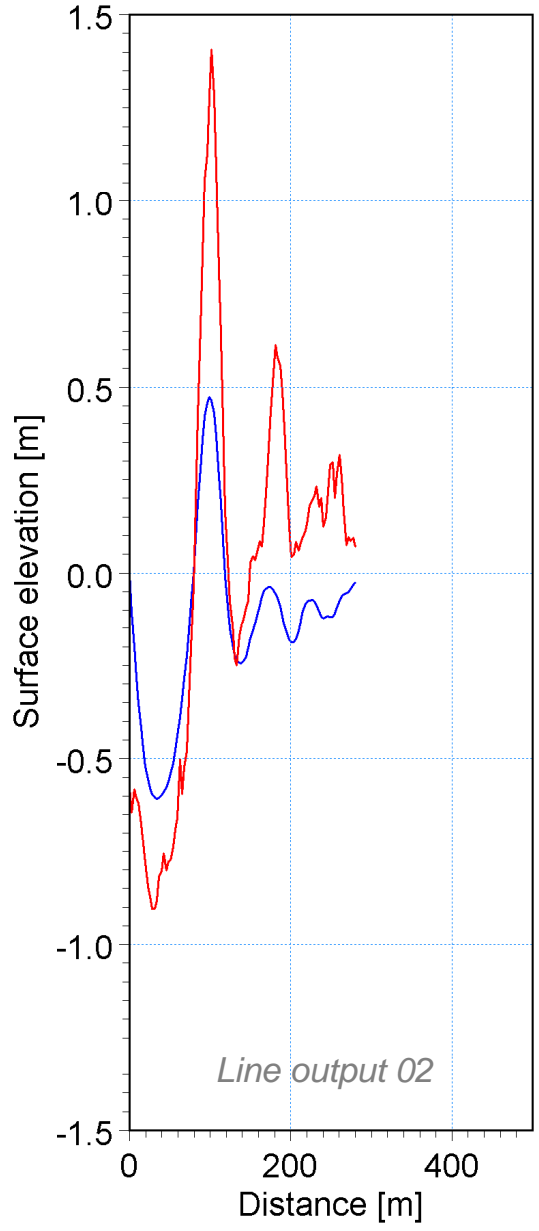
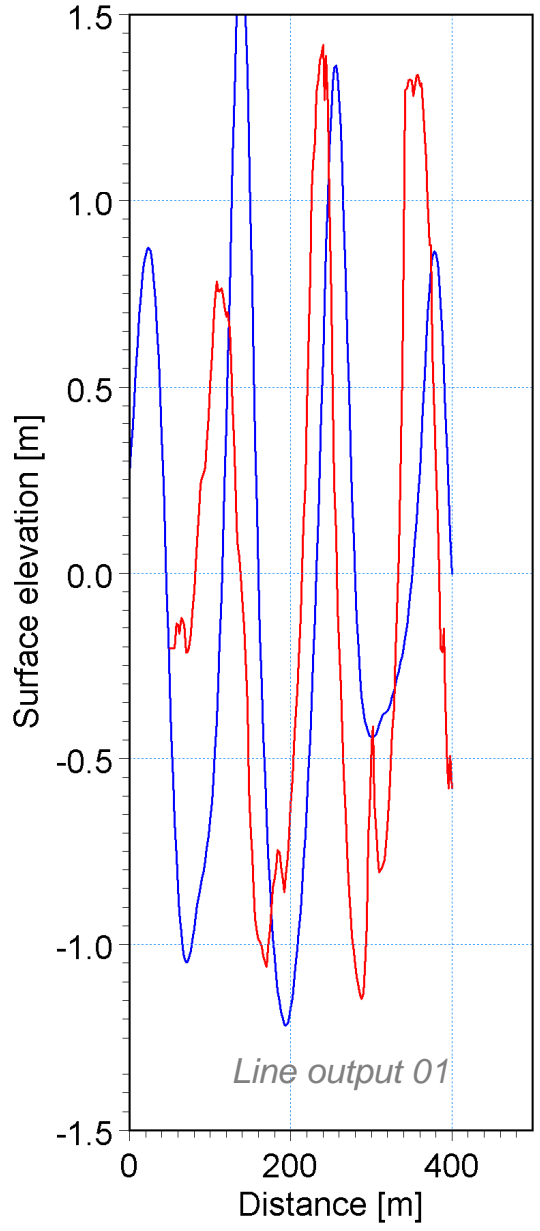


Title:

**Calibration of Boussinesq Wave modelling using existing Koeberg installation:
Comparison of surface elevation - LIDAR survey (left) and BW model run (right)**

Figure No.

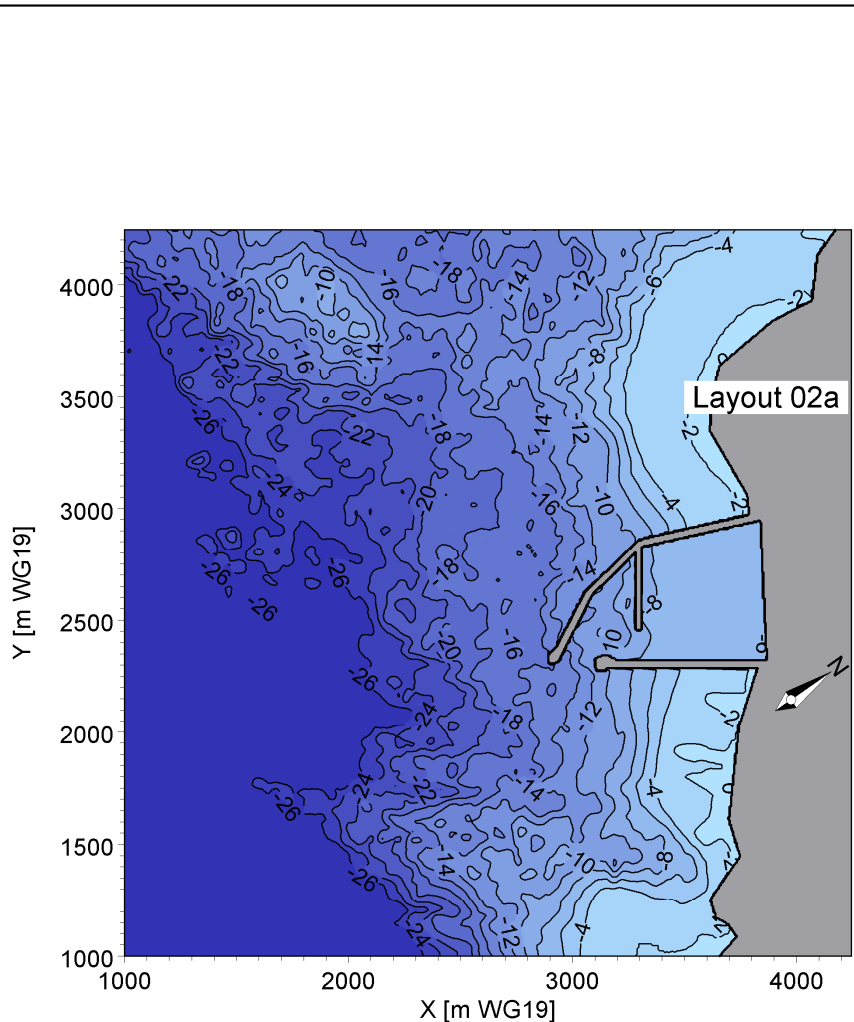
6.3



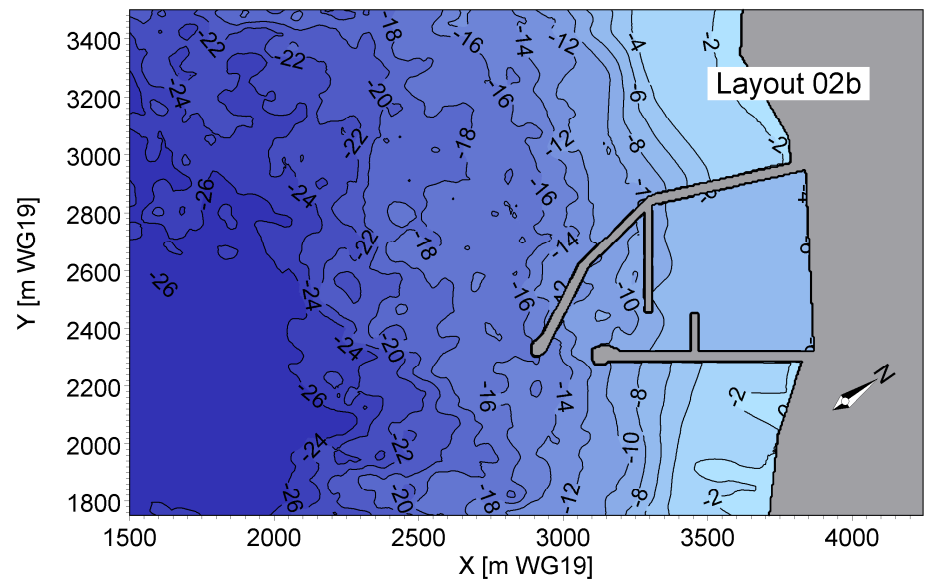
— Measured
— Predicted



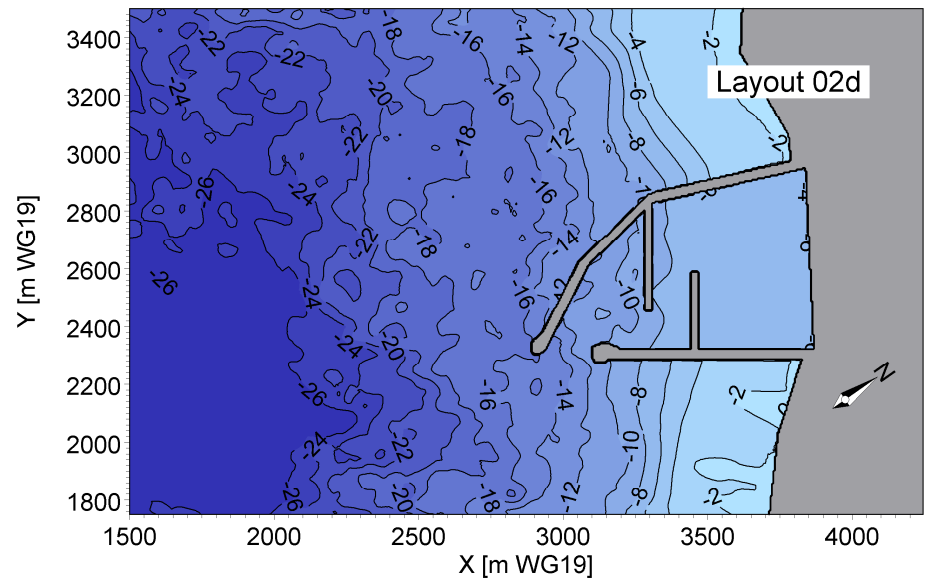
Title: Calibration of Boussinesq Wave modelling using existing Koeberg installation:
Comparison of surface elevation - Line output profiles (Refer to Figure 6.2)



C:\0_Projects\02_ProjectFolder\1010_Nuclear_Sites_BW_Model\Bantamsklip\BWModel\ProductionRuns\Layout02a\Data\Bathy\PR_Layout02a.png



C:\0_Projects\02_ProjectFolder\1010_Nuclear_Sites_BW_Model\Bantamsklip\BWModel\ProductionRuns\Layout02b\Data\Bathy\PR_Layout02b.png



C:\0_Projects\02_ProjectFolder\1010_Nuclear_Sites_BW_Model\Bantamsklip\BWModel\ProductionRuns\Layout02d\Data\Bathy\PR_Layout02d.png

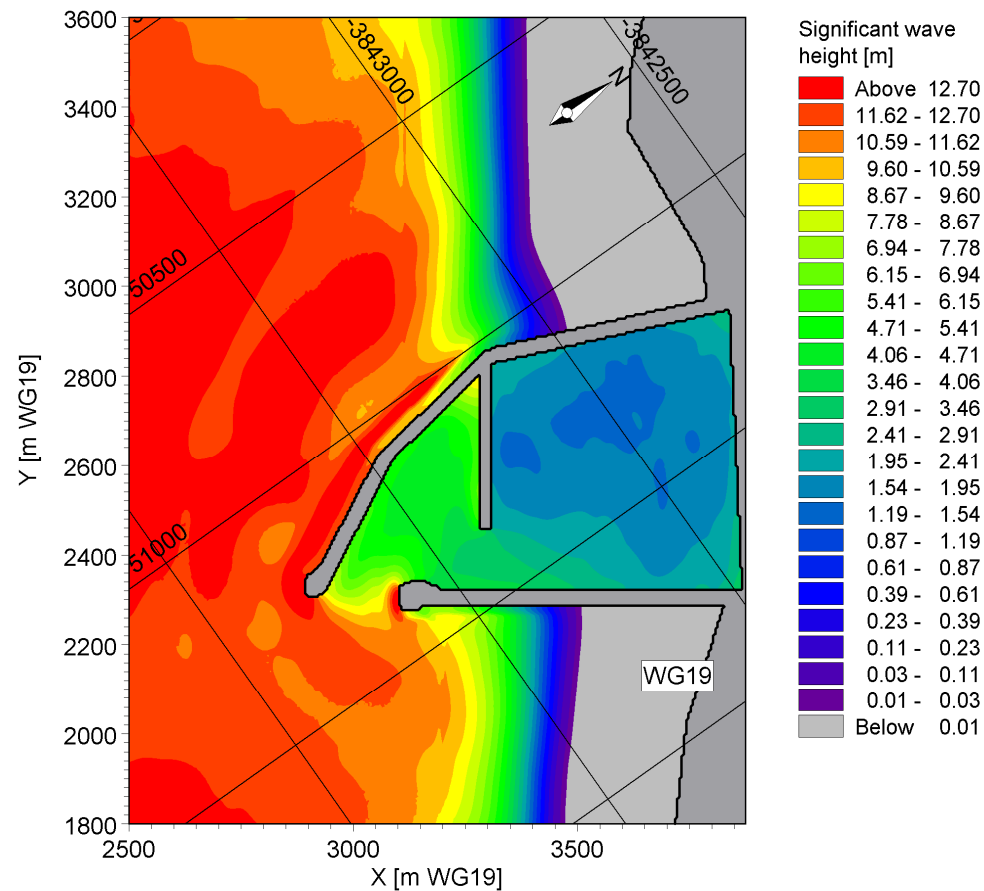
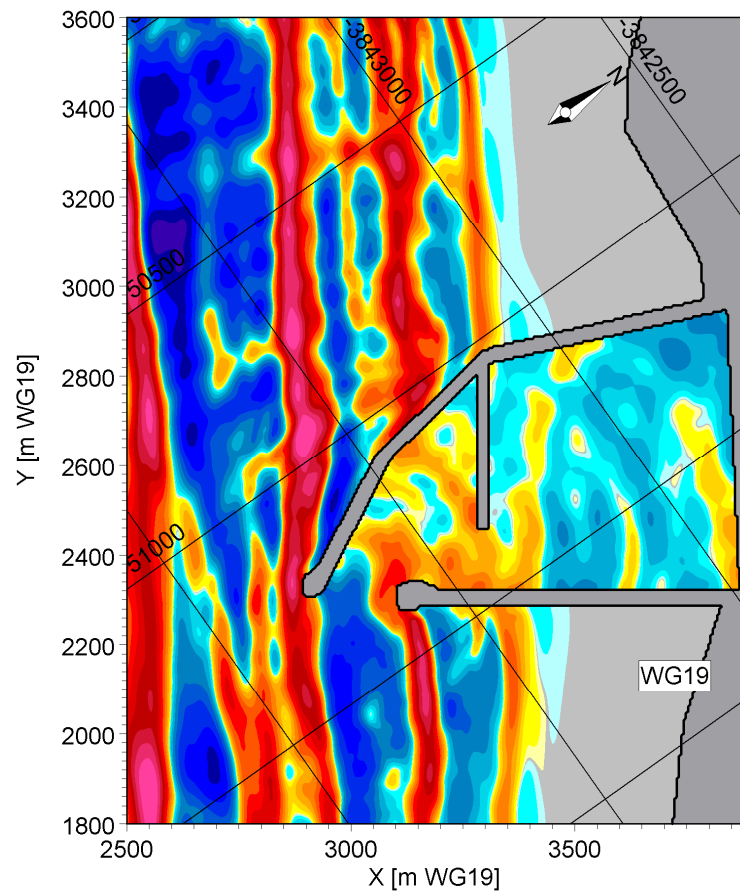


Title:

**Boussinesq Wave modelling Bantamsklip basin layout:
Bathymetry and model orientation**

Figure No.

6.5



01/01/1990 12:40:00 C:\0_Projects\02_ProjectFolder\1010_Nuclear_Sites_BW_Model\Bantamskip\BWMo
 1\ProductionRuns\Layout02a\TR1E6\21.bw - Result Files\Deterministic.Plan.png

01/01/1990 12:40:00 C:\0_Projects\02_ProjectFolder\1010_Nuclear_Sites_BW_Model\Bantamskip\BWMo
 1\ProductionRuns\Layout02a\TR1E6\21.bw - Result Files\PhaseAveraged.Plan.png

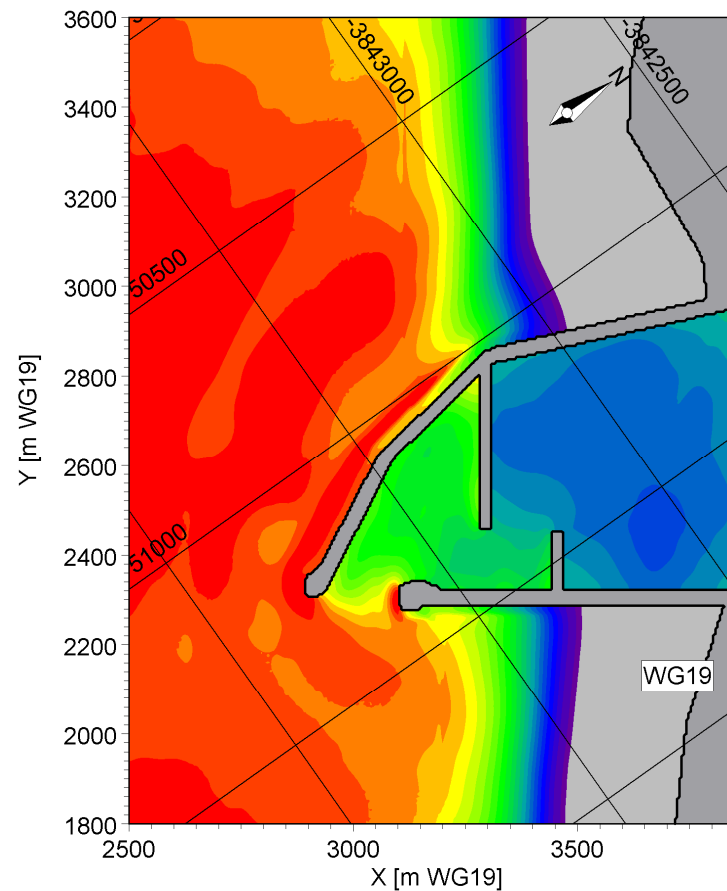
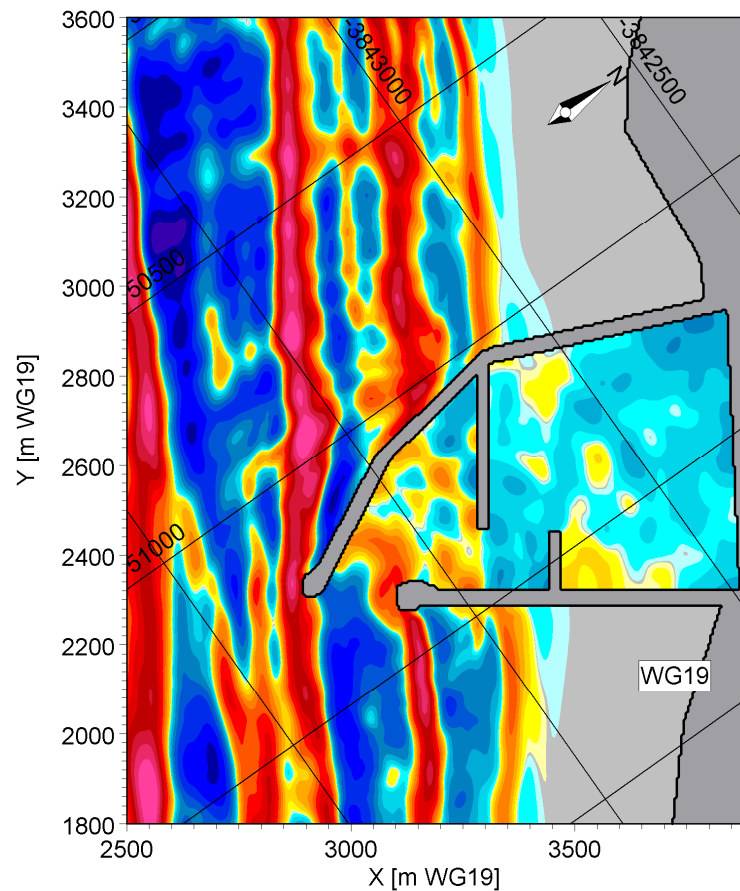


Title:

Boussinesq Wave modelling proposed basin (Layout 02a) results: $H_{m0} = 15.6$ m, $T_p = 24.4$ s
Instantaneous surface elevation (left) Significant wave height (right)

Figure No.

6.6



01/01/1990 12:40:00 C:\0_Projects\02_ProjectFolder\1010_Nuclear_Sites_EW_Model\Bantamskip\BWMo
 1\ProductionRuns\Layout02b\TR1E6\21.bw - Result Files\Deterministic.Plan.png

01/01/1990 12:40:00 C:\0_Projects\02_ProjectFolder\1010_Nuclear_Sites_EW_Model\Bantamskip\BWMo
 1\ProductionRuns\Layout02b\TR1E6\21.bw - Result Files\PhaseAveraged.Plan.png

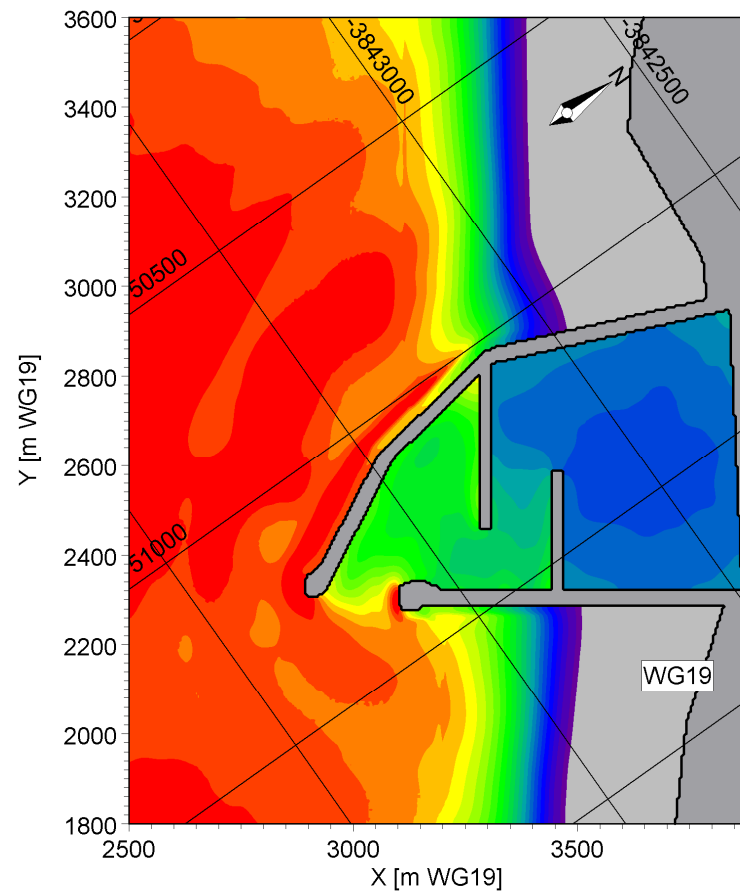
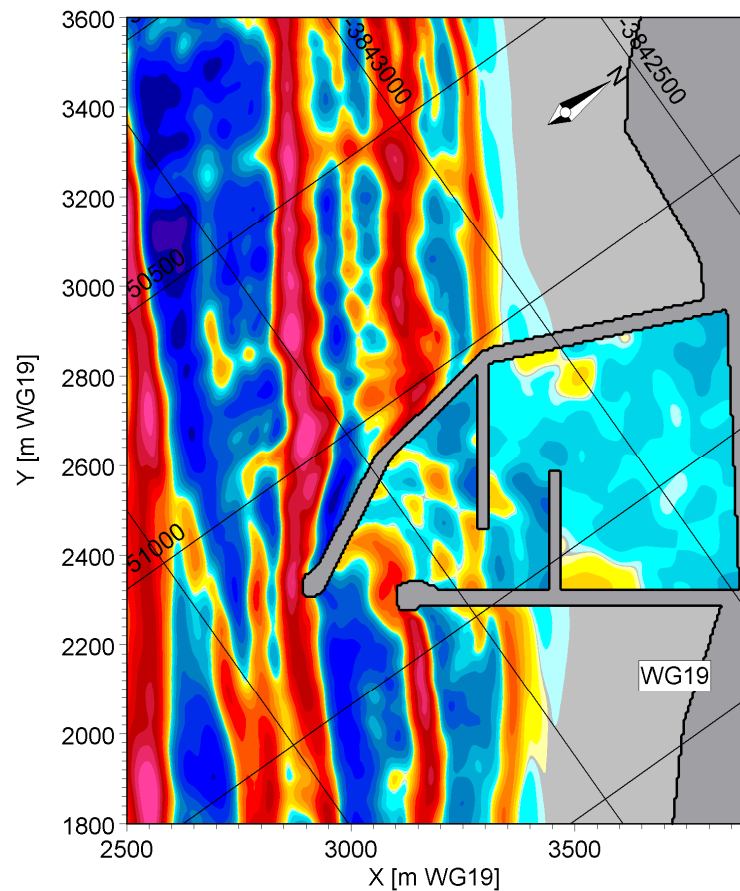


Title:

Boussinesq Wave modelling proposed basin (Layout 02b) results: $H_{m0} = 15.6$ m, $T_p = 24.4$ s
Instantaneous surface elevation (left) Significant wave height (right)

Figure No.

6.7



01/01/1990 12:40:00 C:\0_Projects\02_ProjectFolder\1010_Nuclear_Sites_BW_Model\Bantamskip\BWMo
 1\ProductionRuns\Layout02d\TR1E6\21.bw - Result Files\Deterministic.Plan.png

01/01/1990 12:40:00 C:\0_Projects\02_ProjectFolder\1010_Nuclear_Sites_BW_Model\Bantamskip\BWMo
 1\ProductionRuns\Layout02d\TR1E6\21.bw - Result Files\PhaseAveraged.Plan.png

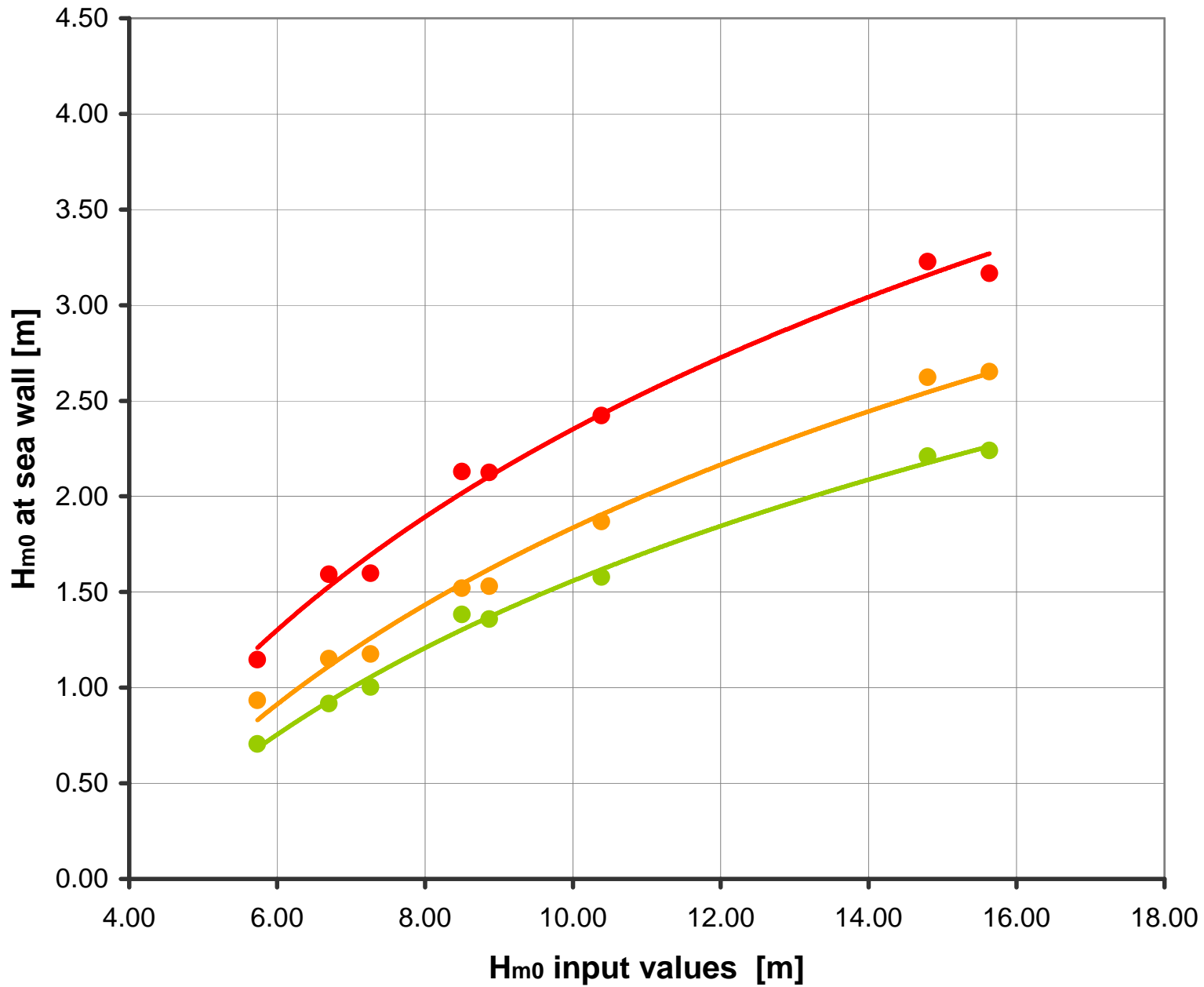


Title:

Boussinesq Wave modelling proposed basin (Layout 02d) results: $H_{m0} = 15.6$ m, $T_p = 24.4$ s
Instantaneous surface elevation (left) Significant wave height (right)

Figure No.

6.8

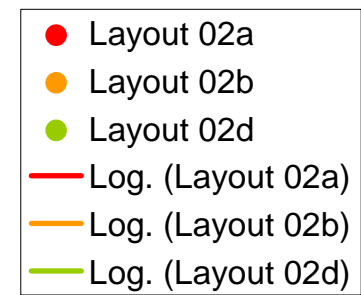
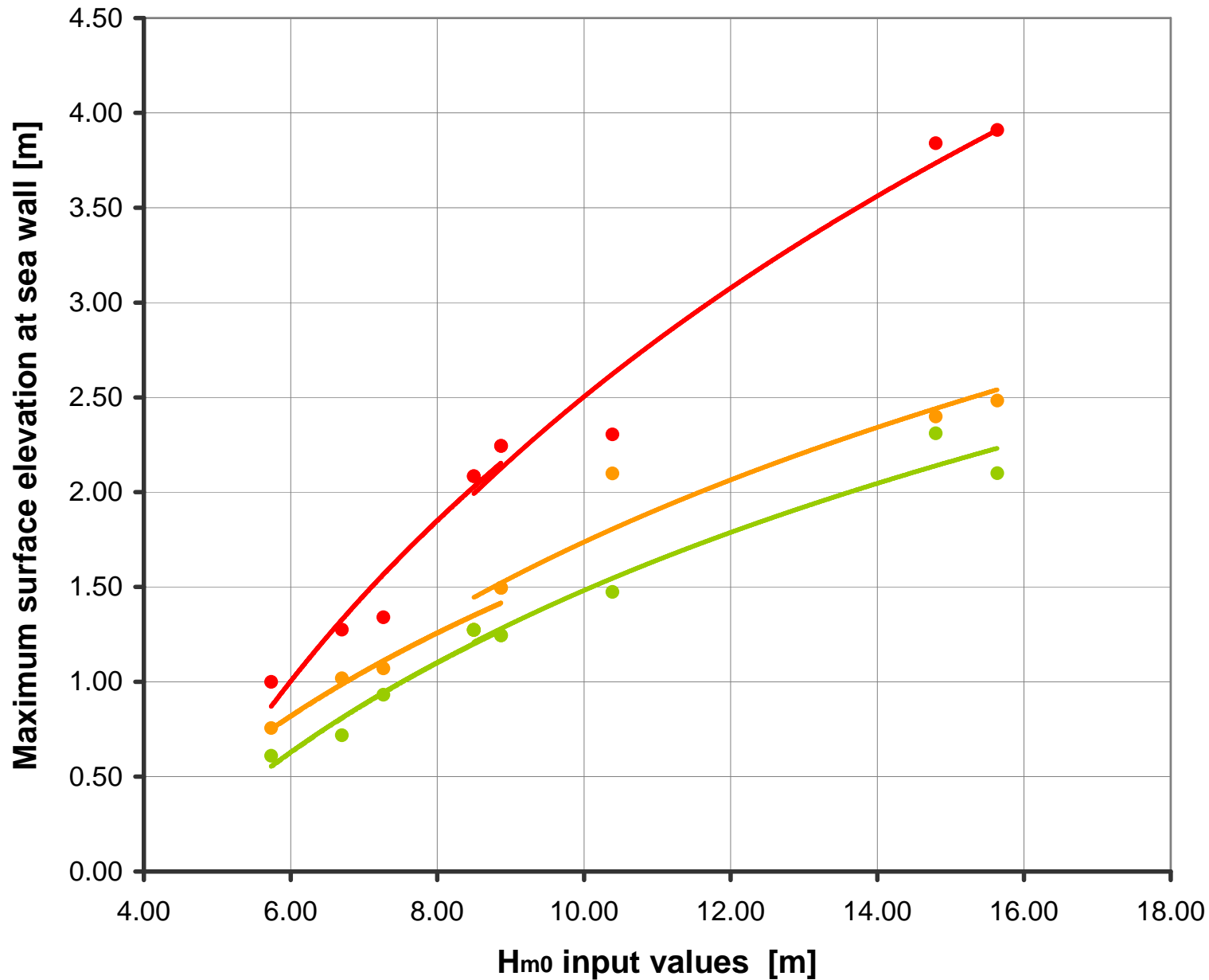


Title:

Logarithmic interpolation of extracted results of H_{m0} along the pump house sea wall as a function of input H_{m0} values from the 95% confidence level

Figure No.

6.9

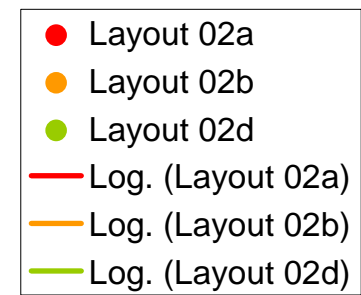
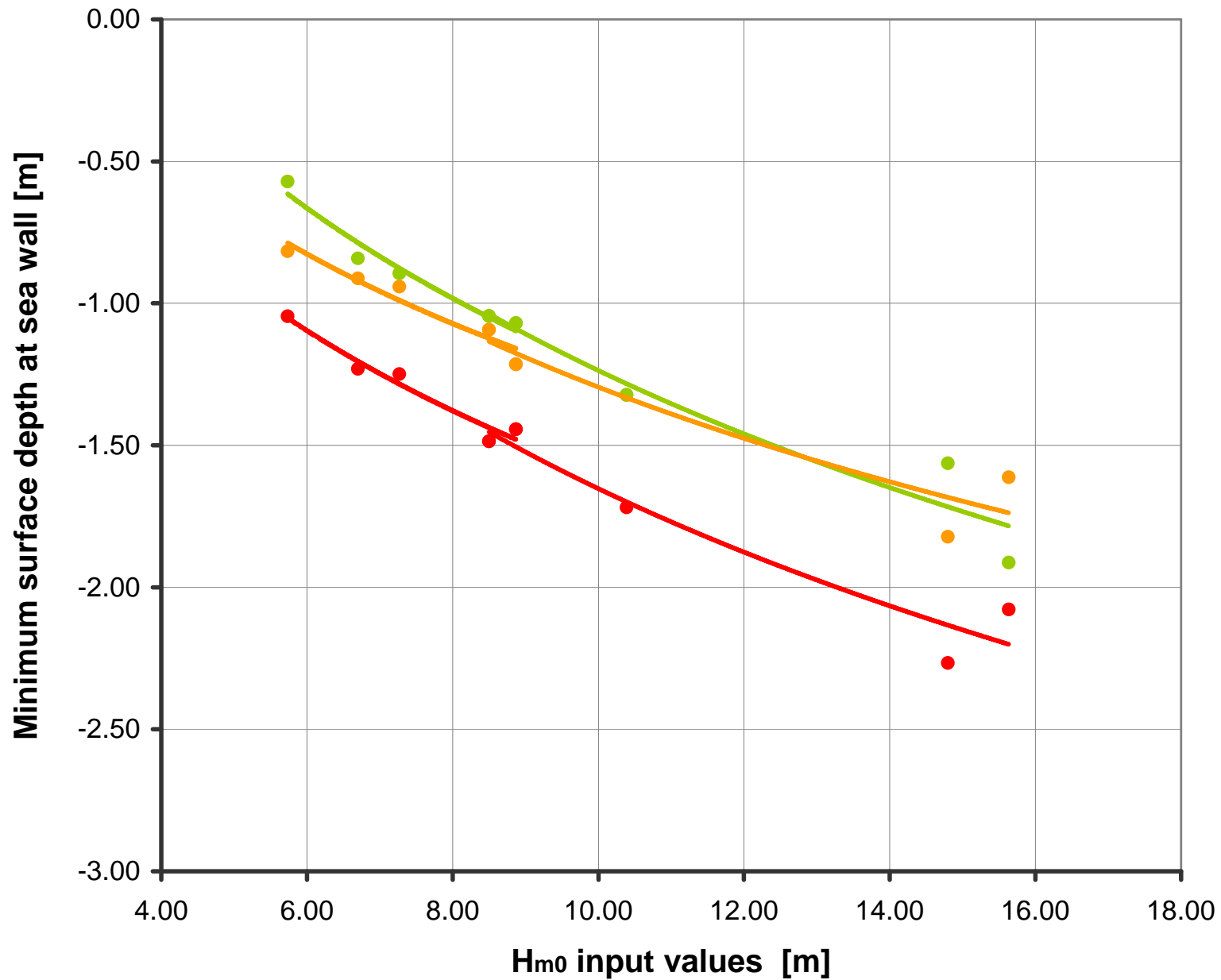


Title:

Logarithmic interpolation of extracted results of maximum surface elevation along the pump house sea wall as a function of input H_{m0} values from the 95% confidence level

Figure No.

6.10

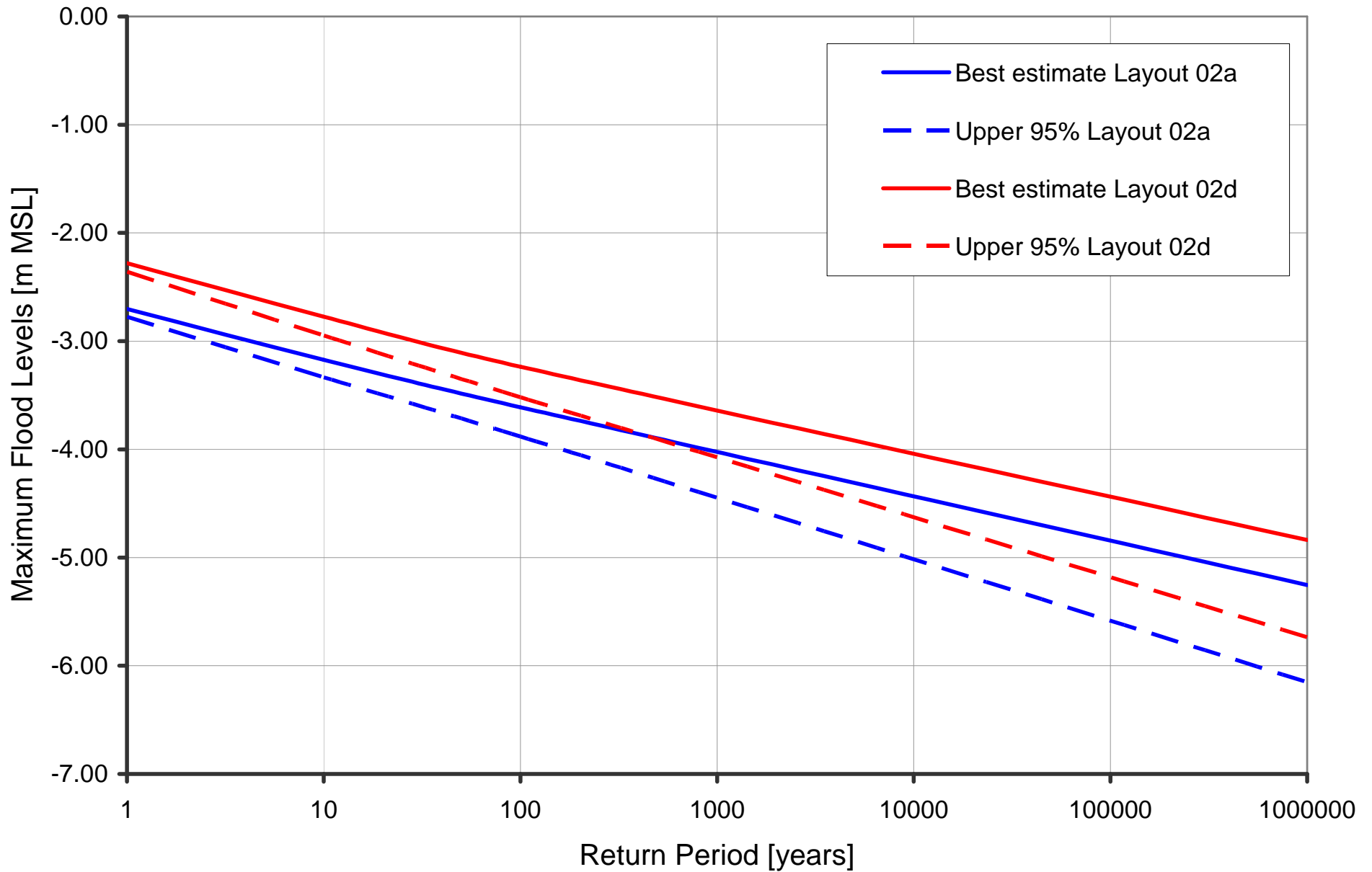


Title:

Logarithmic interpolation of extracted results of minimum surface depth along the pump house sea wall as a function of input H_{m0} values from the 95% confidence level

Figure No.

6.11

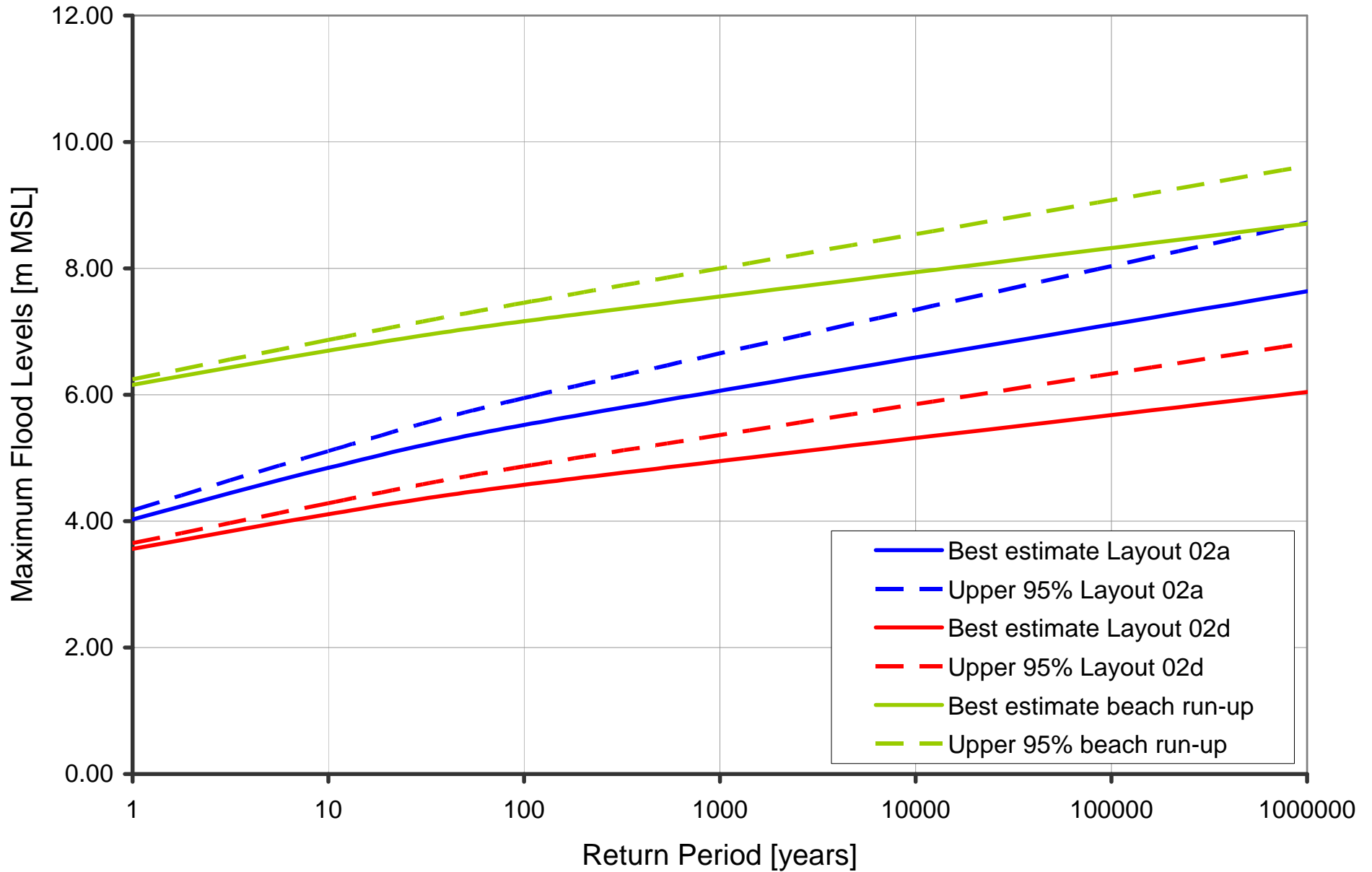


Title:

**Comparison of extreme low water levels:
Proposed Layout 02a and Proposed Layout 02d**

Figure No.

7.1

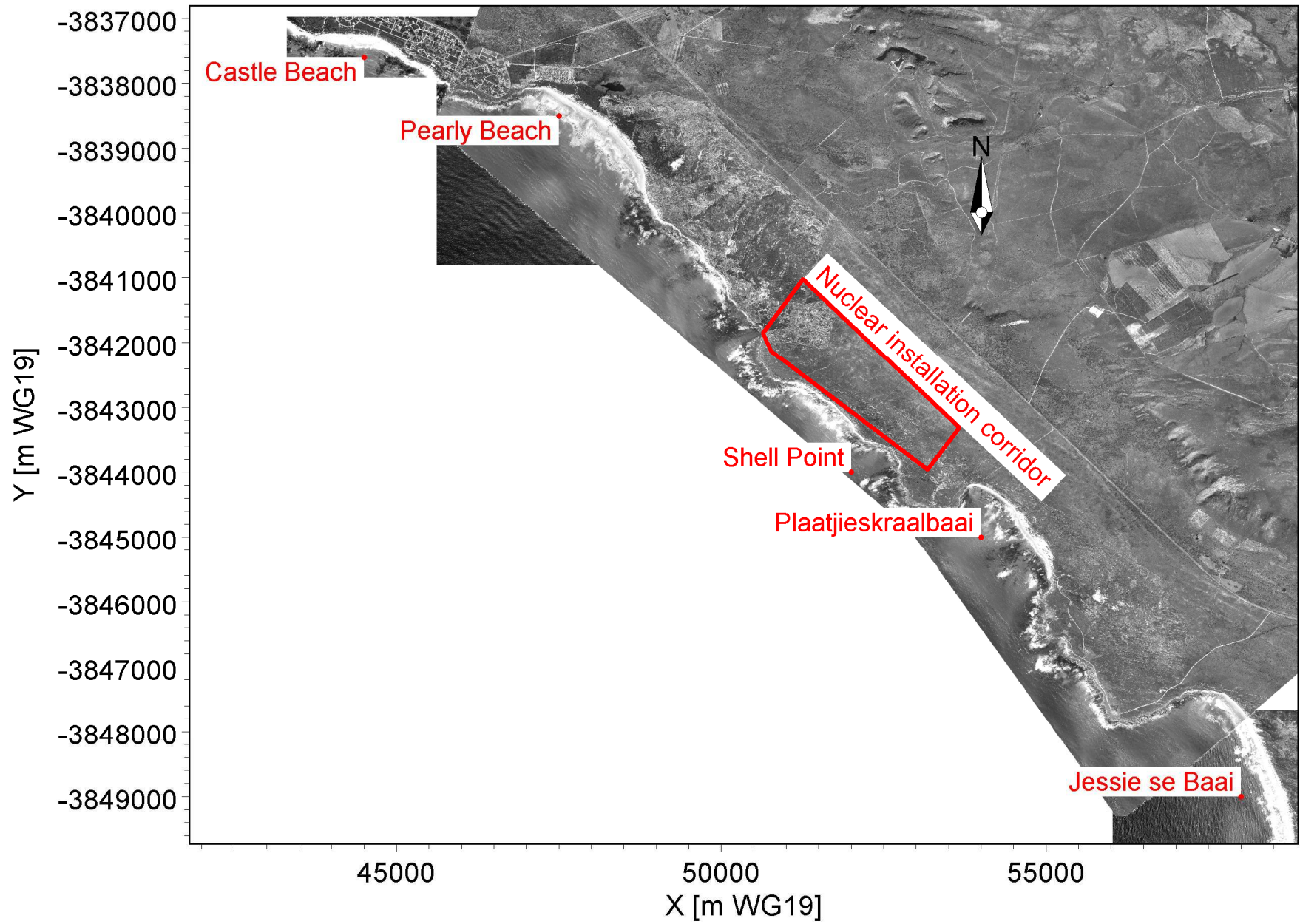


Title:

Comparison of extreme high water levels: Proposed Layout 02a, Proposed Layout 02d and Profile 04 Beach run-up (including climate change parameters)

Figure No.

7.2

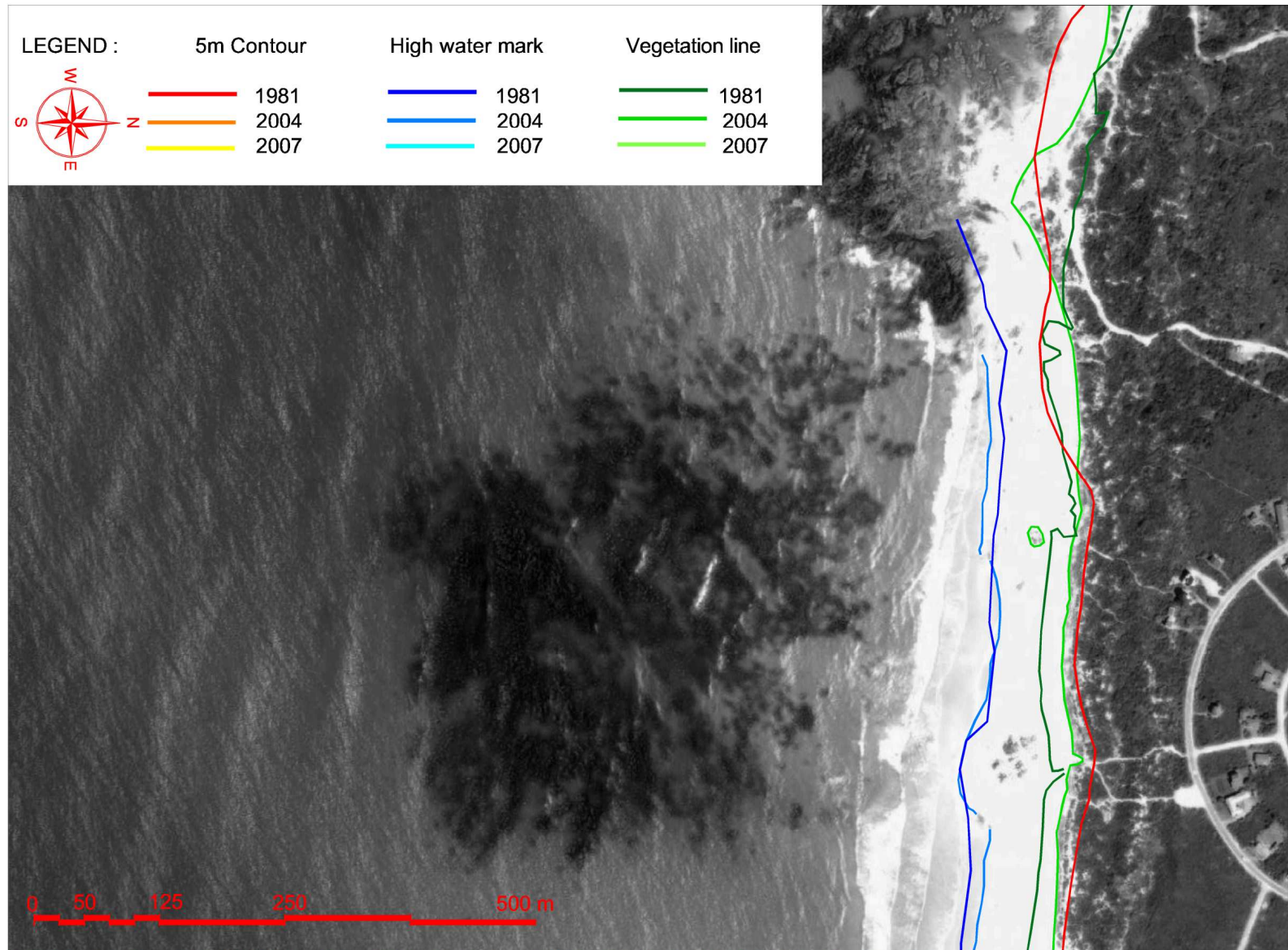


Title:

Combined image of the Bantamsklip site showing beach locations used for the coastline study

Figure No.

8.1



X:\PRDW Projects\Current\SA (1010) Nuclear Sites SSRs\Working\Engineers\RLH\Coastline\Bantamsklip\Plots\Scaled\Coastline_Contours_Comparison_11.png

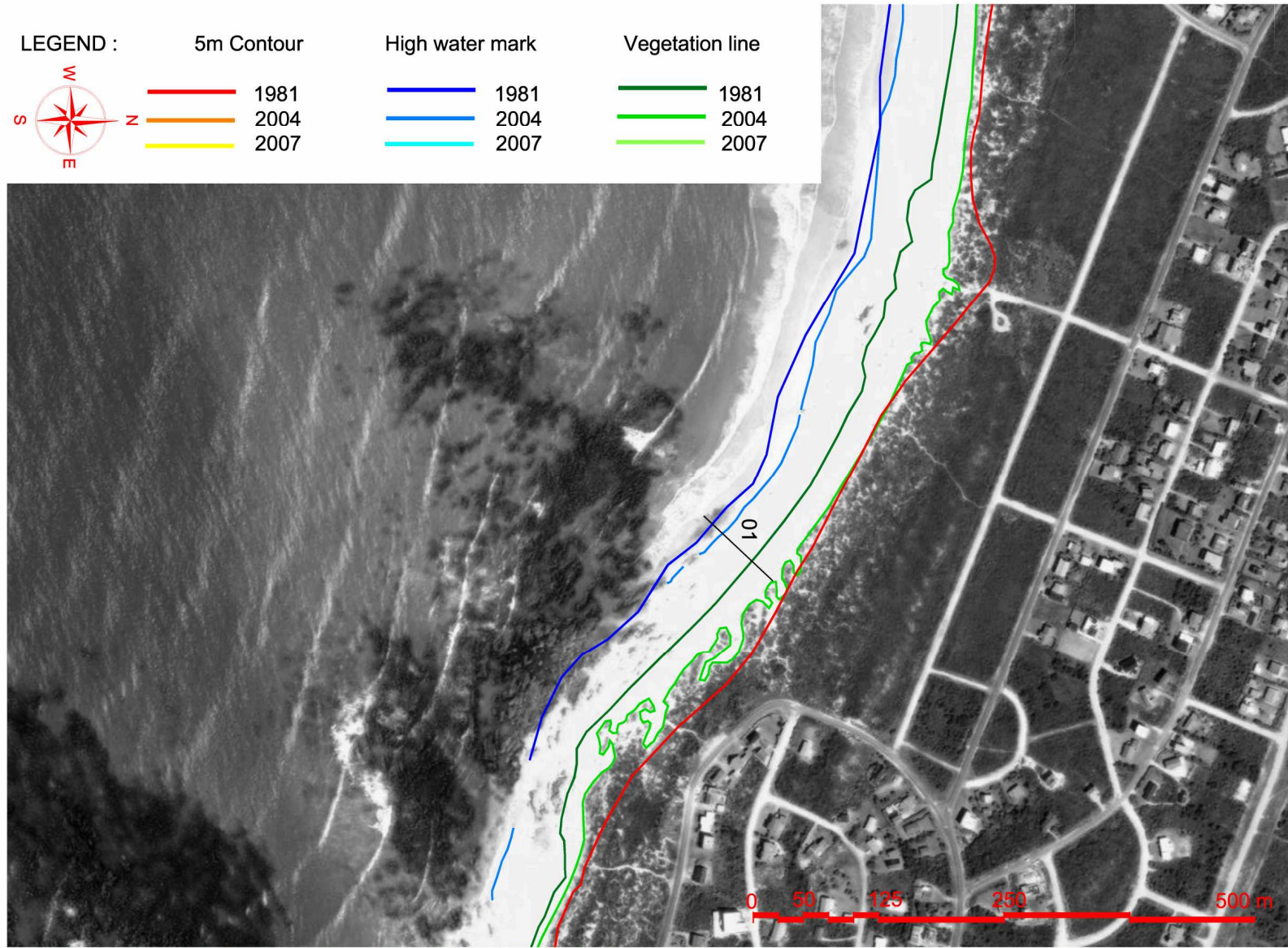


Title:

**Plan view of historical coastline trends from aerial photographs
Castle Beach**

Figure No.

8.2



X:\PRDW Projects\Current\SA (1010) Nuclear Sites SSRs\Working\Engineers\RLH\Coastline\Bantamsklip\Plots\Scaled\Coastline_Contours_Comparison_10.png

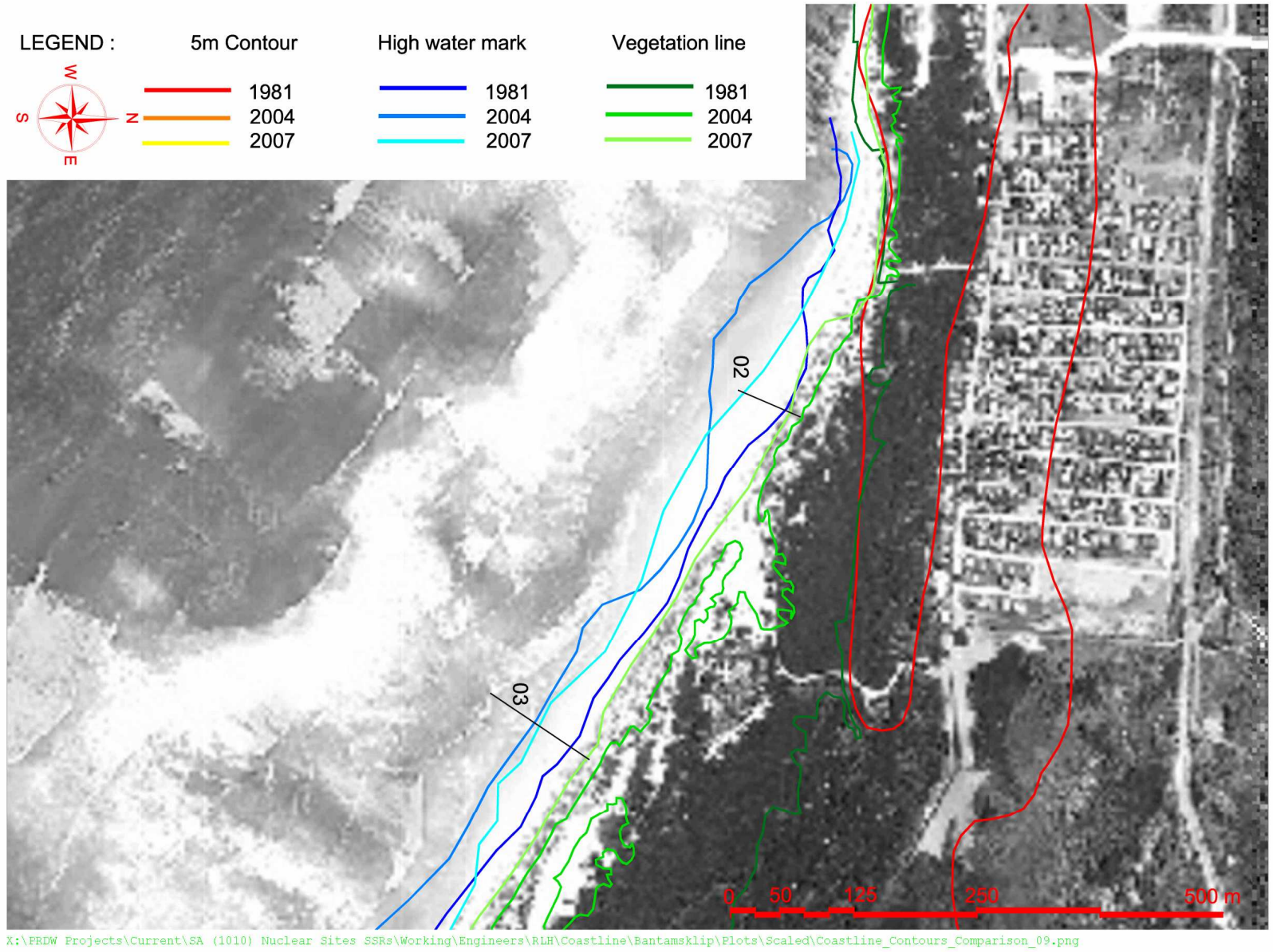


Title:

**Plan view of historical coastline trends from aerial photographs
Castle Beach**

Figure No.

8.3

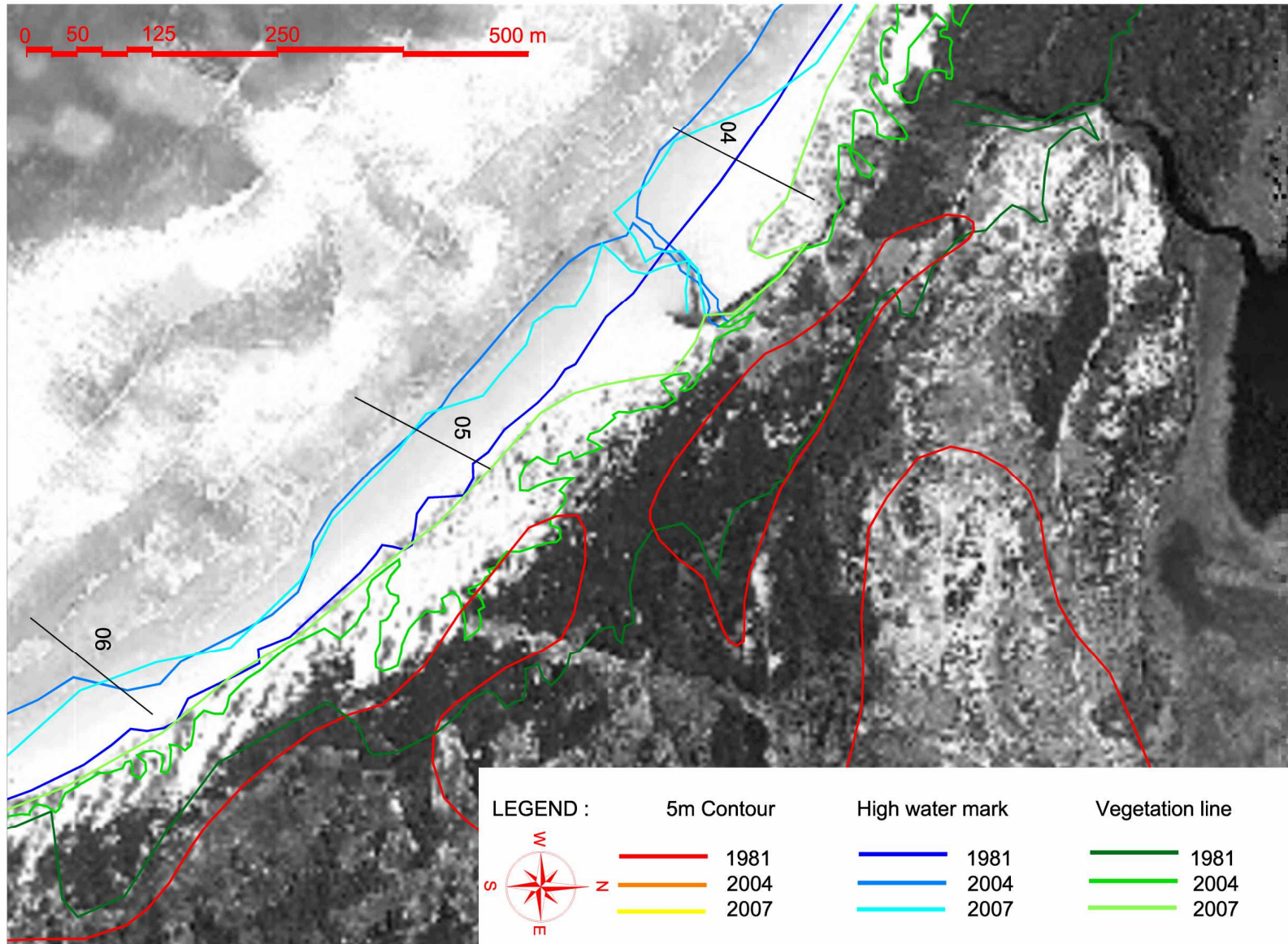


Title:

**Plan view of historical coastline trends from aerial photographs
Pearly Beach**

Figure No.

8.4



X:\PRDW Projects\Current\SA (1010) Nuclear Sites SSRs\Working\Engineers\RLH\Coastline\Bantamsklip\Plots\Scaled\Coastline_Contours_Comparison_08.png

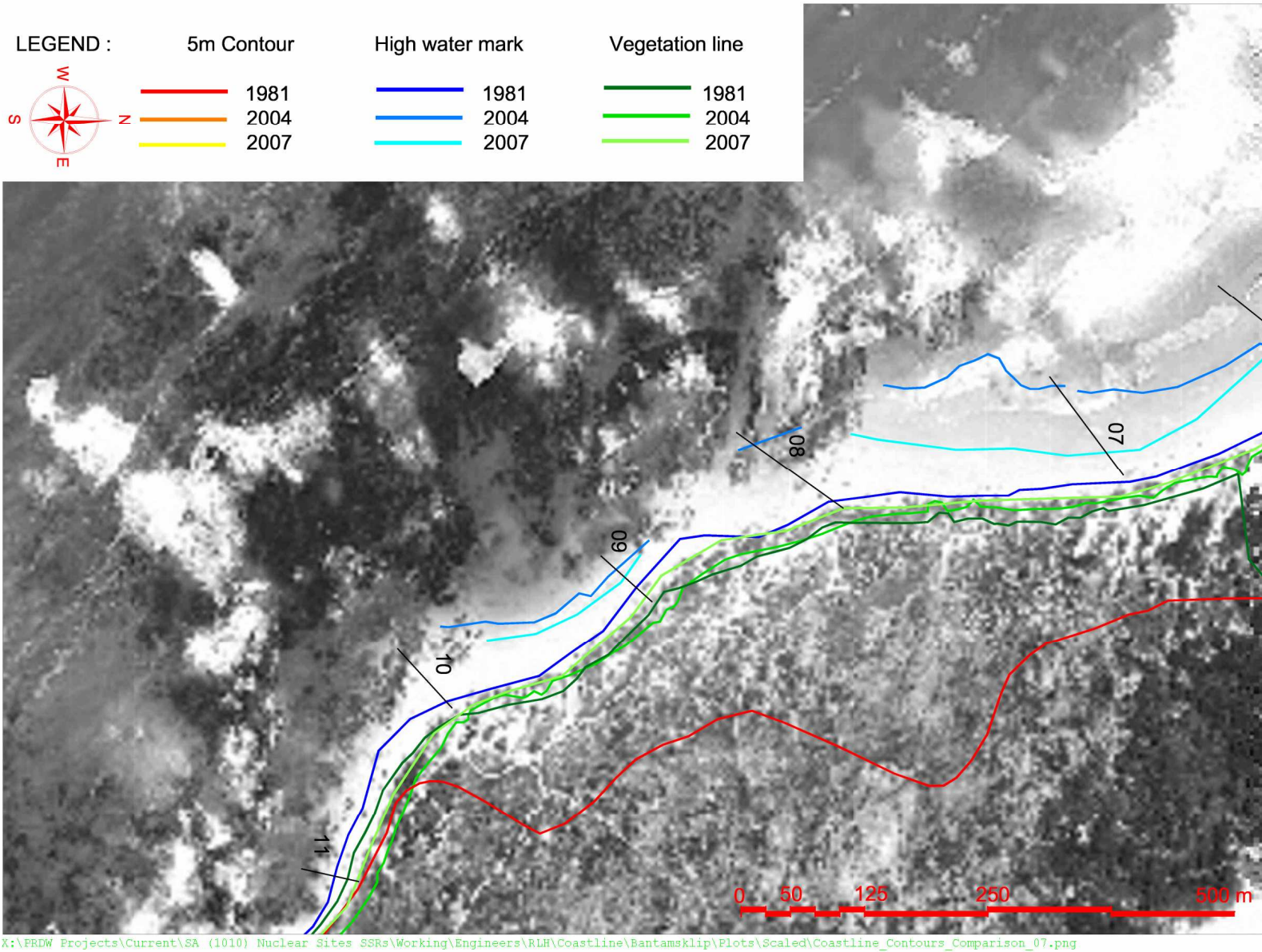


Title:

**Plan view of historical coastline trends from aerial photographs
Pearly Beach**

Figure No.

8.5

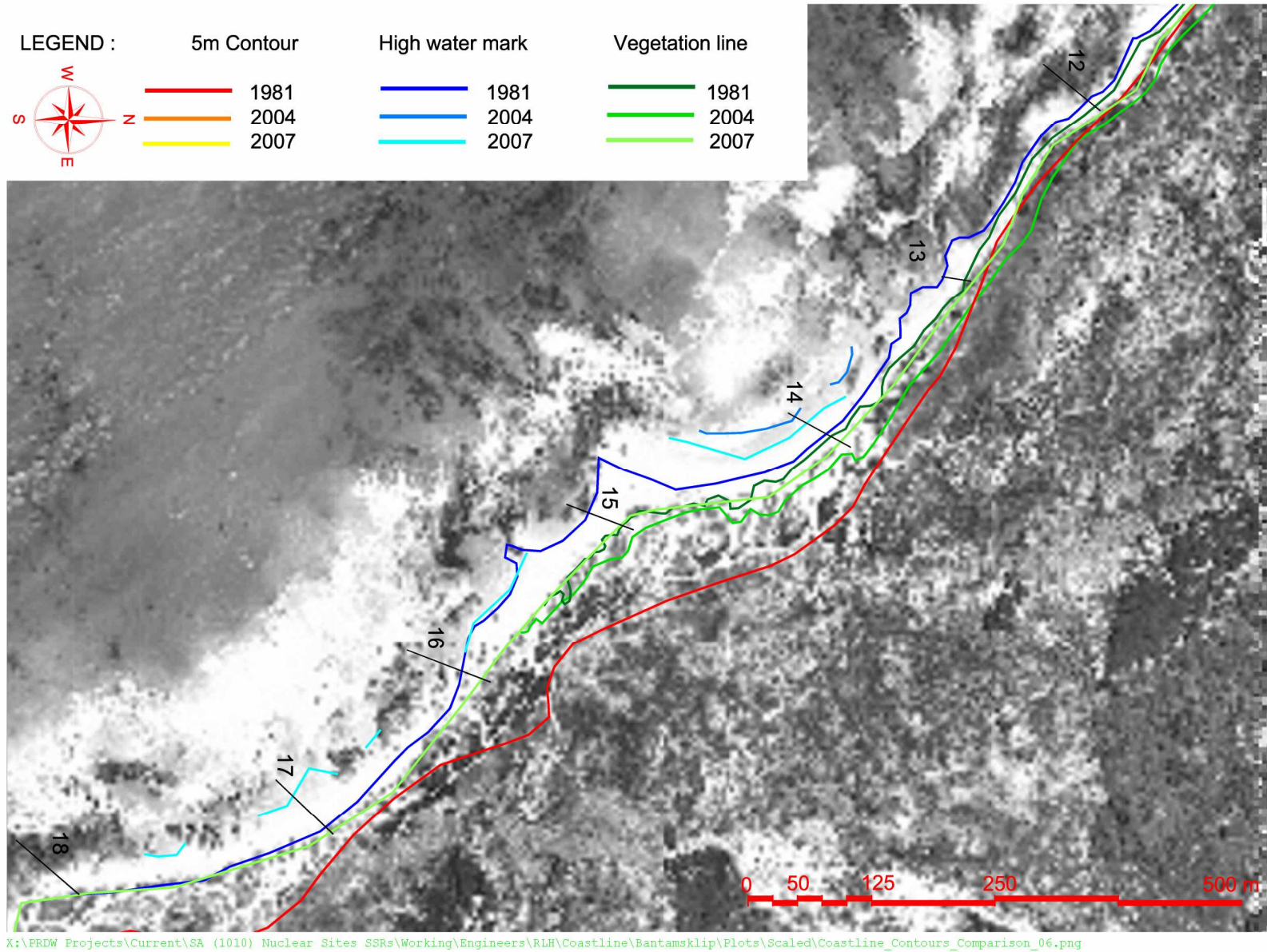


Title:

**Plan view of historical coastline trends from aerial photographs
Pearly Beach**

Figure No.

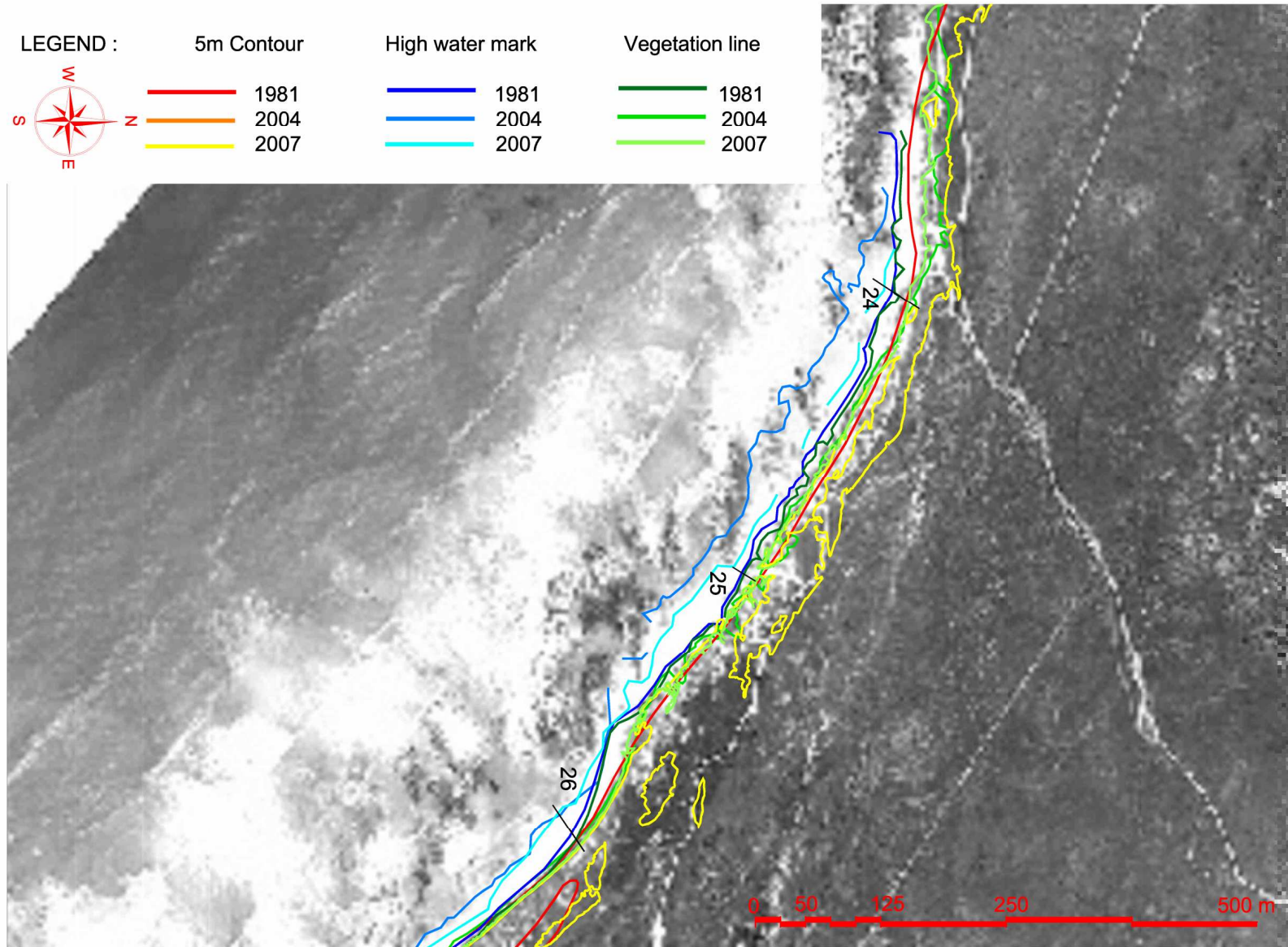
8.6



Title:

**Plan view of historical coastline trends from aerial photographs
Shell Point**

**Figure No.
8.7**



X:\PRDW Projects\Current\SA (1010) Nuclear Sites SSRs\Working\Engineers\RLH\Coastline\Bantamsklip\Plots\Scaled\Coastline_Contours_Comparison_05.png

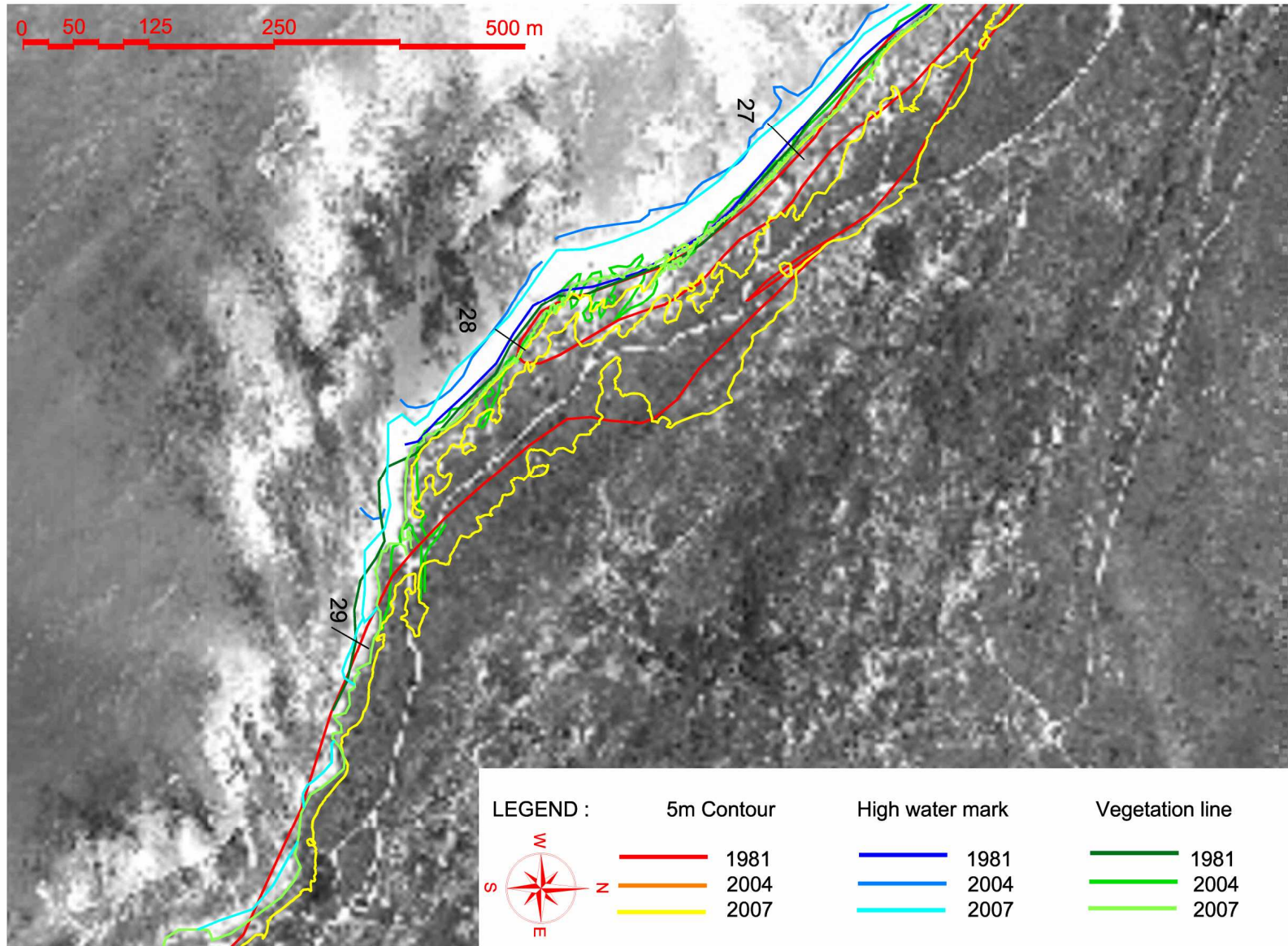


Title:

**Plan view of historical coastline trends from aerial photographs
Shell Point**

Figure No.

8.8



X:\PRDW Projects\Current\SA (1010) Nuclear Sites SSRs\Working\Engineers\RLH\Coastline\Bantamsklip\Plots\Scaled\Coastline_Contours_Comparison_04.png

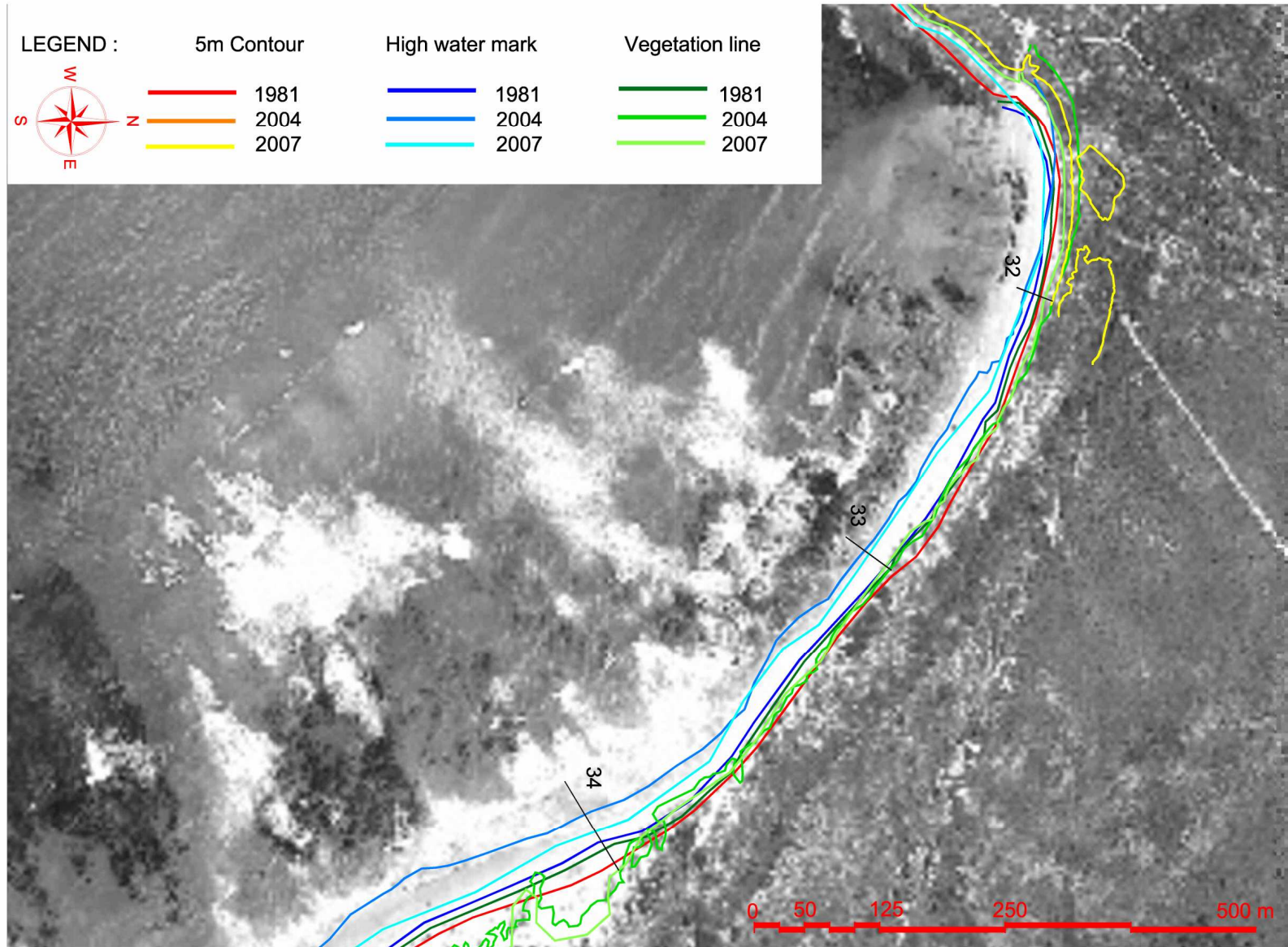


Title:

**Plan view of historical coastline trends from aerial photographs
Shell Point**

Figure No.

8.9



X:\PRDW Projects\Current\SA (1010) Nuclear Sites SSRs\Working\Engineers\RLH\Coastline\Bantamsklip\Plots\Scaled\Coastline_Contours_Comparison_03.png

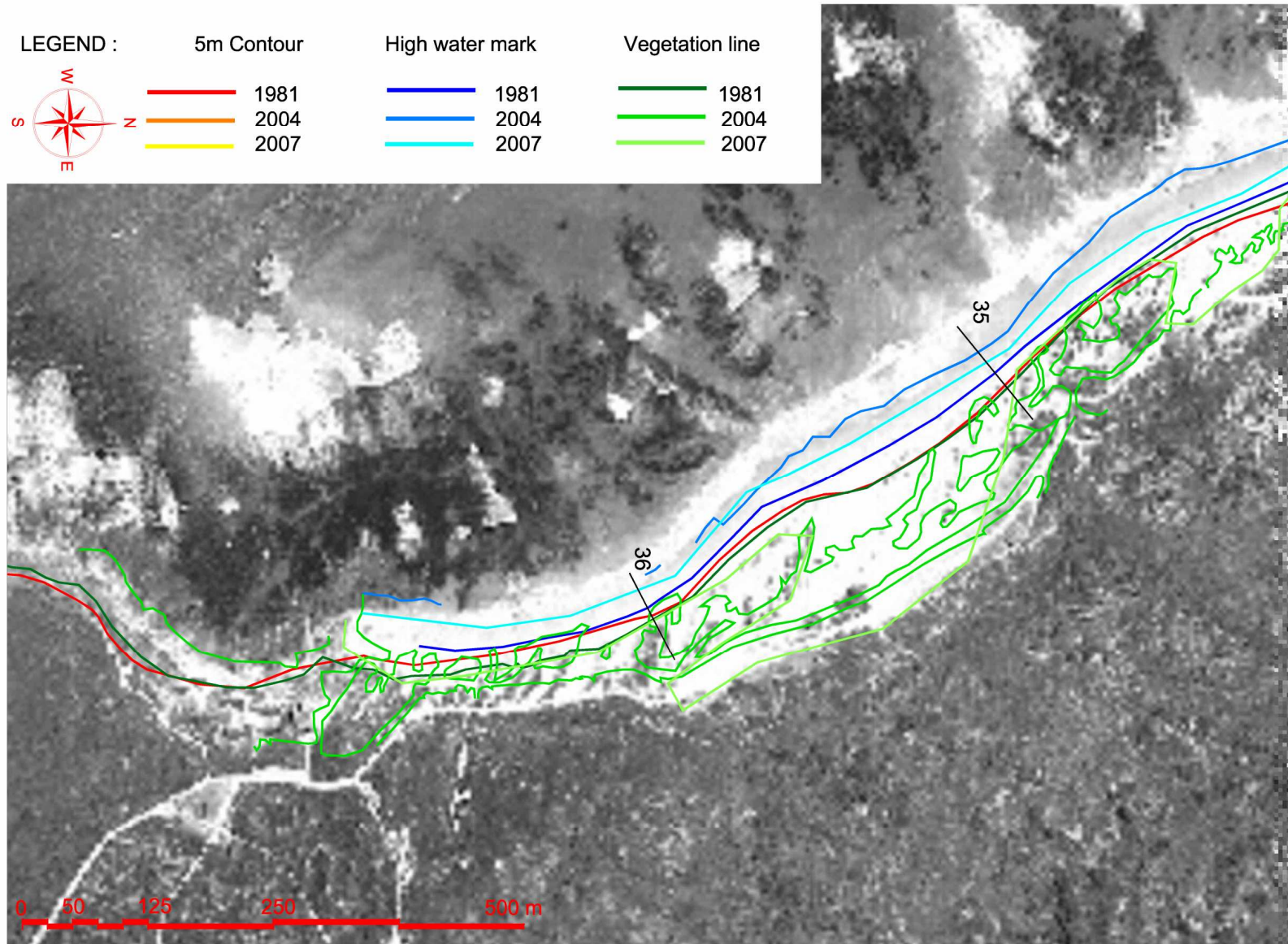


Title:

**Plan view of historical coastline trends from aerial photographs
Plaatjieskraalbaai**

Figure No.

8.10

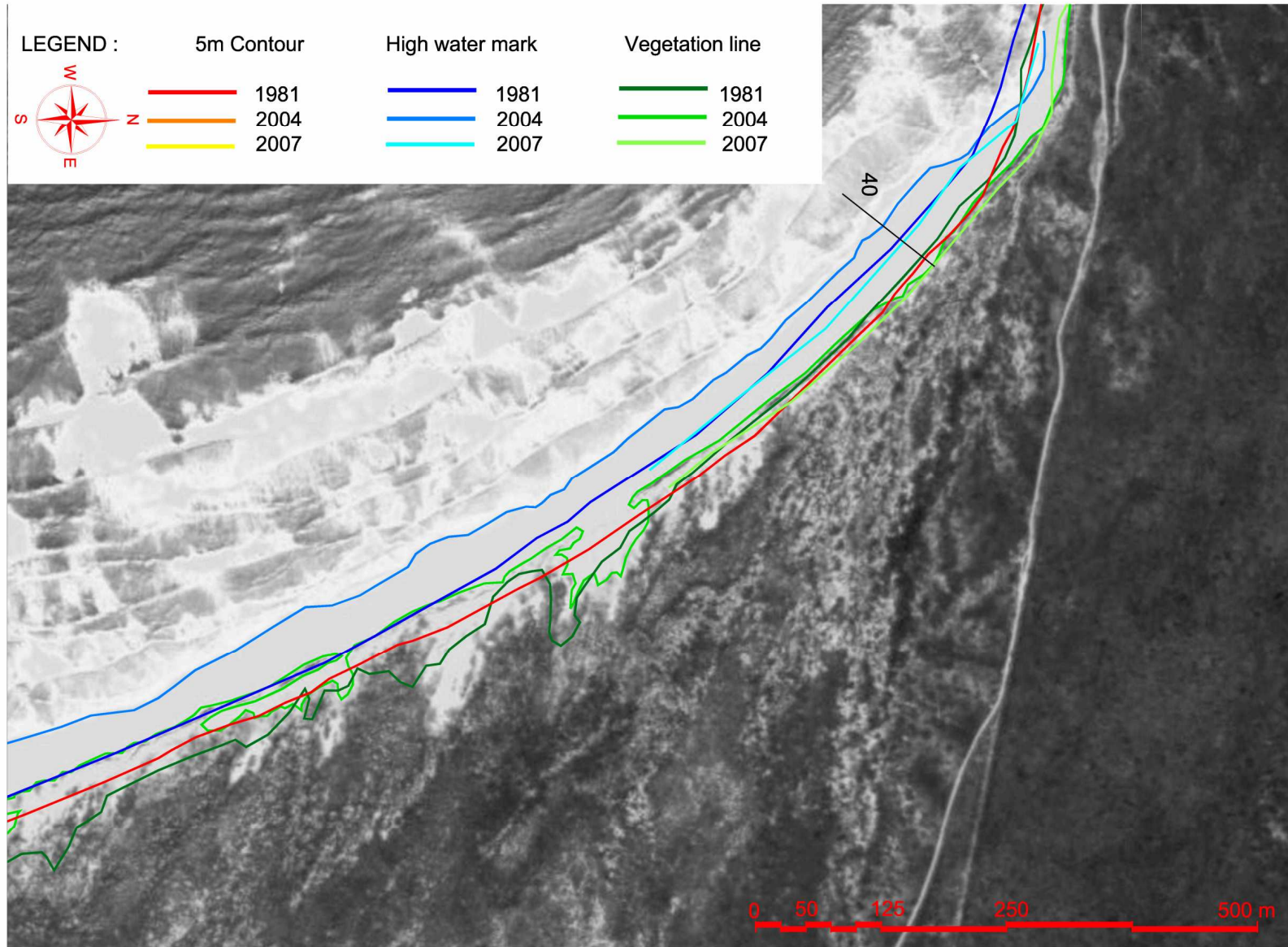


Title:

**Plan view of historical coastline trends from aerial photographs
Plaatjieskraalbaai**

Figure No.

8.11



X:\PRDW Projects\Current\SA (1010) Nuclear Sites SSRs\Working\Engineers\RLH\Coastline\Bantamsklip\Plots\Scaled\Coastline_Contours_Comparison_01.png

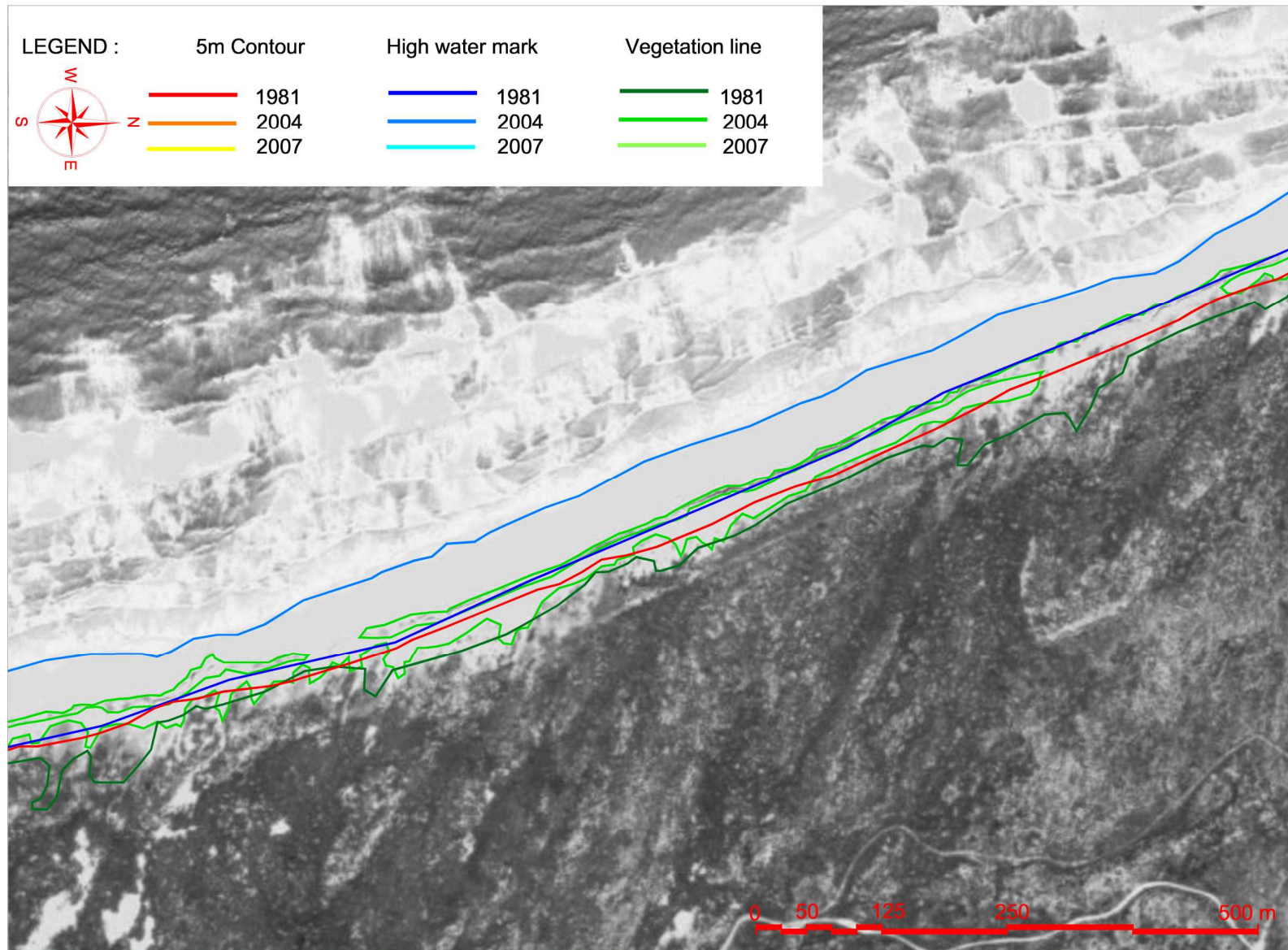


Title:

**Plan view of historical coastline trends from aerial photographs
Jessie se Baai**

Figure No.

8.12



X:\PRDW Projects\Current\SA (1010) Nuclear Sites SSRs\Working\Engineers\RLH\Coastline\Bantamsklip\Plots\Scaled\Coastline_Contours_Comparison_00.png

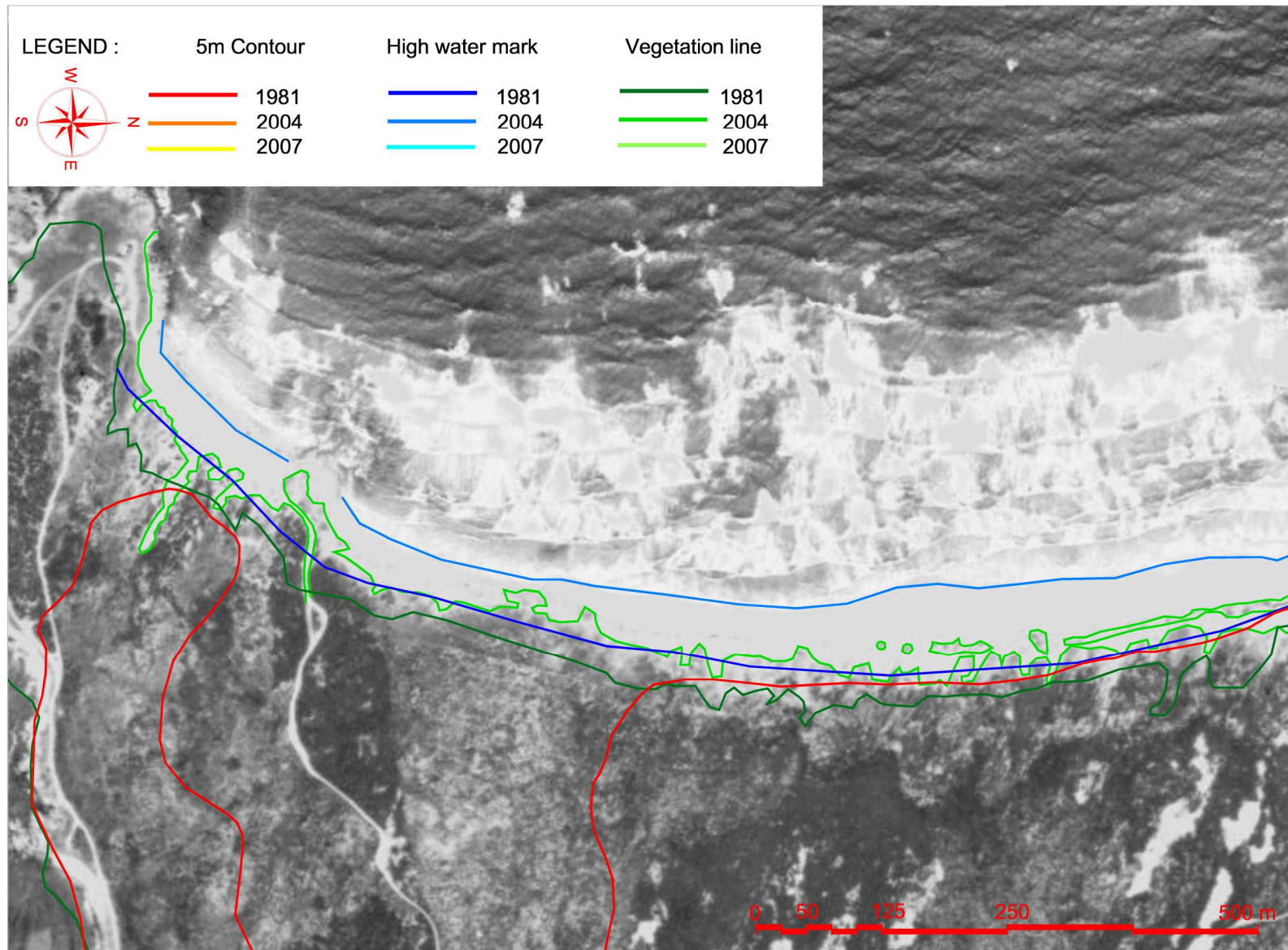


Title:

**Plan view of historical coastline trends from aerial photographs
Jessie se Baai**

Figure No.

8.13



X:\PRDW Projects\Current\SA (1010) Nuclear Sites SSRs\Working\Engineers\RLH\Coastline\Bantamsklip\Plots\Scaled\Coastline_Contours_Comparison_-01.png

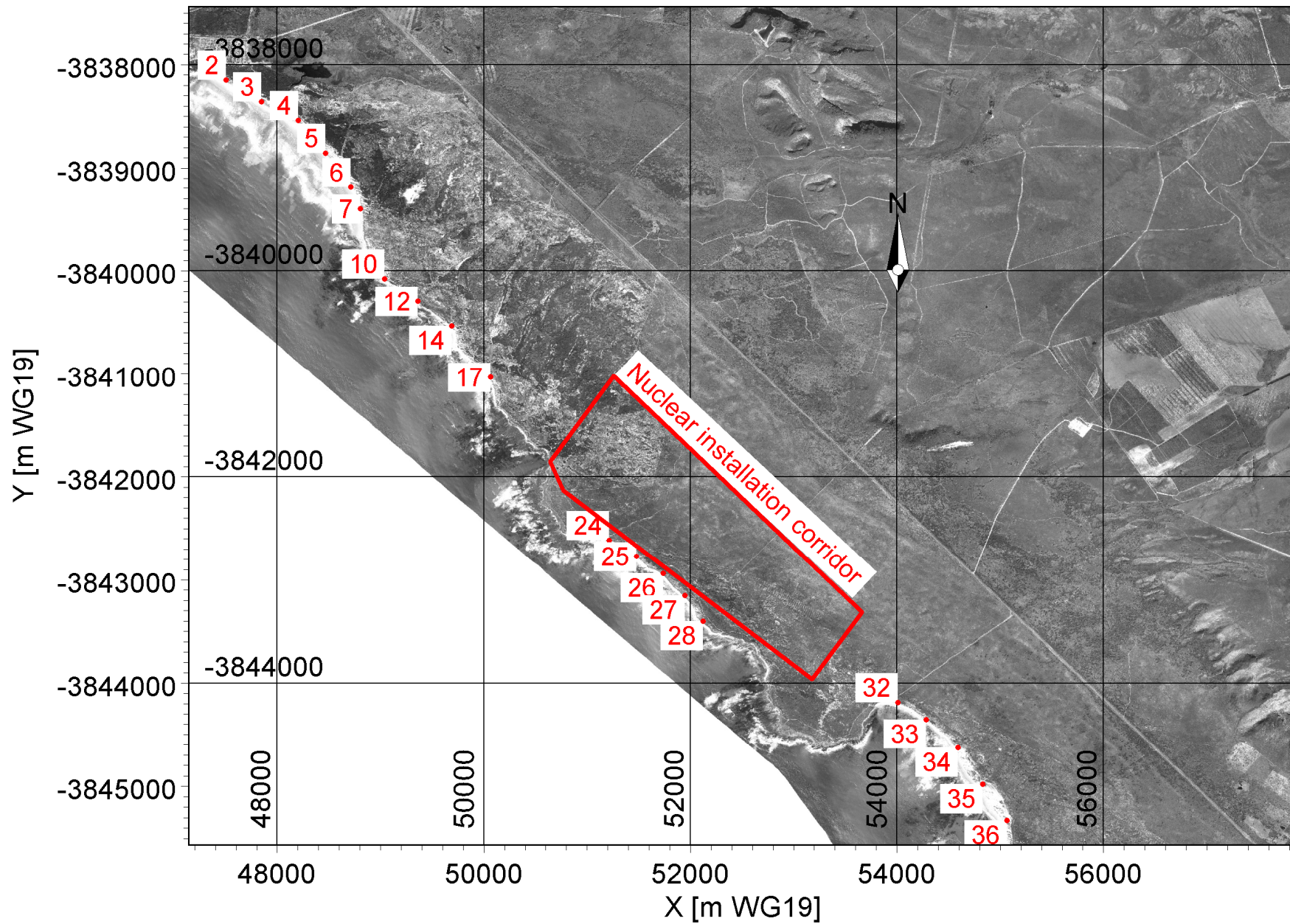


Title:

**Plan view of historical coastline trends from aerial photographs
Jessie se Baai**

Figure No.

8.14

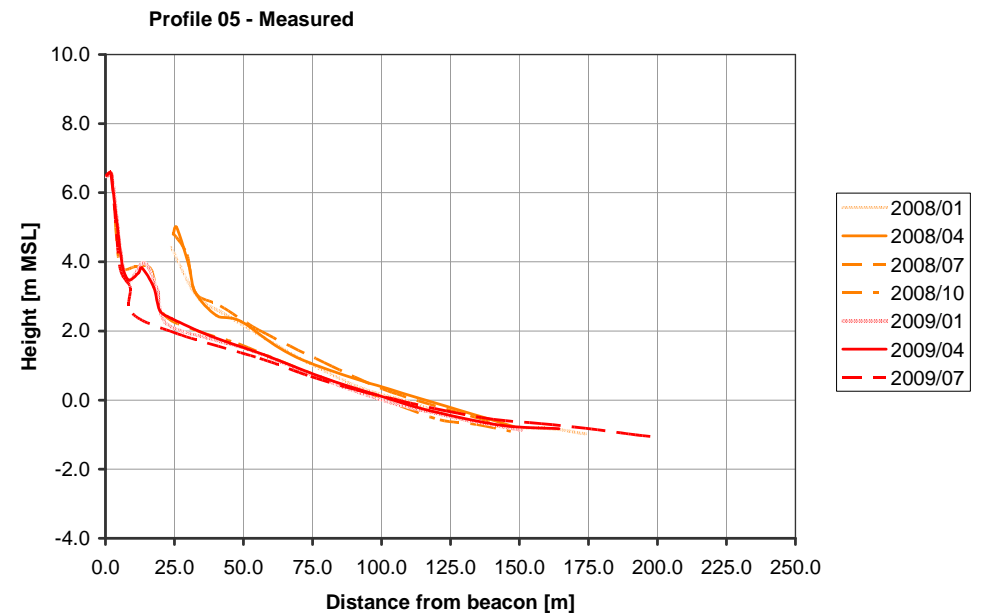
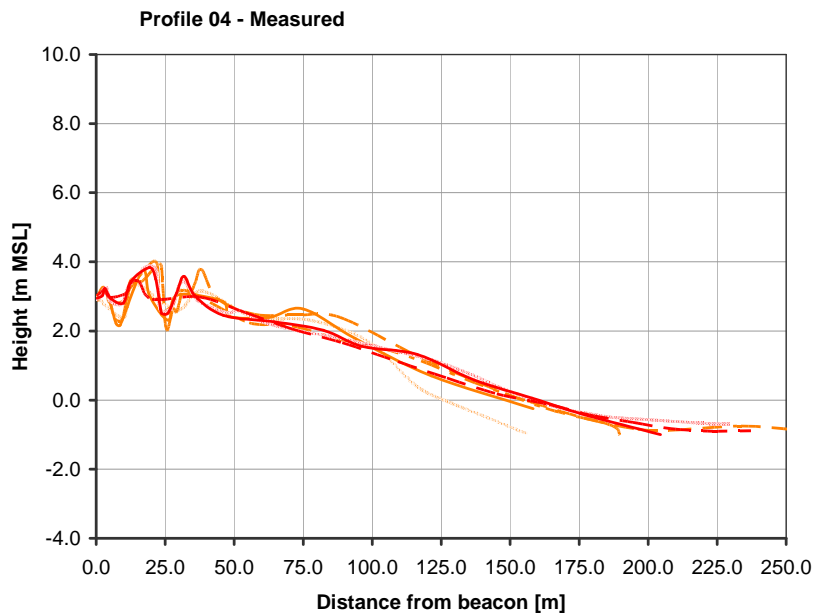
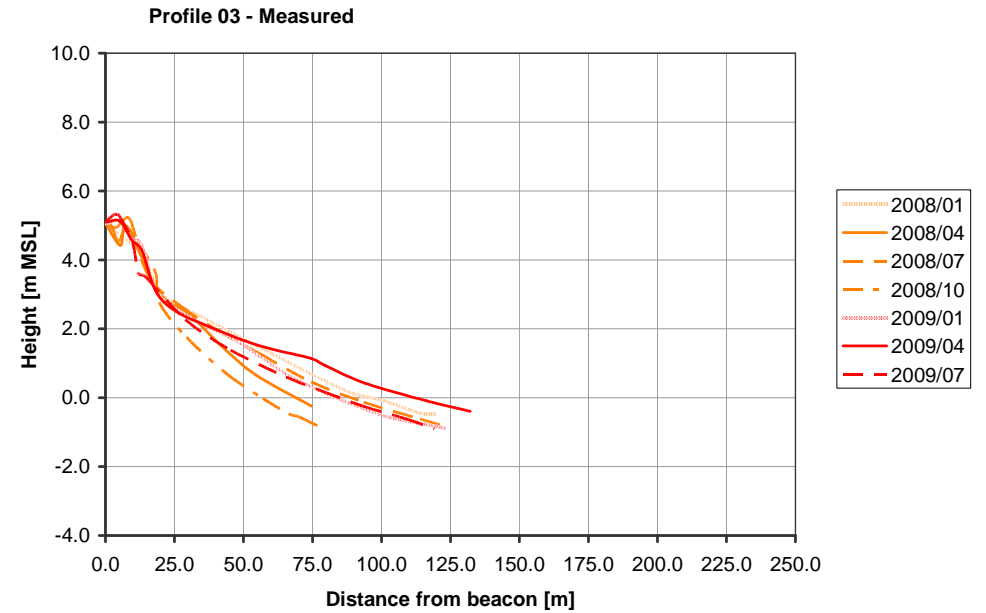
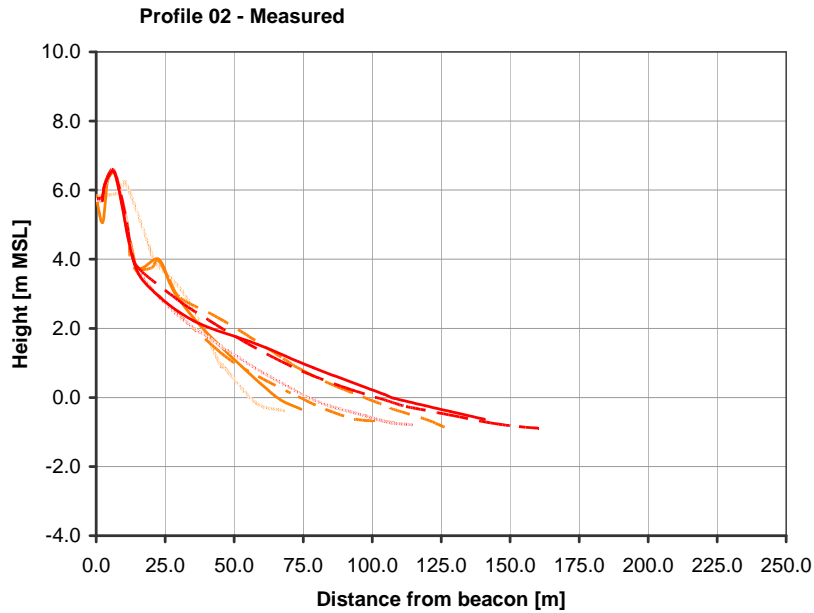


Title:

Satellite image of the Bantamsklip site showing profile locations used for the coastline study

Figure No.

8.15

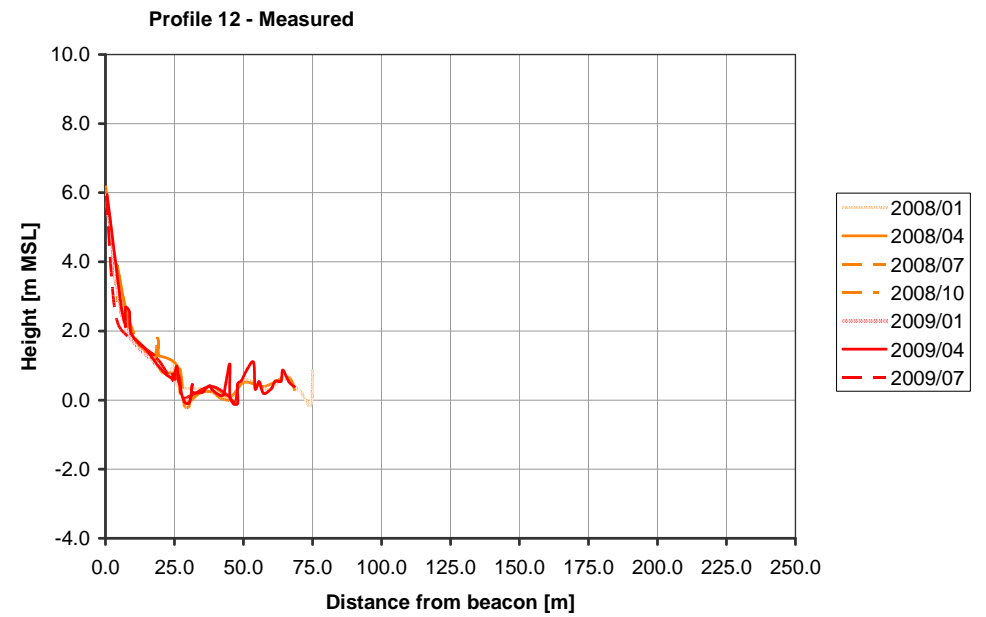
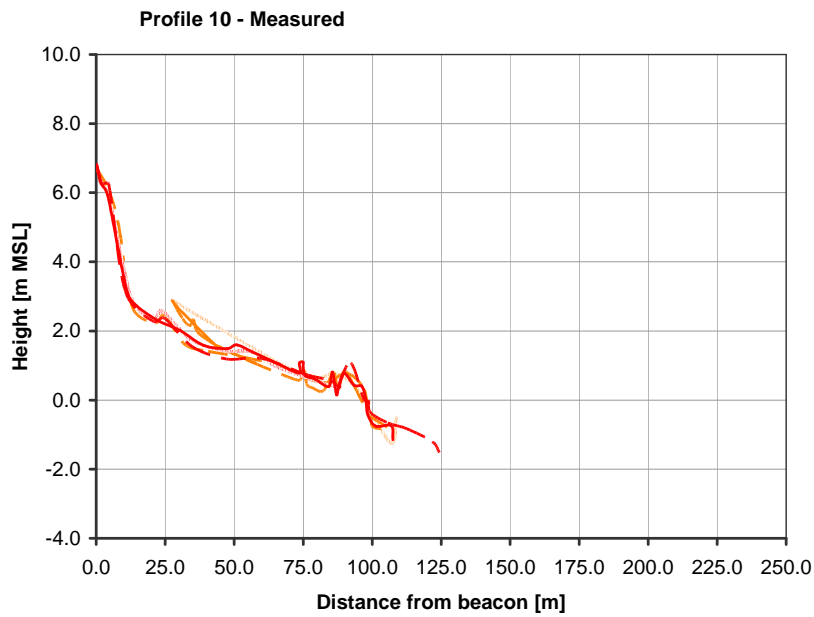
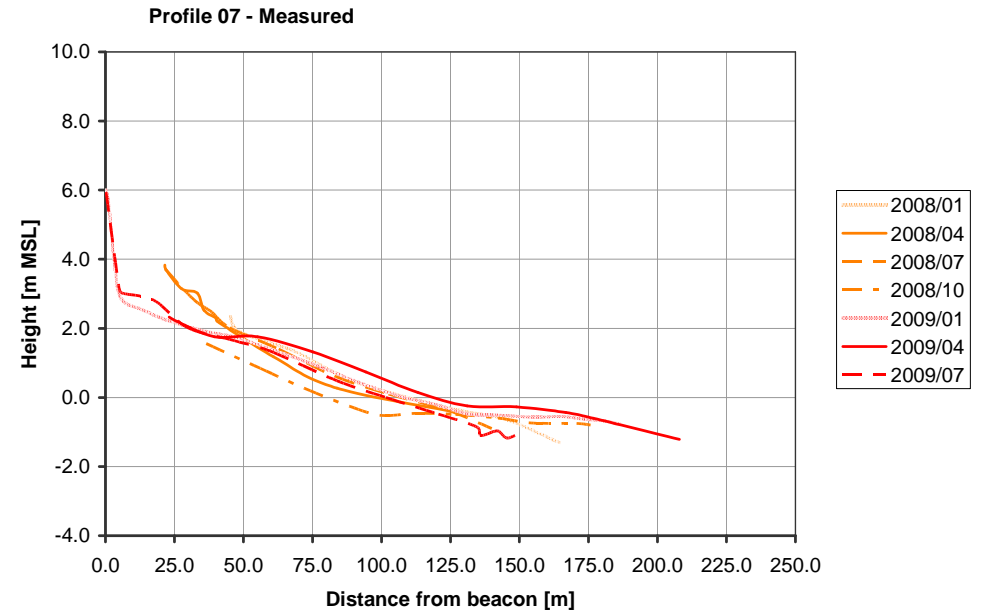
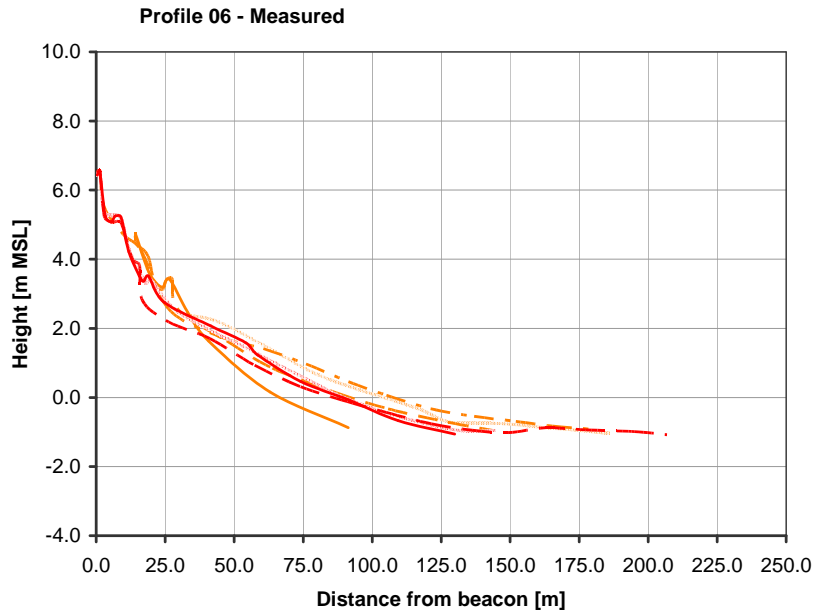


Title:

**Measured beach profiles showing seasonal variations:
Profiles 02 to 05 (refer to Figure 8.15 for positions of profiles)**

Figure No.

8.16

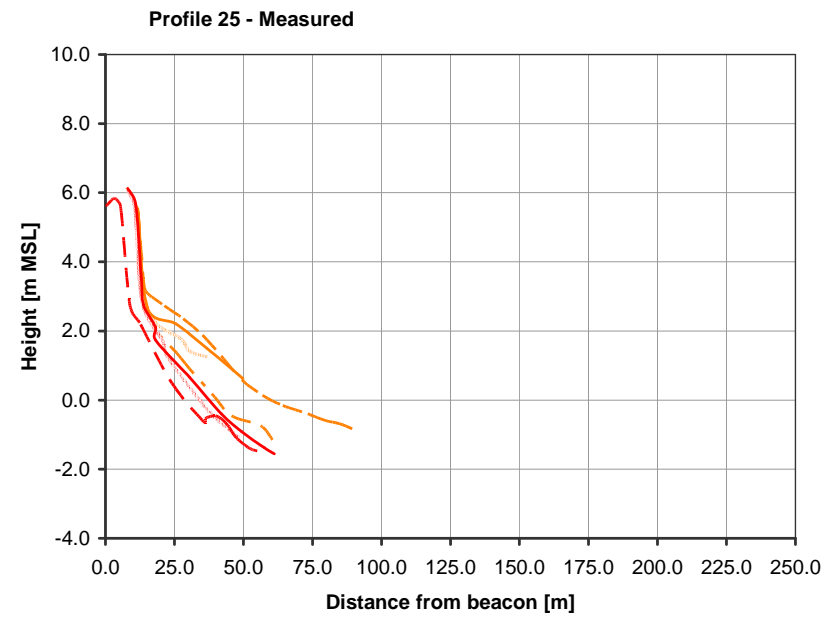
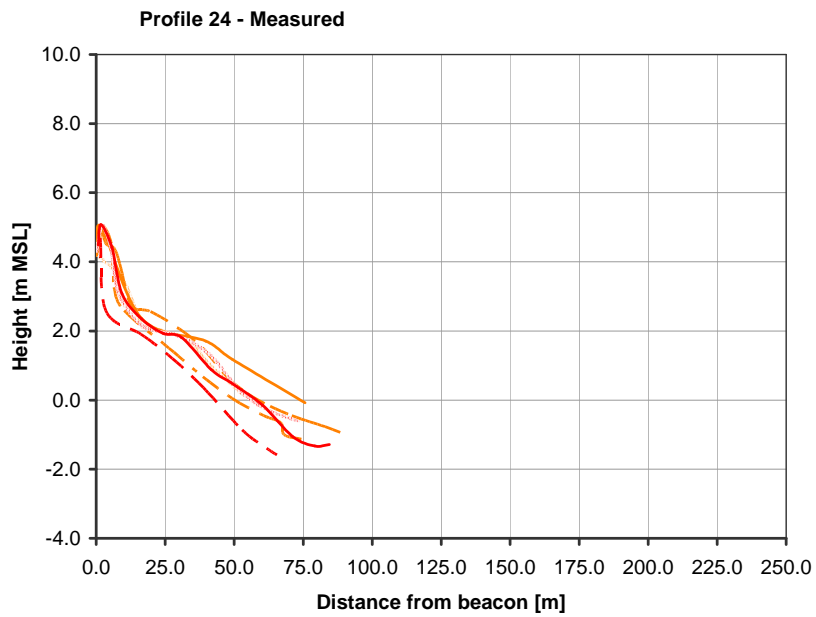
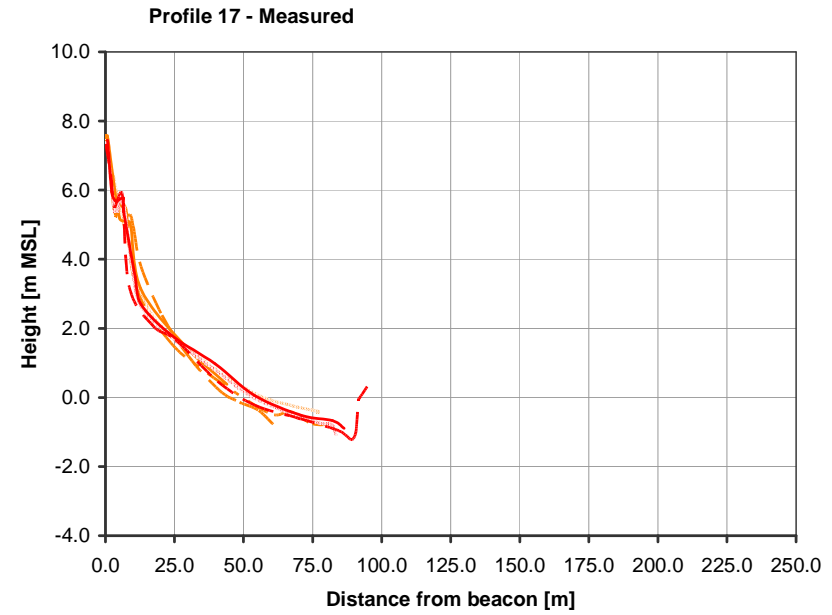
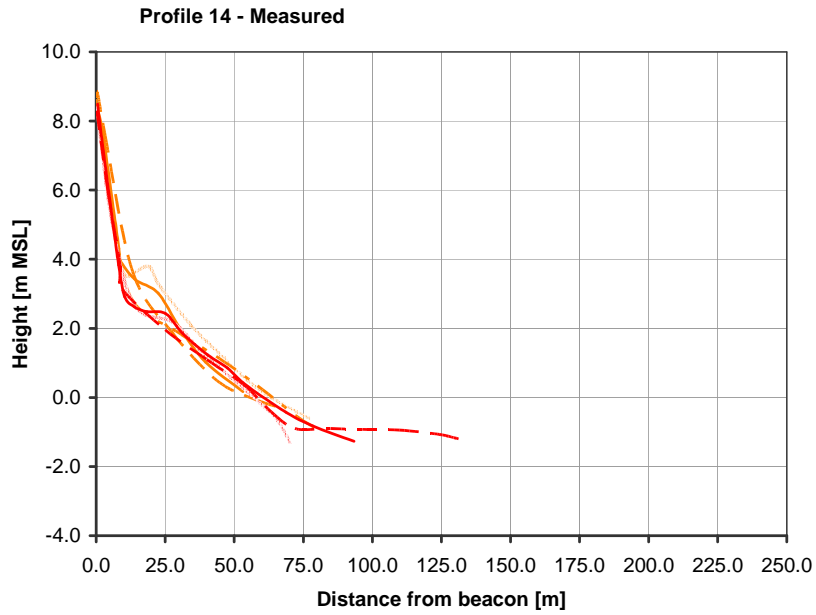


Title:

**Measured beach profiles showing seasonal variations:
Profiles 06, 07, 10, 12 (refer to Figure 8.15 for positions of profiles)**

Figure No.

8.17

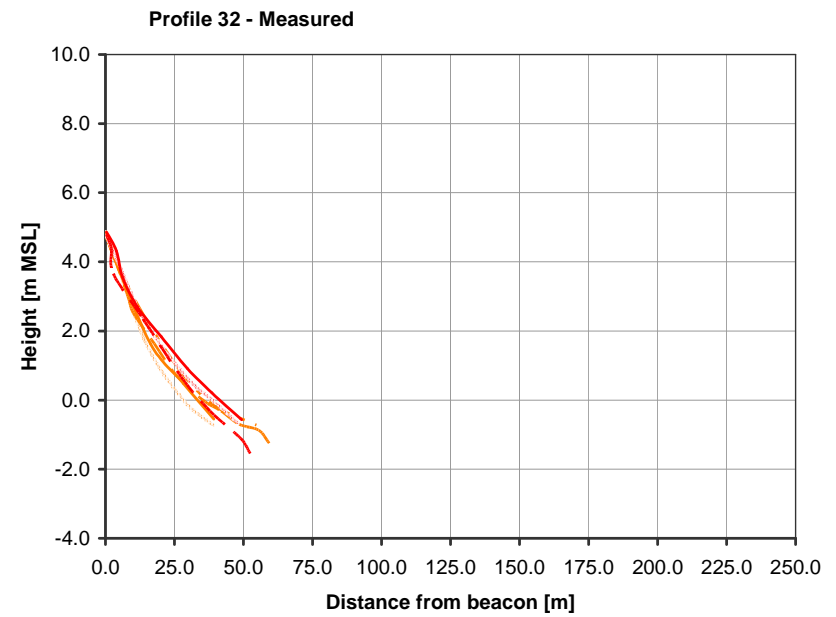
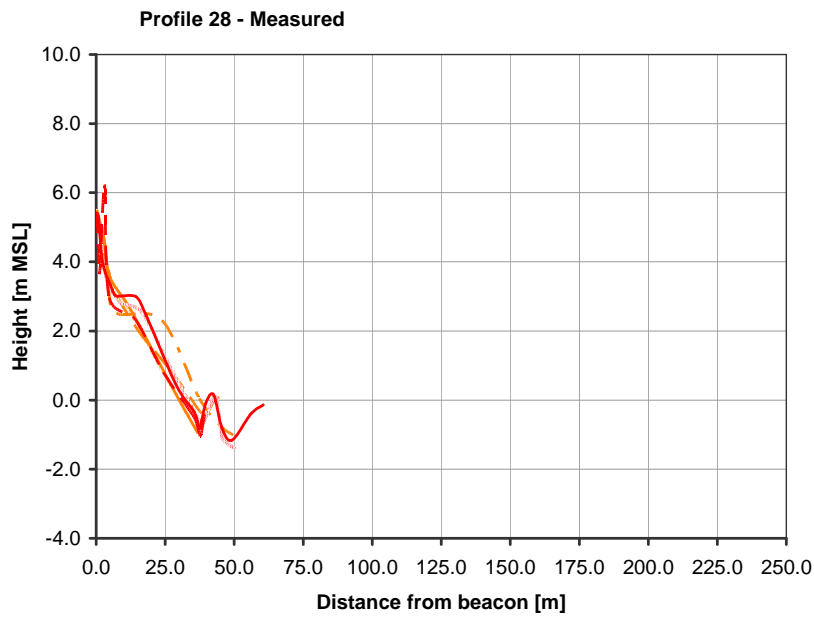
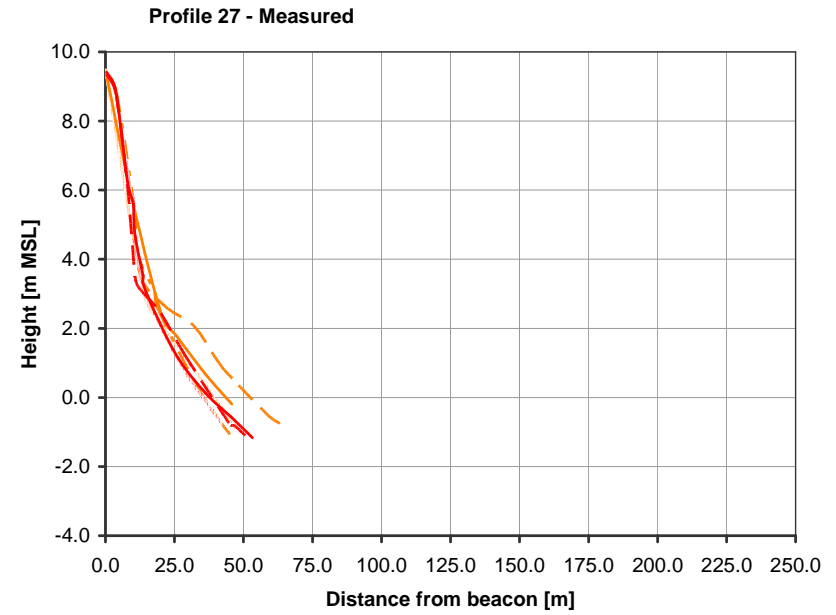
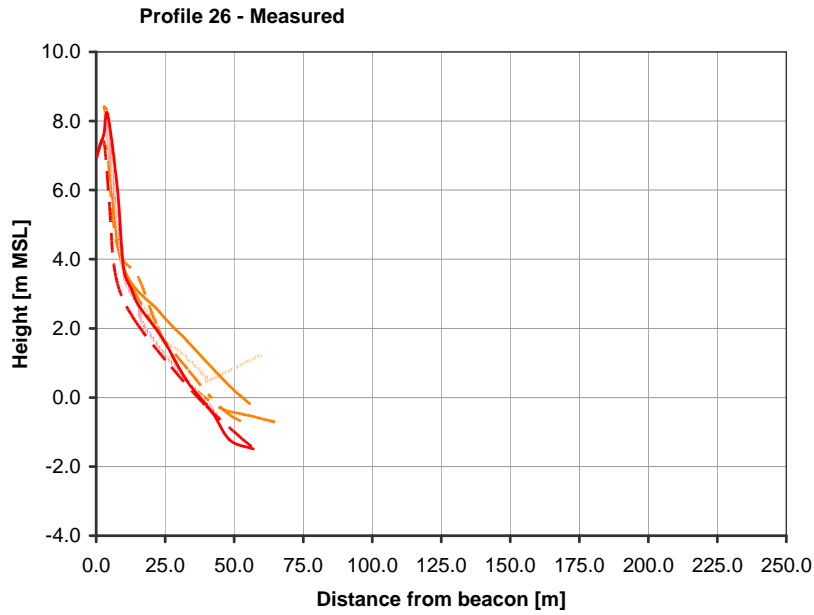


Title:

**Measured beach profiles showing seasonal variations:
Profiles 14, 17, 24, 25 (refer to Figure 8.15 for positions of profiles)**

Figure No.

8.18

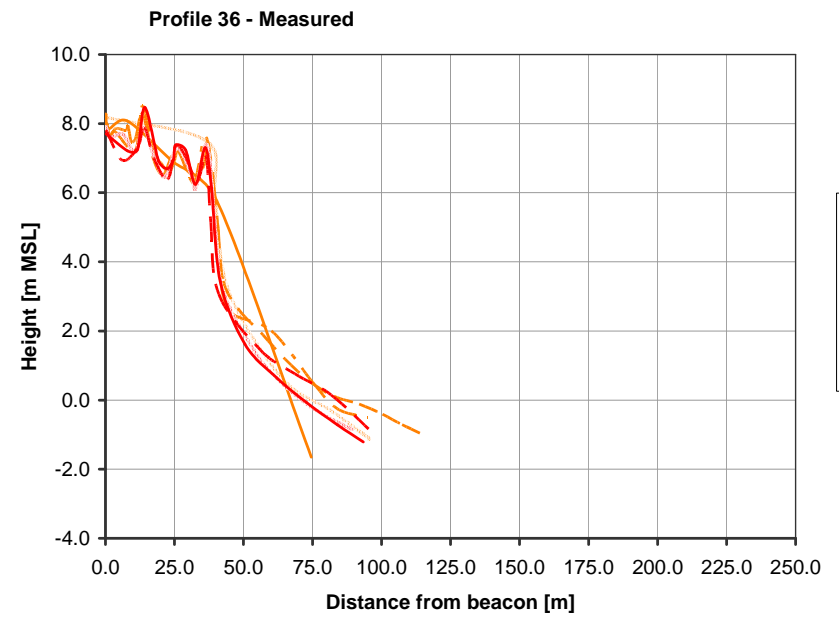
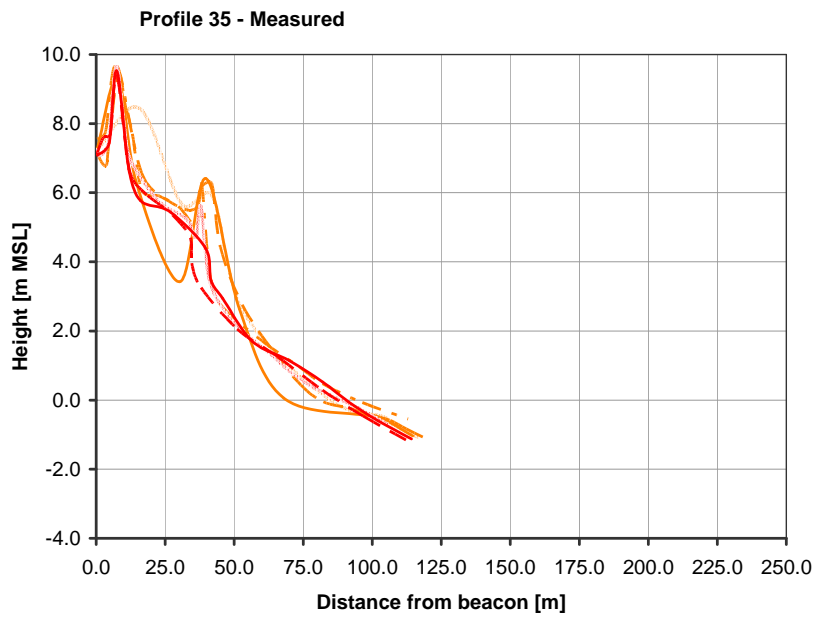
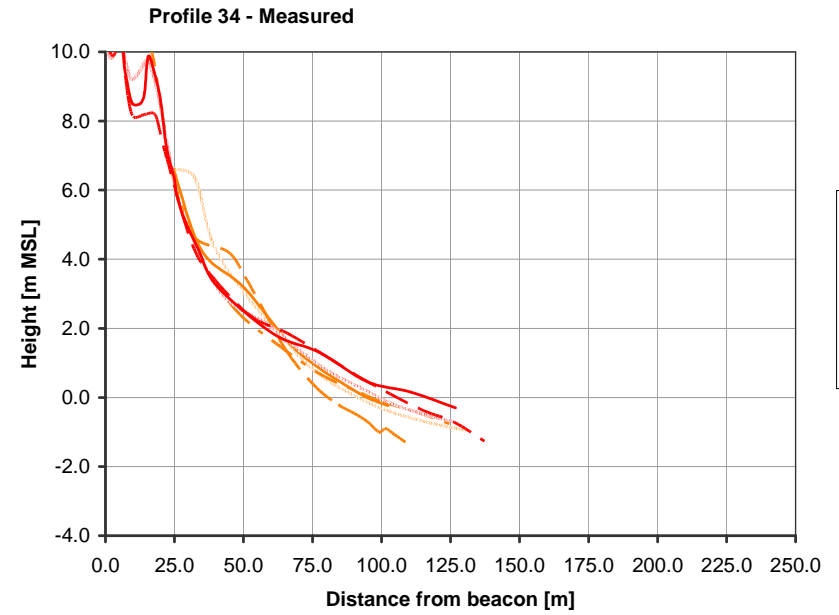
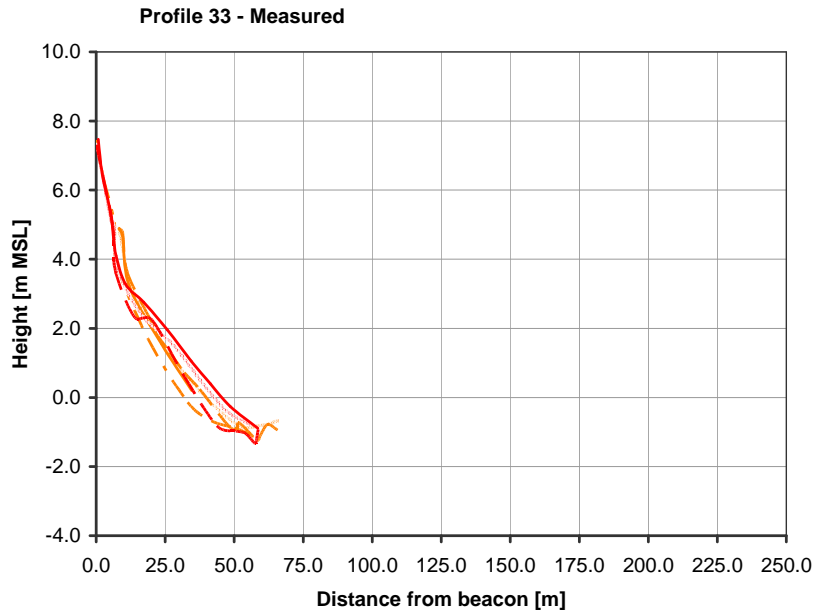


Title:

**Measured beach profiles showing seasonal variations:
Profiles 26, 27, 28, 32 (refer to Figure 8.15 for positions of profiles)**

Figure No.

8.19

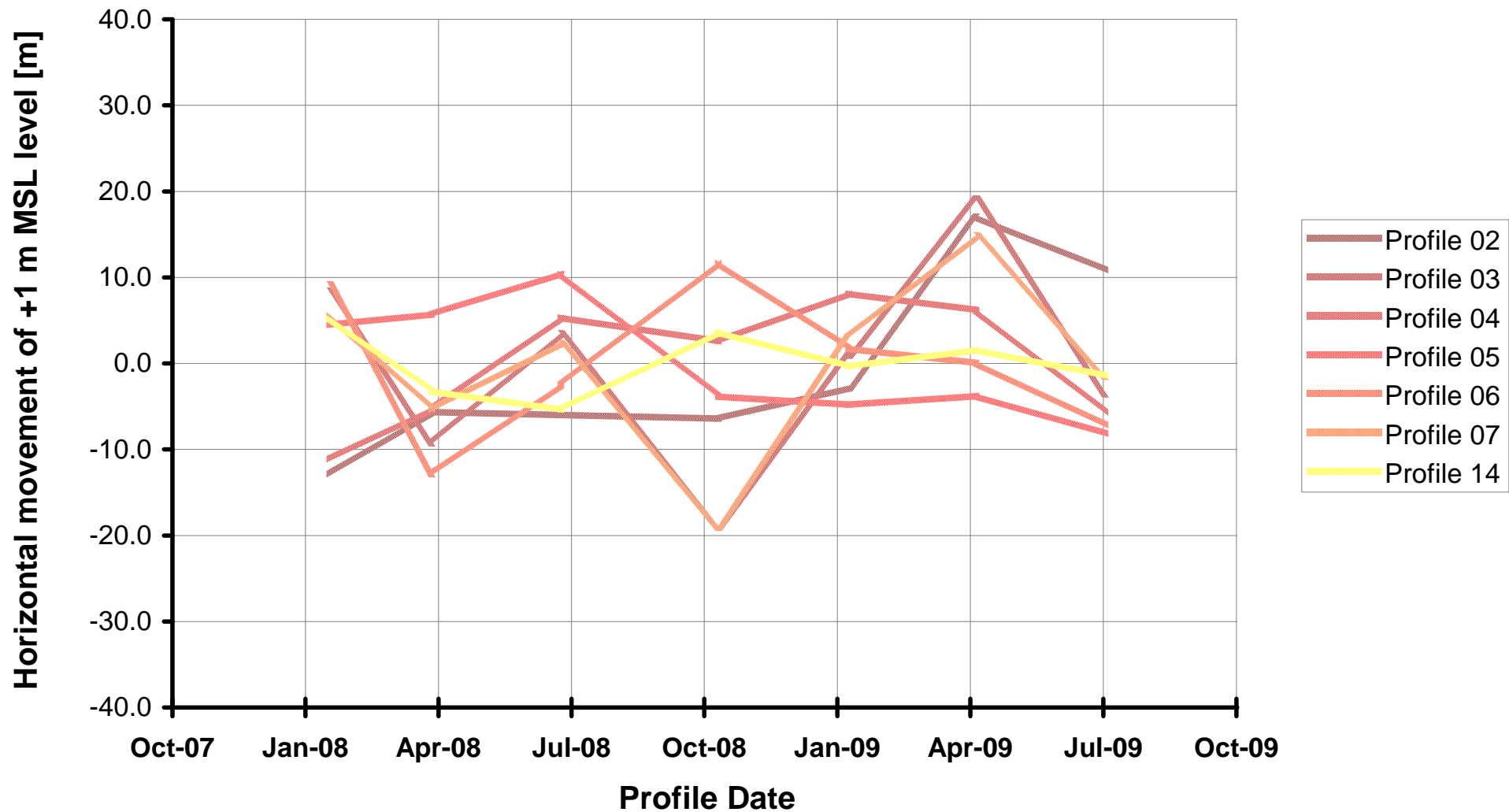


Title:

**Measured beach profiles showing seasonal variations:
Profiles 33 to 36 (refer to Figure 8.15 for positions of profiles)**

Figure No.

8.20



+ Values indicate accretion, -ve values indicate erosion

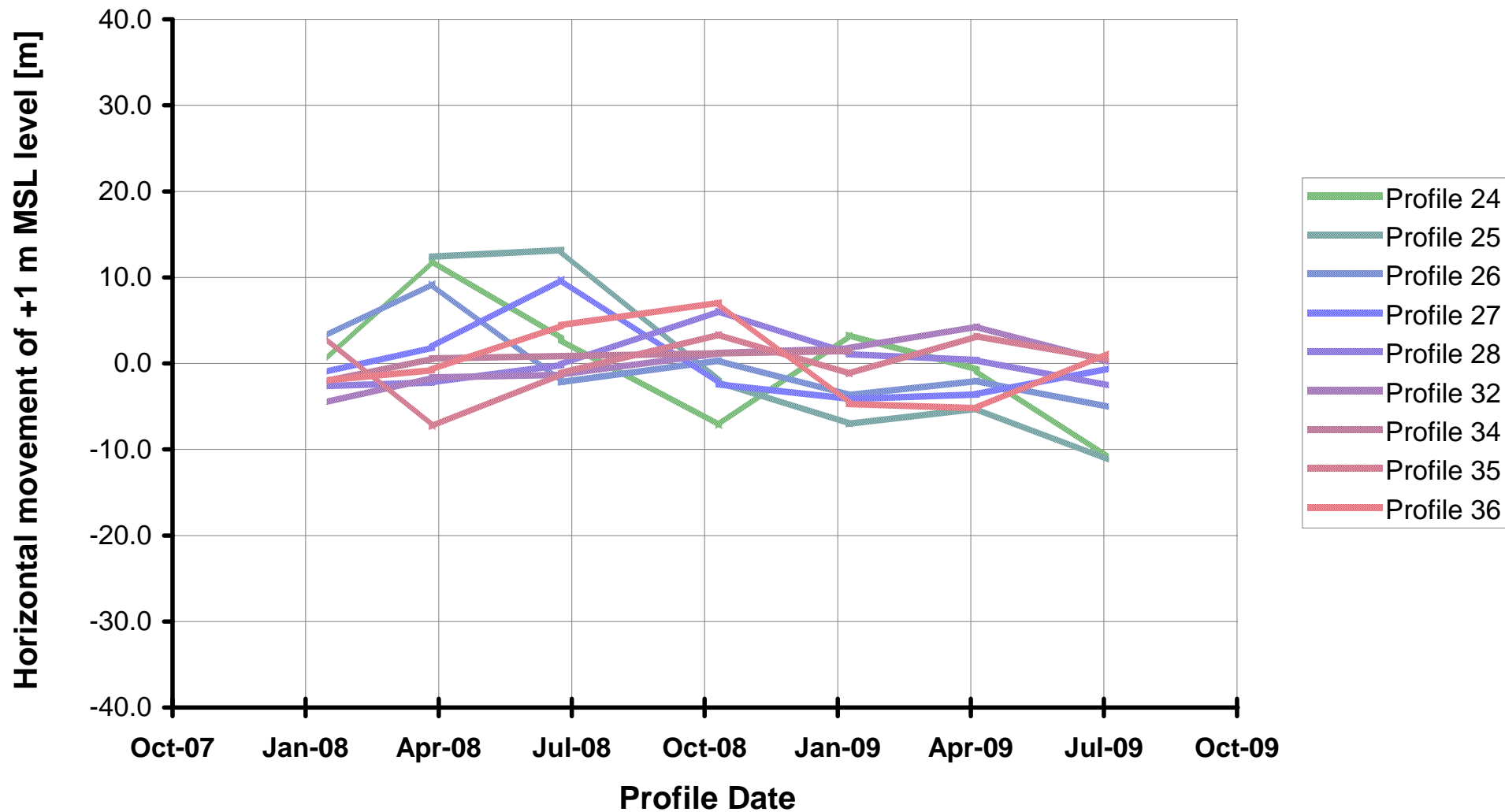


Title:

Seasonal erosion/accretion variation from mean: 2008 to 2009
Distance from beacon at +1 m MSL (northern beaches)

Figure No.

8.21



+ Values indicate accretion, -ve values indicate erosion

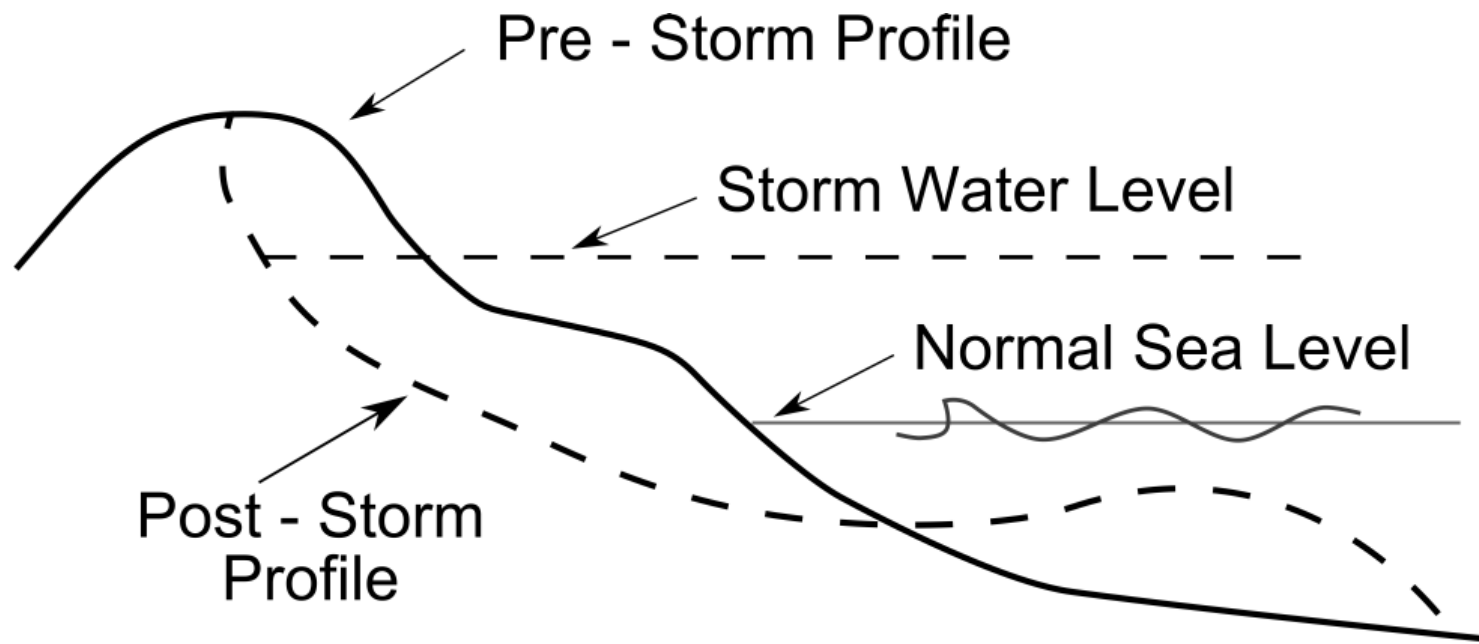


Title:

Seasonal erosion/accretion variation from mean: 2008 to 2009
Distance from beacon at +1 m MSL (southern beaches)

Figure No.

8.22

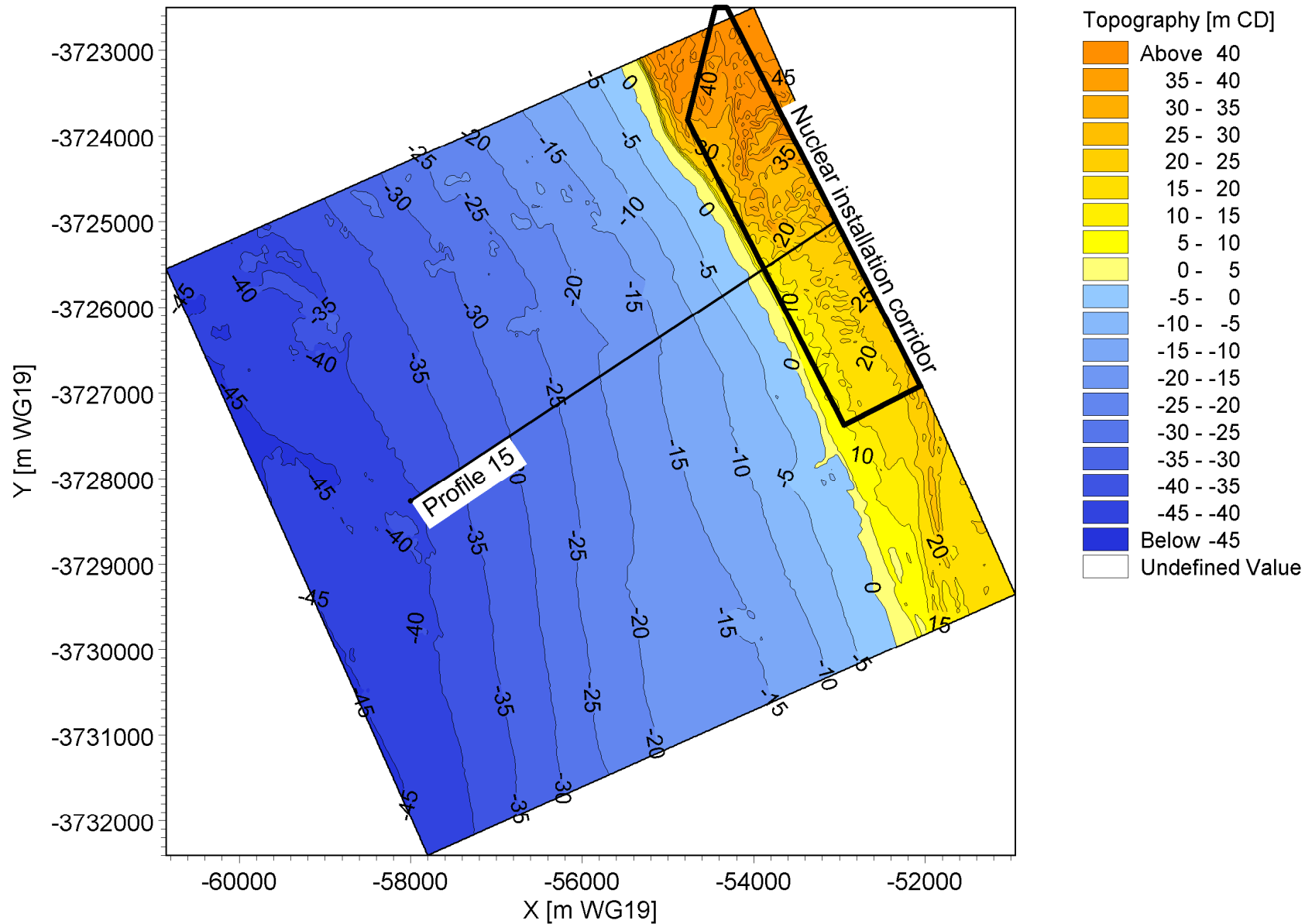


Title:

Beach profile instability due to extreme storm events

Figure No.

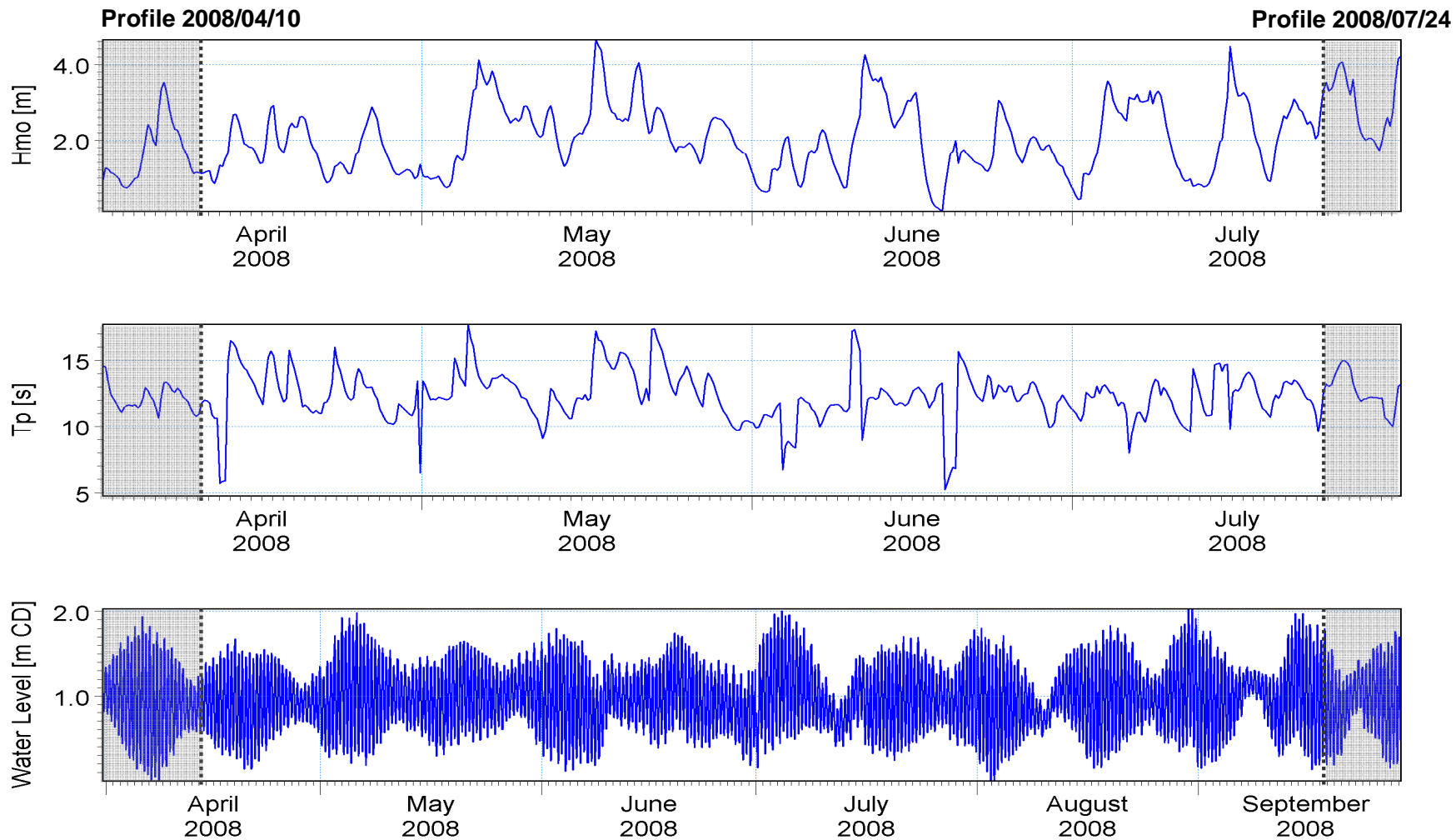
8.23



X:\PRDW Projects\Current\SA (1010) Nuclear Sites
 SSRs\Working\Engineers\RLH\CoastalEngineeringModelling\Duynefontein\Data\Bathy\Koeberg_WG19_CD_AutoCad_CalibrationP15.png



Title: Duynefontein storm erosion model verification: Extrapolation of measured beach Profile 15 from available bathymetric data - Plan view

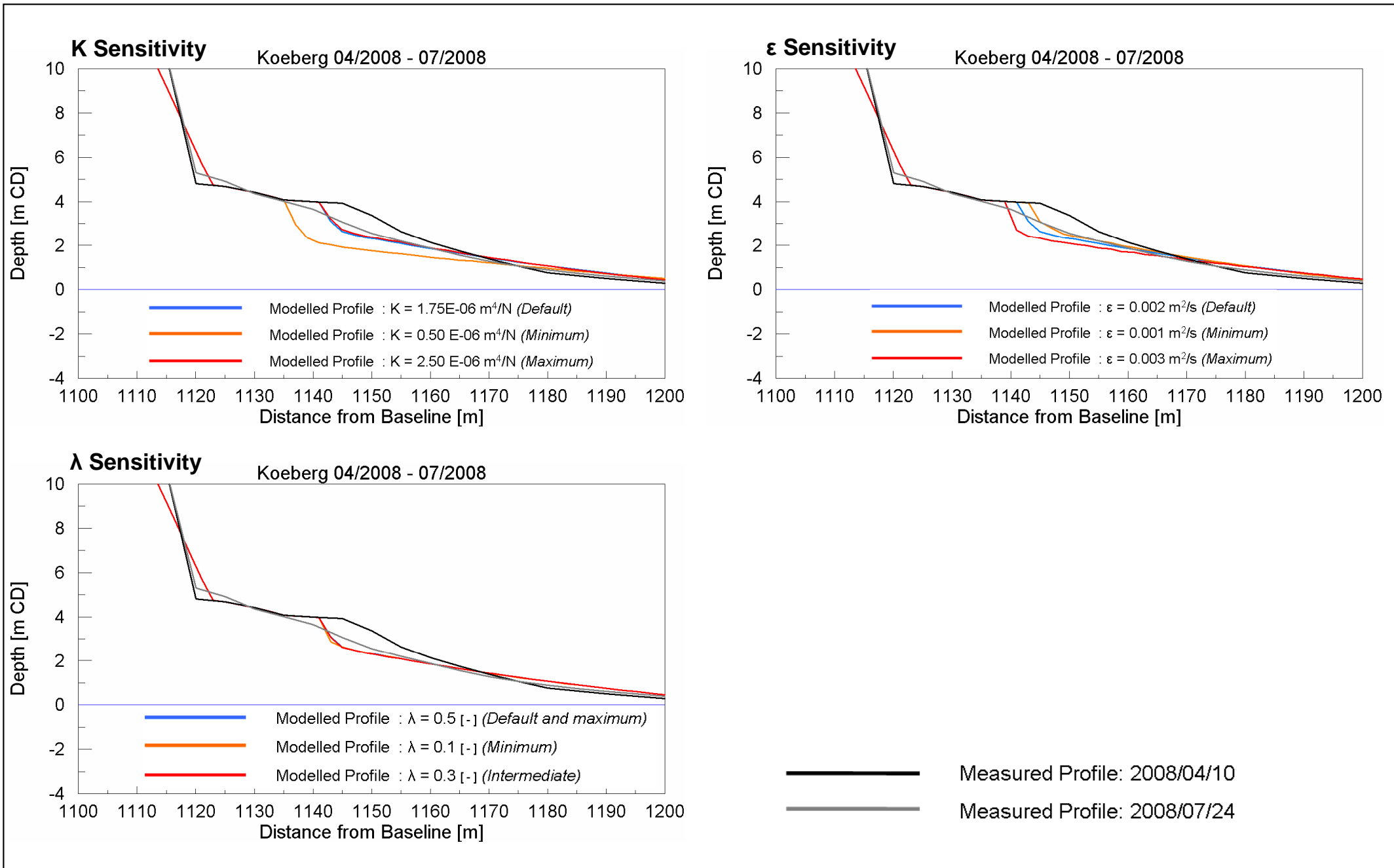


Title:

**Duynfontein storm erosion model verification: Measured wave and water levels
April 2008 to July 2008**

Figure No.

8.25

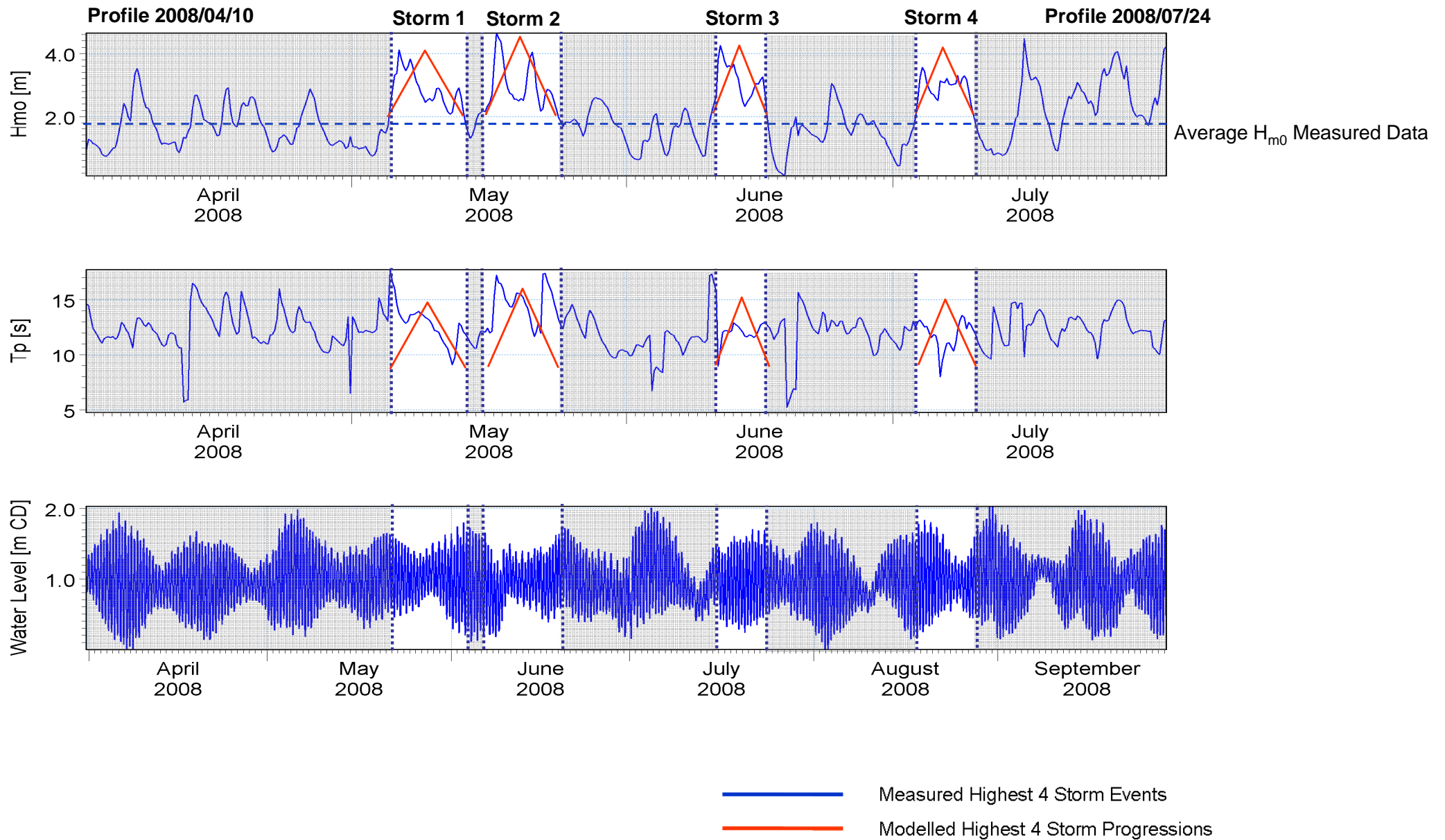


Title:

Duynfontein storm erosion model verification: Comparison of modelled profile response of SBEACH calibration parameters against measured profile data

Figure No.

8.26

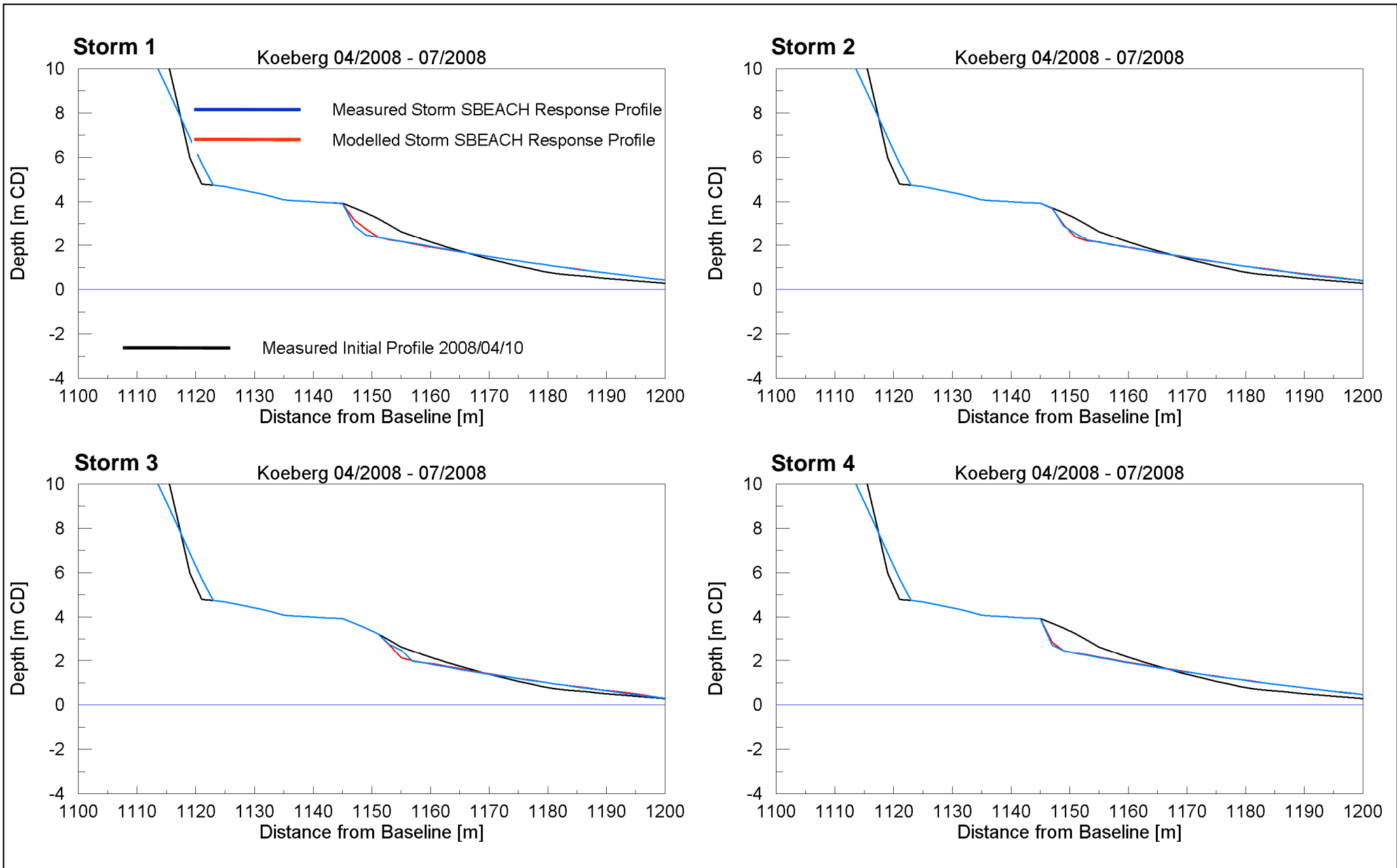


Title:

Duynfontein storm erosion model verification: Comparison of measured storm events and modelled storm progressions

Figure No.

8.27

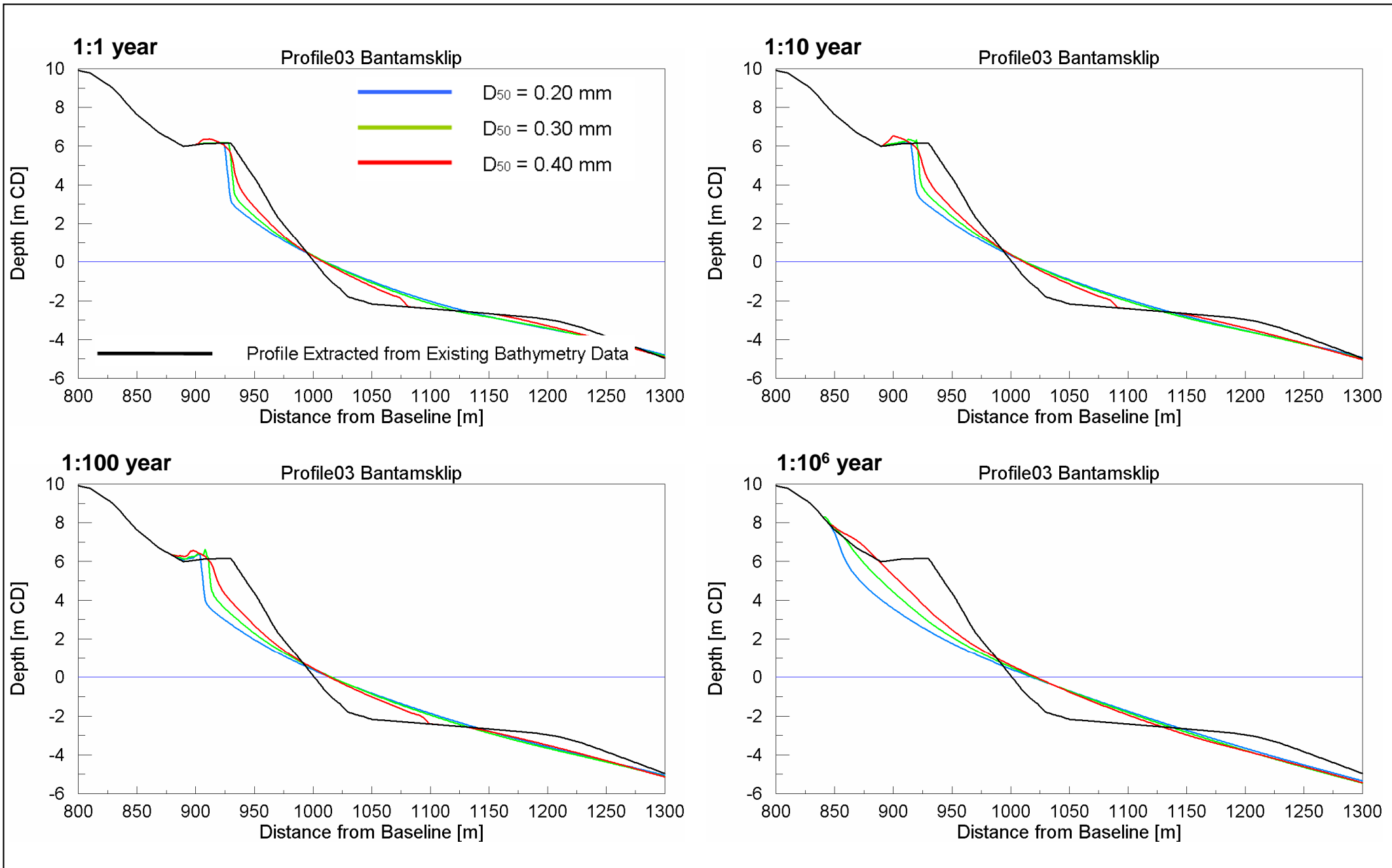


Title:

Duynfontein storm erosion model verification: SBEACH modelled beach response profiles for measured storms and modelled storms

Figure No.

8.28

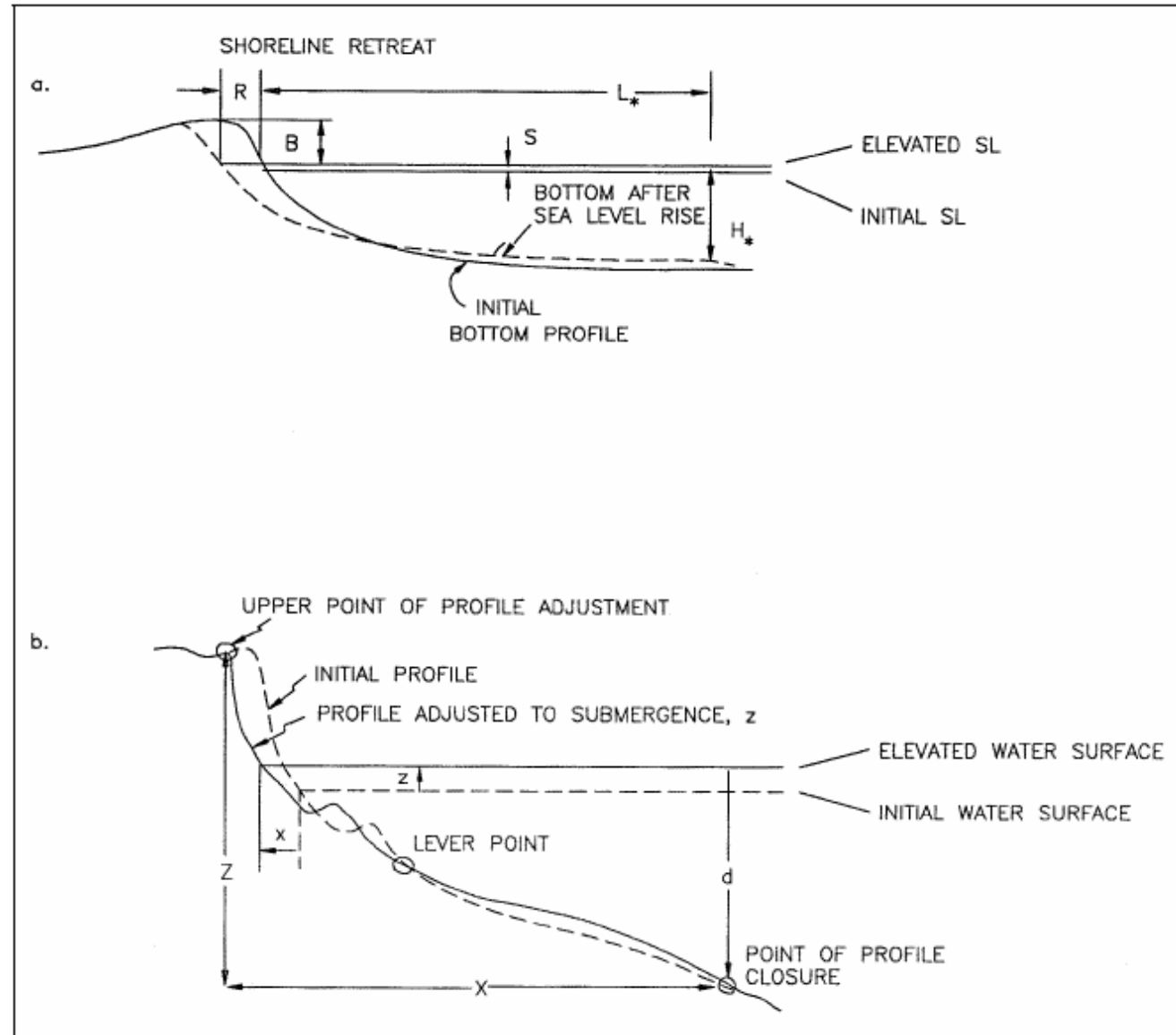


Title:

**Bantamsklip beach storm erosion Profile 03 - Excluding climate change:
Comparison of SBEACH response profiles using varying D_{50} values**

Figure No.

8.29



Original Bruun's Rule

Implemented Modification

Ref: CEM (2003)



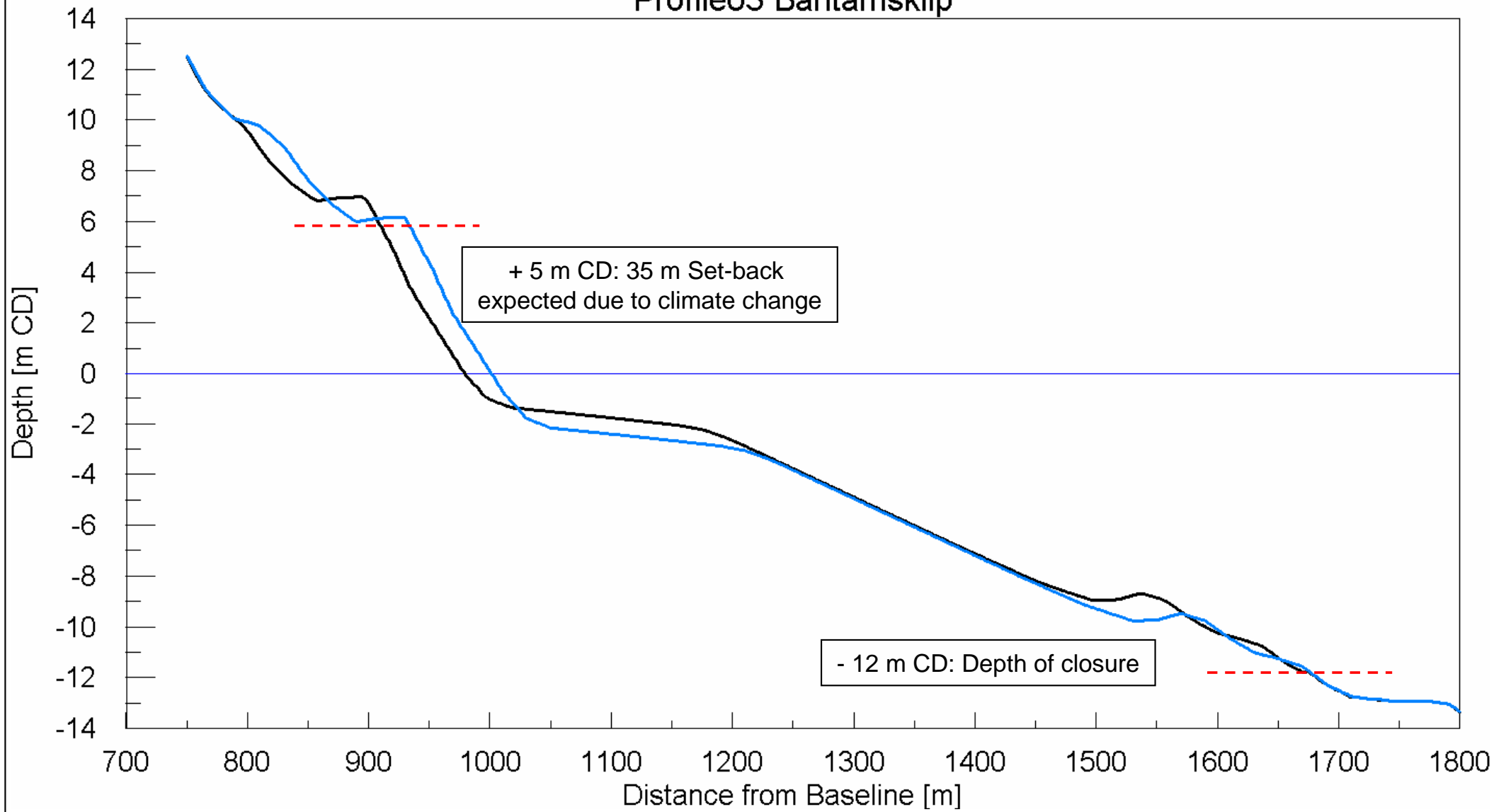
Title:

Schematic diagrams of original Bruun's rule and implemented modification

Figure No.

8.30

Profile03 Bantamsklip

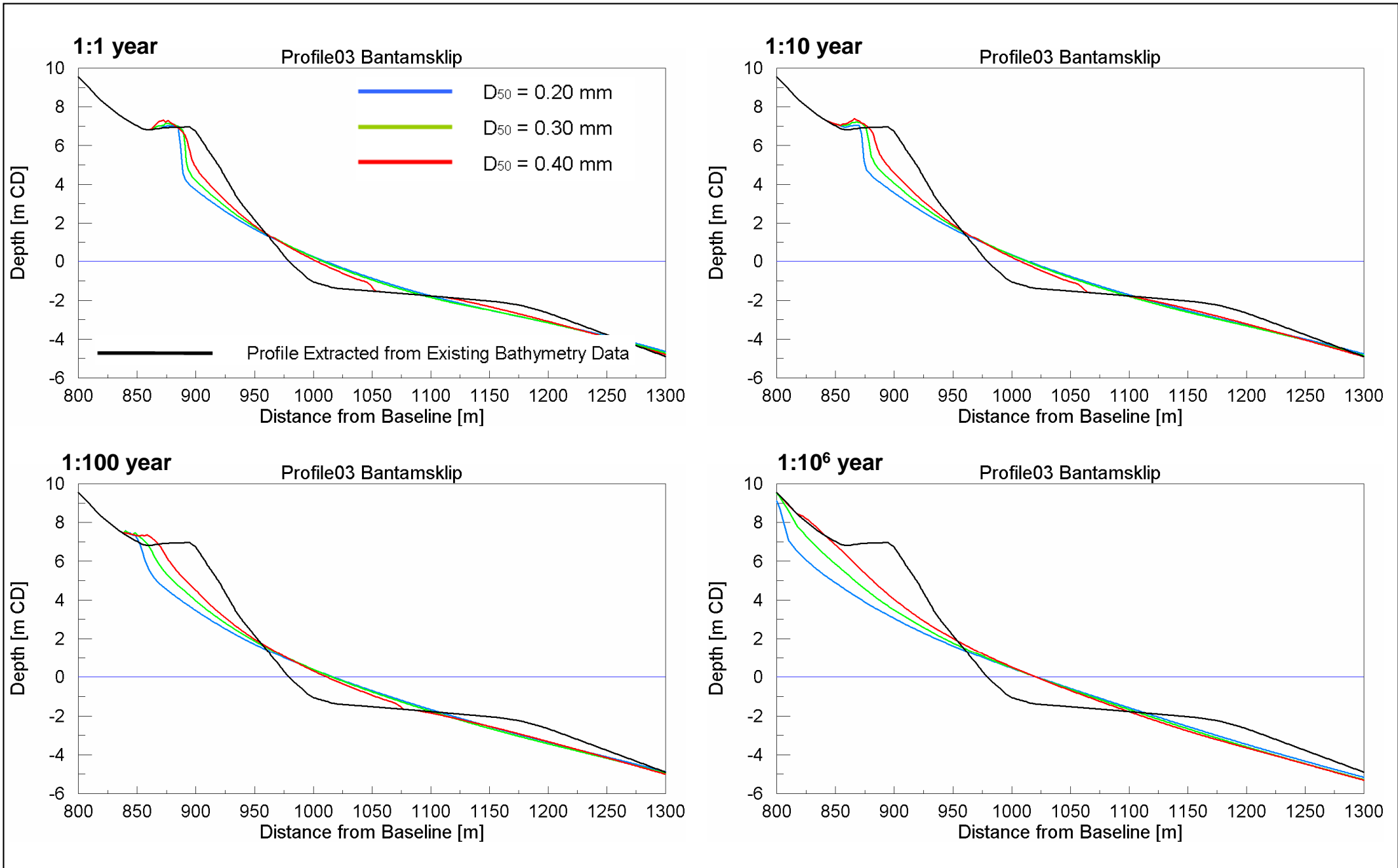


Title:

Coastal morphology: Application of Bruun's rule to Profile 03 from existing bathymetric data

Figure No.

8.31



Title:

**Bantamsklip beach storm erosion Profile 03 - Including climate change:
Comparison of SBEACH response profiles using varying D_{50} values**

Figure No.

8.32

ESKOM

**NUCLEAR SITES
SITE SAFETY REPORTS**

**COASTAL ENGINEERING
INVESTIGATIONS**

BANTAMSKLIP

Report No. 1010/3/102

APPENDICES

APPENDIX A: Global Climate Change: Consequences for Coastal Engineering Design

APPENDIX A:
Global Climate Change: Consequences for Coastal Engineering Design

**GLOBAL CLIMATE CHANGE:
CONSEQUENCES FOR COASTAL
ENGINEERING DESIGN**


POSITION PAPER

REPORT NO. 939/1/001

SEPTEMBER 2009



**PRESTEDGE RETIEF DRESNER WIJNBERG (PTY) LTD
CONSULTING PORT AND COASTAL ENGINEERS**

Global Climate Change: Consequences for Coastal Engineering Design Report No. 939/1/001					
Revision	Date	Author	Checked	Status	Approved
01	September 2009	SAL	ARW	For Use	

Keywords: Climate change, coastal engineering design

GLOBAL CLIMATE CHANGE: CONSEQUENCES FOR COASTAL ENGINEERING DESIGN

POSITION PAPER

TABLE OF CONTENTS

	PAGE NO.
1. SCOPE.....	1
2. SEA LEVEL RISE	1
3. WIND.....	6
4. STORM SURGE.....	7
5. WAVES	7
6. CURRENTS	9
7. SEAWATER TEMPERATURE	9
8. RECOMMENDED DESIGN APPROACH	10
REFERENCES	12

APPENDIX A: ADAPTIVE VERSUS PRECAUTIONARY APPROACH

LIST OF TABLES

Table 1: Projected sea level rise during this century (2000 - 2100)	3
Table 2: Recommended increase in design parameters due to climate change	10

LIST OF FIGURES

Figure 1: Historical and projected future sea level rise for emissions scenario A1B (IPCC, 2007).....	2
Figure 2: Projections and uncertainties (5 to 95% ranges) of global average sea level rise and its components in 2090 to 2099 (relative to 1980 to 1999) for the six emissions scenarios (Meehl <i>et al</i> , 2007).	2
Figure 3: Estimated UK absolute sea level (ASL) rise time-series for the 21 st century. High emissions scenario. Central estimates (thick lines) are shown together with range given by 5 th and 95 th percentiles (thin Lines). (Lowe <i>et al</i> , 2009).	5
Figure 4: Estimates of linear trends in significant wave height for regions along the major ship routes for 1950 to 2002. Trends are shown only for locations where they are significant at the 5% level. (Trenberth <i>et al</i> , 2007).....	8

1. SCOPE

The purpose of this document is to summarize PRDW's position on the effects of climate change on coastal engineering design. The consequences of climate change are the subject of ongoing research work which will require that this paper be reviewed on an annual basis. Specific parameters to be reviewed include sea level rise and wind-generated waves.

The following parameters relevant to coastal engineering design are expected to be affected by climate change and are assessed in this position paper:

- Sea level rise
- Wind
- Storm surge
- Waves
- Currents
- Seawater temperature.

Since sediment transport is a function of water level, waves and currents, any climate-induced changes to sediment transport will require a site-specific analysis based on changes to the primary forcing parameters listed above.

This position paper considers climate changes to the end of this century only. Due to a lack of local data the changes described here are generally global changes rather than local changes.

2. SEA LEVEL RISE

There has been approximately 0.17 m of sea level rise in the 20th century and an accelerating trend is predicted in the 21st century (see Figure 1). The rise is mainly due to thermal expansion of the ocean, decreases in glaciers and ice caps and losses from the polar ice sheets (see Figure 2). The main source of uncertainty is the melting of the Greenland and Antarctic ice sheets (IPCC, 2007).

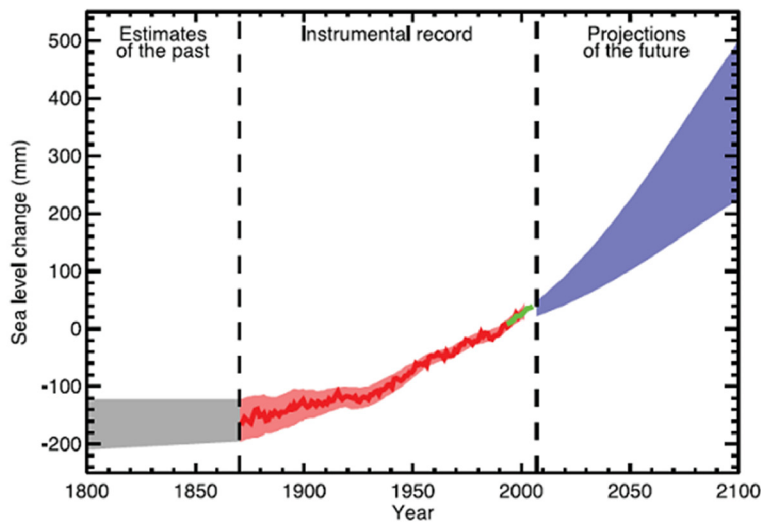


FIGURE 1: HISTORICAL AND PROJECTED FUTURE SEA LEVEL RISE FOR EMISSIONS SCENARIO A1B (IPCC, 2007).

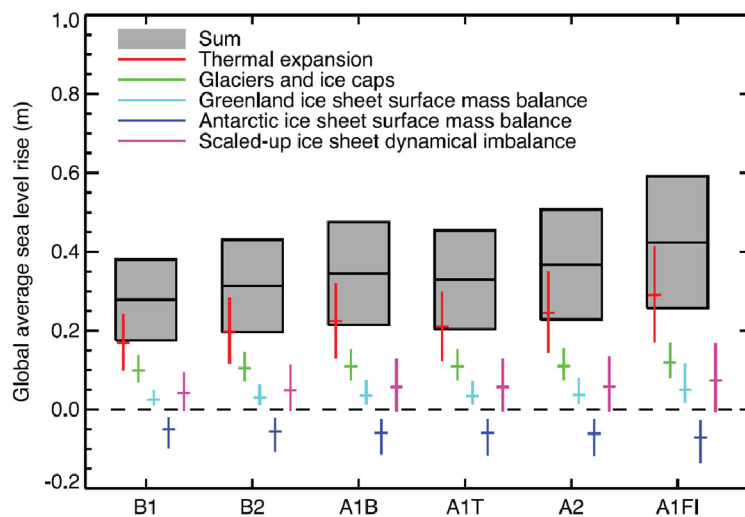


FIGURE 2: PROJECTIONS AND UNCERTAINTIES (5 TO 95% RANGES) OF GLOBAL AVERAGE SEA LEVEL RISE AND ITS COMPONENTS IN 2090 TO 2099 (RELATIVE TO 1980 TO 1999) FOR THE SIX EMISSIONS SCENARIOS (MEEHL *ET AL*, 2007).

Table 1 summarises the projected sea level rise for this century extracted from a number of recent sources and arranged chronologically.

TABLE 1: PROJECTED SEA LEVEL RISE DURING THIS CENTURY (2000 - 2100)*

Sea Level Rise [m]	Source	Comment
0.35 - 0.85	IAEA (2003)	<ul style="list-style-type: none"> ▪ Recommended values for 100 year lifetime of a nuclear power plant by the International Atomic Energy Agency. ▪ Estimate from 2003.
0.86	Defra (2006)	<ul style="list-style-type: none"> ▪ Guidelines from Department for Environment, Food and Rural Affairs, UK Government. ▪ Values given exclude local land subsidence.
0.26 - 0.59	IPCC (2007)	<ul style="list-style-type: none"> ▪ Predictions from the Fourth Assessment Report of the Intergovernmental Panel on Climate Change. ▪ These are model predicted ranges for the worst case future emissions scenario A1F1. ▪ Does not address uncertainties in climate-carbon cycle feedbacks nor include the full effects of changes in ice sheet flow, because a basis in published literature is lacking. ▪ Therefore the upper values given are not to be considered upper bounds for sea level rise.
0.79	IPCC (2007)	<ul style="list-style-type: none"> ▪ The IPCC projections given above include a contribution due to increased ice flow from Greenland and Antarctica at the rates observed for 1993-2003, but these flow rates could increase or decrease in the future. ▪ If this contribution were to grow linearly with global average temperature change, the upper ranges of sea level rise would increase by 0.1 - 0.2 m. ▪ Adding 0.2 m to 0.59 m increases the upper range to 0.79 m.
0.5 - 1.4	Rahmstorf (2007)	<ul style="list-style-type: none"> ▪ A semi-empirical relation is presented that connects global sea-level rise to global mean surface temperature. ▪ When applied to future warming scenarios of the IPCC, this relationship results in a projected sea-level rise in 2100 of 0.5 to 1.4 m above the 1990 level. ▪ Concludes that a rise of over 1 m by 2100 for strong warming scenarios cannot be ruled out.
1.6	Rohling <i>et al</i> (2008)	<ul style="list-style-type: none"> ▪ Based on average rise each century during the interglacial period ~120 000 years ago during which sea levels reached 6 m above where they are now. ▪ Data from the Red Sea indicates a rise of 1.6 ± 0.8 m per century.
0.79	Pfeffer <i>et al</i> (2008)	<ul style="list-style-type: none"> ▪ The study addresses the plausibility of very rapid sea level rise from land ice occurring this century by considering kinematic constraints on glacier contributions. ▪ “Low 1” scenario: a low range estimate based on specific adjustments to dynamic discharge in certain potentially vulnerable locations.
0.83	Pfeffer <i>et al</i> (2008)	<ul style="list-style-type: none"> ▪ “Low 2” scenario: in addition to the assumptions made in Low 1, the authors integrated presently observed rates of change in dynamic discharge forward in time.
2.0	Pfeffer <i>et al</i> (2008)	<ul style="list-style-type: none"> ▪ “High 1” scenario: combines all eustatic sources taken as high but reasonable values. No firm upper limit can be established so the values chosen represent judged upper limits of likely behaviour on the century timescale. ▪ The Greenland and Antarctic Glacier velocities required for very large increases in sea level (2-5 m) are found to be far beyond the range of observations, and while no physical proof is offered that these velocities cannot be reached, the authors recommend that they should not be adopted as a central working hypothesis.
0.5	PIANC (2008)	<ul style="list-style-type: none"> ▪ Recommendation by The International Navigation Association (PIANC), based on average values in IPCC (2007).

0.55 - 1.2	Deltacommissie (2008)	<ul style="list-style-type: none"> ▪ Commission set up by Dutch government to recommend how to protect the Dutch coast and the low-lying hinterland against the consequences of climate change. ▪ Based on research conducted by 20 leading national and international climate experts, including several IPCC authors. ▪ Supplements the scenarios for 2100 produced by the IPCC (2007). ▪ Regarded as <i>plausible upper limit scenarios</i>, which are regarded as possible by the group of sea level experts consulted, based on current scientific knowledge. ▪ Note that the values given exclude land subsidence, which will increase the relative sea level rise locally in the Netherlands by 0.1 m.
2.0	Ananthaswamy (2009)	<ul style="list-style-type: none"> ▪ With climate change modelling being so uncertain, with many ice dynamics not included due to lack of knowledge of those systems, this article states that climate scientists are looking for other ways to predict sea level rise. Some approaches being explored may take a more black box approach, where the rate of sea level rise is proportional to the increase in temperature: the warmer Earth gets, the faster ice melts and the oceans expand. This held true for the last 120 years at least. ▪ A worst case scenario indicated in this article would present up to 2 m sea level rise by 2100.
0.15 - 0.76	Lowe <i>et al</i> (2009)	<ul style="list-style-type: none"> ▪ This is from the recent UK Climate Projections Report of June 2009. ▪ Based on a UK regionalisation of the IPCC (2007) projections. ▪ Based on the high emissions scenario including ice melt. ▪ Range represents 5th – 95th confidence intervals (see Figure 3).
0.93 - 1.9	Lowe <i>et al</i> (2009)	<ul style="list-style-type: none"> ▪ This is the so-called “High-plus-plus” (H++) scenario from the UK Climate Projections Report of June 2009. ▪ The top of the H++ scenario range is derived from indirect observations of sea level rise in the last interglacial period, at which time the climate bore some similarities to the present day, and from estimates of maximum glacial flow rate. ▪ This is a UK regionalisation of an upper limit global rise from Rohling <i>et al</i> (2008) of 2.5 m \approx 1.6+0.8 m, taking glacial-isostatic adjustment (GIA) of the earth’s crust into account. ▪ This value might be used for contingency planning and to help users thinking about the limits to adaptation. It is very unlikely that the upper limit of this scenario will occur during the 21st century, but it cannot yet be ruled out completely given past climate proxy observations and current model limitations.

* The IPCC projections are from 1980-1999 until 2090-2099.

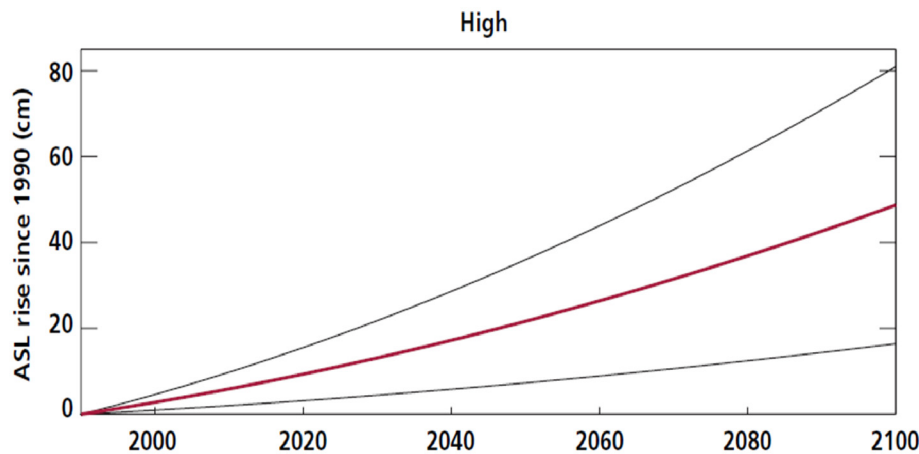


FIGURE 3: ESTIMATED UK ABSOLUTE SEA LEVEL (ASL) RISE TIME-SERIES FOR THE 21ST CENTURY. HIGH EMISSIONS SCENARIO. CENTRAL ESTIMATES (THICK LINES) ARE SHOWN TOGETHER WITH RANGE GIVEN BY 5TH AND 95TH PERCENTILES (THIN LINES). (LOWE *ET AL*, 2009).

The first issue is whether these global sea level rises apply locally to Southern Africa. Mechanisms for local sea level changes include vertical land movement, atmospheric pressure changes, ocean density variations, circulation changes and differential heating. Local sea level change due to ocean density and circulation change relative to the global average have been modelled (Meehl *et al*, 2007). For Southern Africa the predicted changes are approximately 0.05 m above the global average over the 21st century.

The rate of sea level rise measured by tide gauge between 1970 and 2003 at Durban is $+2.7 \pm 0.05$ mm/y, which is similar to recently published results of global sea-level rise calculations over the last ten years derived from worldwide tide gauge and TOPEX/Poseidon altimeter measurements, which range between 2.4 and 3.2 mm/y (Mather, 2007). An analysis of tide gauge records around Southern Africa (Mather *et al*, 2009) indicates that regional sea level trends vary, with the West Coast rising relative to land by +1.87 mm/y (1959–2006), the South Coast by +1.48 mm/y (1957 and 2006) and the East Coast by +2.74 mm/y (1967–2006). Vertical crust movements in Southern Africa are upwards (i.e. the sea level rise relative to land will be reduced compared to the global sea level rise) and increase from approximately +0.3 mm/y on the West Coast to +1.1 mm/y at Richards Bay (Mather *et al*, 2009). Mather *et al* (2009) also identify atmospheric pressure trends as contributing to the measured regional sea level trends given above.

Since the observed regional trends in relative sea level rise described above are relatively small compared to the uncertainties in the long-term global projections, for long-term design purposes it is proposed to apply the global sea level rise projections directly to Southern Africa.

Since the Intergovernmental Panel on Climate Change (IPCC) is the primary consensus reference on this subject, the sea level rise projections from the IPCC's Fourth Assessment Report (IPCC, 2007) are

summarised below. Referring to Table 1, the mid-point of the sea level rise projections for the worst emissions scenario is $(0.26 + 0.59) / 2 \approx 0.4$ m by 2100. The maximum sea level rise projection is $0.59 + 0.2 \approx 0.8$ m by 2100, which is the upper range modelled under the worst emissions scenario and includes a contribution due to increased ice flow from Greenland and Antarctica.

Since the IPCC's Fourth Assessment Report there has been an increased effort to understand the factors influencing sea-level rise, specifically the melting of the ice caps. The results of this research are summarised in Table 1 and provide an upper limit to sea level rise of 2.0 m by 2100.

Our recommended design approach (see Section 8) is to consider the implications for design of the following three sea level rise scenarios to 2100: the mid-point of the IPCC (2007) projections of 0.4 m, the upper end of the IPCC (2007) projections of 0.8 m, and in specific cases the design should also be evaluated for future design adaptations or contingency planning in the event of an extreme upper limit sea level rise of 2.0 m.

3. WIND

Based on a range of models, it is likely that future tropical cyclones (typhoons and hurricanes) will become more intense, with larger peak wind speeds associated with ongoing increases of tropical sea-surface temperatures. Extra-tropical storm tracks are projected to move poleward, with consequent changes in wind, precipitation and temperature patterns, continuing the broad pattern of observed trends over the last half century (IPCC, 2007).

For Cape Town, the south-east winds, which typically prevail along the Cape coast during the summer months, are projected to become stronger as climate change progresses and may become an increasing feature of the winter months. It is important to note that the north-west winds that prevail in winter do not, as yet, show a statistically discernable change as a result of climate forcing and are not projected in regional climate forecasts to change (MacDeevitt and Hewitson, 2007, cited in LaquaR Consultants, 2008).

The International Atomic Energy Agency (IAEA, 2003) recommends that an increase in wind strength between 5 and 10% be considered over a 100 year lifetime of a nuclear power plant. This is a global estimate from 2003.

The Department for Environment, Food and Rural Affairs of the UK Government (Defra, 2006) recommends that sensitivity testing be performed taking into account a 5% increase in offshore wind speed to the year 2055 and a 10% increase to the year 2115.

Due to the inherent uncertainties in long-term regional climate forecasts and the requirement for a precautionary approach, an increase in wind speed of 10% to the year 2100 is recommended for design, based on IAEA (2003) and Defra (2006). Ongoing research work on regional wind climate

projections should be reviewed annually, considering that the Ferrel Westerly winds are the main drivers for winter storm events along the South-Western and Southern Cape coastlines. Changes in wind direction are likely to be localised, with little information currently available.

4. STORM SURGE

Storm-induced surges can produce short-term increases in water level that rise to an elevation considerably above tidal levels. Storm surge is mainly composed of an atmospheric pressure component (low pressure for positive storm surge and high pressure for a negative storm surge) and a wind-induced component.

The gradient in atmospheric pressure and thus the atmospheric pressure component of storm surge is proportional to the wind speed, while the wind set-up component of storm surge is proportional to the square of the wind speed. With a 10% increase in wind speed due to climate change (see Section 3) the total storm surge is thus likely to increase by between 10% and 21%, depending on the relative contribution of the pressure and wind components, respectively.

The UK Climate Projections Report (Lowe *et al*, 2009) applied sophisticated surge models and found that around the United Kingdom the 1:50 year surge is projected to increase by less than 0.09 m by 2100 (not including the mean sea level change). In addition, a “High-plus-plus” (H++) model scenario was also considered (Lowe *et al*, 2009). Whilst the top end of this scenario cannot be ruled out based on current understanding, it is regarded as very unlikely to occur during the 21st century. For the H++ scenario the 1:50 year surge in the Thames Estuary is projected to increase by approximately 0.2 - 0.95 m.

In the absence of downscaled storm surge model data for Southern Africa, it is conservatively recommended to increase the storm surge by 21% to the year 2100, based on a 10% increase in wind speed.

Since shelf waves, edge waves and meteo-tsunamis have similar forcing mechanisms to storm surge, i.e. changes in wind or atmospheric pressure, is recommended to also increase the water level changes caused by these processes by 21%. Note that tsunamis due to geological forcing mechanisms, e.g. earthquakes, are unlikely to be influenced by climate change (IPPC, 2007).

5. WAVES

As part of the Fourth Assessment Report of the Intergovernmental Panel on Climate Change, Trenberth (2007) reports on historical trends in significant wave height (H_{m0}) obtained from Voluntary Observing Ships (VOS) data between 1950 and 2002 (see Figure 4). These results show that around Southern Africa the increase in H_s is around 0.4 cm/decade, whilst significantly higher increases up to

1.2 cm/decade are found in the Northern Atlantic and Northern Pacific Oceans. These results suggest that future wave height changes will not be uniform.

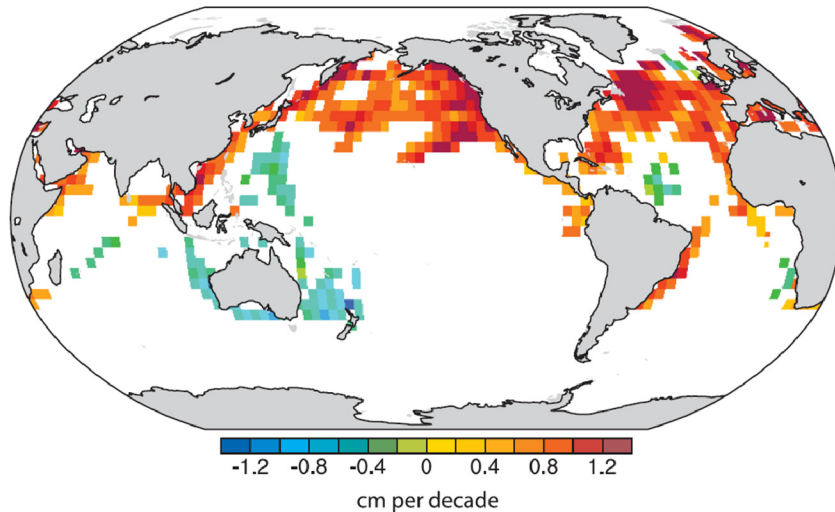


FIGURE 4: ESTIMATES OF LINEAR TRENDS IN SIGNIFICANT WAVE HEIGHT FOR REGIONS ALONG THE MAJOR SHIP ROUTES FOR 1950 TO 2002. TRENDS ARE SHOWN ONLY FOR LOCATIONS WHERE THEY ARE SIGNIFICANT AT THE 5% LEVEL. (TRENBERTH *ET AL*, 2007).

The UK Climate Projections Report (Lowe *et al*, 2009) applied sophisticated wave models and found that around the United Kingdom for the medium emissions scenario, the projected changes to 2100 in the winter mean H_{m0} are between -0.35 and $+0.05$ m. Changes in the annual maxima are projected to be between -1.5 and $+1.0$ m. Changes in wave period and direction were found to be rather small and more difficult to interpret.

The Department for Environment, Food and Rural Affairs of the UK Government (Defra, 2006) recommends sensitivity testing taking into account a 5% increase in wave height to the year 2055 and a 10% increase to the year 2115. These increases are the same as Defra recommends for wind.

The methods presented in Coastal Engineering Manual (CEM, 2003) have been used to analyse the impact of an increased wind speed on fetch-limited and duration-limited waves. Duration-limited waves show the largest increase, with a 10% increase in wind speed due to climate change (see Section 3) increasing the wave height by 13% for the lower wind speeds and 17% for the higher wind speeds.

Wave data measured offshore of Cape Town and Richards Bay have been analysed to investigate trends in the peak significant wave height of individual storm events (Guastella and Rossouw, 2009). The Cape Town data suggests an increasing trend during winter of approximately 0.5 m over the 14 year period from 1994 to 2008, and a general decreasing trend during summer. The Richards Bay data do not show any conclusive trends over the 30 year period from 1979 to 2008. The study also identifies

cold fronts and their associated low pressure systems as the major cause of extreme wave events along the South-Western Cape coastline. On the East Coast of South Africa tropical cyclones and cut-off lows were identified as being responsible for the extreme wave events.

In the absence of downscaled wave generation model data for Southern Africa, it is conservatively recommended to increase the wave height by 17% to the year 2100, based on a 10% increase in wind speed. The impact on wave period can be estimated from the present day H_{m0} - T_p relationship. We are not aware of data on changes in wave directions for South Africa. Sensitivity testing to wave direction should be considered on a project-specific basis.

6. CURRENTS

Ocean circulations could be affected by climate change, and these effects could be either gradual or sudden. For example, it is very likely that the Atlantic Ocean Meridional Overturning Circulation (MOC), which transports relatively warm upper-ocean waters northward (including the Gulf Stream), and relatively cold deep waters southward, will slow down during the course of the 21st century. It is however very unlikely that the MOC will undergo a large abrupt transition during the 21st century. (IPCC, 2007). No reference to possible changes in the Agulhas Current is made in IPCC (2007).

Coastal hydrodynamics will be affected by changes in wind, wave height, wave direction and sea level. Wind-driven currents will tend to increase linearly with wind speed, while wave-driven currents will depend both on wave height and wave direction. These changes will vary from one location to another and can only be quantified through detailed site-specific modelling.

7. SEAWATER TEMPERATURE

From a coastal engineering design perspective, seawater temperature is relevant for cooling water studies and also has a small effect on sediment settling velocities and thus sediment transport. Impacts on marine ecology are beyond the scope of this position paper.

The UK Climate Projections Report (Lowe *et al*, 2009) applied sophisticated hydrodynamic models and found that the seas around the UK are projected to be 1.5 - 4°C warmer, depending on location, and ~0.2 psu fresher by the end of the 21st century, using the medium emissions scenario. Seasonal stratification strength is projected to increase but not by as much as in the open ocean.

The International Atomic Energy Agency (IAEA, 2003) recommends an increase in sea temperature of 3°C be considered over a 100 year lifetime of a nuclear power plant.

Additional factors to be considered include:

- changes in large ocean currents on temperature, e.g. Agulhas Current

- changes in coastal upwelling due to changes in wind speed or direction.

8. RECOMMENDED DESIGN APPROACH

The recommended design approach is to first calculate the present day design parameters based on historical datasets, e.g. determine the 1:100 year wave height from an Extreme Value Analysis of measured Waverider data or wave hindcast data. The present day parameters should then be increased to account for climate change using the values in Table 2. In some cases a conservative design will be achieved by excluding the effect of climate change, e.g. for entrance channel depths and minimum seawater intake depths it is recommended not to include sea level rise.

Although the rate of change is expected to increase over time (see for example Figures 1 and 3), because of the uncertainty attached to these rates and to be conservative, we have assumed a linear increase over the 21st century, with 50% of the change predicted to the year 2100 occurring by 2050. The recommended increases are given in Table 2; refer to Sections 2 to 7 for the supporting information.

TABLE 2: RECOMMENDED INCREASE IN DESIGN PARAMETERS DUE TO CLIMATE CHANGE

Parameter		Increase to 2050	Increase to 2100
Sea level rise	Mid-point of projections ⁽¹⁾	+ 0.2 m	+ 0.4 m
	Upper end of projections ⁽²⁾	+ 0.4 m	+ 0.8 m
	Extreme upper limit ⁽³⁾	+ 1.0 m	+ 2.0 m
Wind speed		+ 5%	+ 10%
Storm surge (including shelf-waves, edge waves and meteo-tsunami)		+ 10%	+ 21%
Wave height		+ 8.5%	+ 17%
Wave period		Obtain from present day H_{m0} - T_p relationship.	
Wave direction		No data, consider sensitivity testing.	
Seawater temperature		+ 1.5°C	+ 3°C
Currents and sediment transport		Use site-specific modelling with the forcing parameters increased by the values given above.	

Notes:

- (1) Although engineering judgement is required on a case by case basis, this value would typically be recommended for minor structures with a short design life, or structures that can relatively easily be adapted to accommodate possible accelerated sea level rise in future.
- (2) Recommended for the majority of large coastal structures.
- (3) In specific cases the design should also be evaluated for future design adaptations or contingency planning in the event of an extreme upper limit sea level rise of 2.0 m by 2100. See below for further details.

In specific cases an extreme upper limit sea level rise of 2.0 m by 2100 should be considered as part of the design process. This will depend inter alia on the type of structure, the design life and the consequences of failure. Examples of the issues that should be considered include:

- The survivability of the structure under the extreme upper limit climate change projections.
- The design should consider making allowance for future adaptations, e.g. increase the breakwater crest width to allow for future raising of the crest level, allow space for future revetments in front of structure.
- Consider the cost implications of an adaptive versus precautionary approach (see Appendix A for more details).
- Consider the impacts of the structure on the adjacent coastline or adjacent structures, and vice versa, e.g. raising the structure levels may increase the flooding risk for adjacent structures.

REFERENCES

1. Ananthaswamy, A (2009) Sea level rise: It is worse than we thought. *New Scientist*, 2715, 28-33.
2. CEM (2003) CEM Part II Chapter 2 - Meteorology and Wave Climate, US Army Corps of Engineers, July 2003.
3. Defra (2006) Department for Environment, Food and Rural Affairs. Flood and Coastal Defence Appraisal Guidance: FCDPAG3 Economic appraisal: Supplementary note to operating authorities – Climate change impacts October 2006.” Defra, UK Government.
4. Deltacommissie (2008) Working together with water, A living land builds for its future, Findings of the Deltacommissie 2008.
5. Guastella, L A and Rossouw M (2009) Coastal Vulnerability: Are Coastal Storms Increasing in Frequency and Intensity along the South African Coast? International Multi-purpose reef conference, Jeffrey’s Bay, South Africa, May 2009.
6. IAEA (2003) Flood Hazard for Nuclear Power Plants on Coastal and River Sites. International Atomic Energy Agency. IAEA Safety Standards Series No. NS-G-3.5.
7. IPCC (2007) Climate Change 2007: Synthesis Report. Contribution of Working Groups I, II and III to the Fourth Assessment Report of the Intergovernmental Panel on Climate Change [Core Writing Team, Pachauri, R.K and Reisinger, A. (eds.)]. IPCC, Geneva, Switzerland, 104 pp.
8. LaquaR Consultants (2008) Global Climate Change and Adaptation - A Sea-Level Rise Risk Assessment, prepared by LaquaR Consultants CC for the City of Cape Town, 2008.
9. Lowe, J A, Howard, T P, Pardaens, A, Tinker, J, Holt, J, Wakelin, S, Milne, G, Leake, J, Wolf, J, Horsburgh, K, Reeder, T, Jenkins, G, Ridley, J, Dye, S, Bradley, S (2009). UK Climate Projections science report: Marine and coastal projections. Met Office Hadley Centre, Exeter, UK.
10. MacDeevit, C and Hewitson, B (2007) Sea-level Rise on the Cape Coast. Atmospheric Science Honours Thesis 2007. University of Cape Town.
11. Mather, A A (2007) Linear and nonlinear sea-level changes at Durban, South Africa, *South African Journal of Science*, 103, November/December 2007, 509-512.
12. Mather, A A, Garland G G and Stretch D D (2009). *African Journal of Marine Science* 2009, 31(2), in press.
13. Meehl, G.A., T.F. Stocker, W.D. Collins, P. Friedlingstein, A.T. Gaye, J.M. Gregory, A. Kitoh, R. Knutti, J.M. Murphy, A. Noda, S.C.B. Raper, I.G. Watterson, A.J. Weaver and Z.-C. Zhao, 2007: Global Climate Projections. In: *Climate Change 2007: The Physical Science Basis. Contribution of Working*

- Group I to the Fourth Assessment Report of the Intergovernmental Panel on Climate Change [Solomon, S., D. Qin, M. Manning, Z. Chen, M. Marquis, K.B. Averyt, M. Tignor and H.L. Miller (eds.)]. Cambridge University Press, Cambridge, United Kingdom and New York, NY, USA.
14. Rohling, E J, Grant, K, Hemleben, Ch, Siddal, M, Hoogakker, B A A, Bolshaw, M and Kucera, M (2008). High rates of sea-level rise during the last interglacial period, *Nature Geoscience*, 1, 38-42, 2008.
 15. PIANC (2008) Waterborne transport, ports and waterways: A review of climate change drivers, impacts, responses and mitigation. May 2008.
 16. Pfeffer, W. T., Harper, J. T. & O'Neel, S (2008). Kinematic constraints on glacier contributions to 21st-Century sea-level rise. *Science*, 321, 1340-1343.
 17. Rahmstorf, S. (2007) A Semi-Empirical Approach to Projecting Future Sea-Level Rise. *Science*, 315, 368-370.
 18. Trenberth, K.E., P.D. Jones, P. Ambenje, R. Bojariu, D. Easterling, A. Klein Tank, D. Parker, F. Rahimzadeh, J.A. Renwick, M. Rusticucci, B. Soden and P. Zhai, (2007). Observations: Surface and Atmospheric Climate Change. In: *Climate Change 2007: The Physical Science Basis. Contribution of Working Group I to the Fourth Assessment Report of the Intergovernmental Panel on Climate Change* [Solomon, S., D. Qin, M. Manning, Z. Chen, M. Marquis, K.B. Averyt, M. Tignor and H.L. Miller (eds.)]. Cambridge University Press, Cambridge, United Kingdom and New York, NY, USA.

APPENDIX A: ADAPTIVE VERSUS PRECAUTIONARY APPROACH

Our response to climate change requires appropriate decisions on whether to consider a managed adaptive approach or whether to adopt a more precautionary approach. The following (reproduced from Defra, 2006) provides a brief explanation of this.

Managed adaptive approach

A managed approach allows for adaptation in the future, and is wholly appropriate in the majority of cases where ongoing responsibility can be assigned to tracking the change in risk, and managing this through multiple interventions. This approach provides flexibility to manage future uncertainties associated with climate change, during the whole life of a flood risk management system. To consider a precautionary approach only, could lead to greater levels of investment at fewer locations. A managed approach is therefore important to ensure best value for money.

Both structural (e.g. physical changes to structures, upstream storage or a combination thereof) and non-structural solutions (e.g. land use changes, resilience, statutory objections, relocation, public awareness) are necessary to ensure cost effective adaptation can take place in future years. In order to fully explore non-structural options alongside structural options, the sensitivity analysis of these options should become a more important component of appraisal and decision making, with care needed at screening-out stages to avoid discarding non-structural options without strong justification. See Figure A.1 and the saw-tooth line to illustrate.

Precautionary approach

For some circumstances, future adaptation may be technically infeasible or too complex to administer over the long term of up to 100 years. These circumstances may occur where multiple interventions are not possible to manage the changes in risk. Therefore, a precautionary approach, perhaps with one-off intervention, may be the only feasible option, such as in the design capacity of a major culvert or in the span of a road bridge across a flood plain. See Figure A.1 and the dashed line to illustrate.

REFERENCES

- Defra (2006) Department for Environment, Food and Rural Affairs. Flood and Coastal Defence Appraisal Guidance: FCDPAG3 Economic appraisal: Supplementary note to operating authorities – Climate change impacts October 2006.” Defra, UK Government.

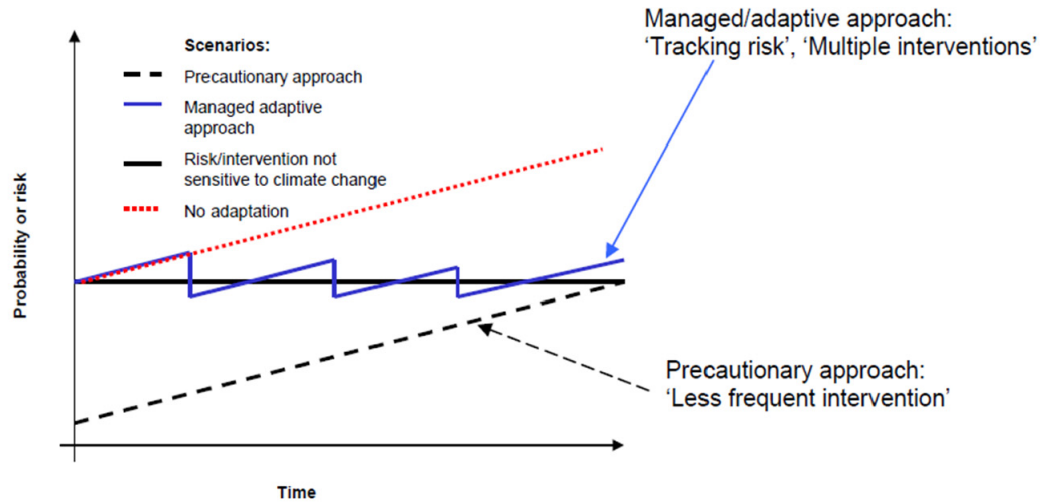


FIGURE A.1: COMPARISON BETWEEN MANAGED ADAPTIVE APPROACH AND PRECAUTIONARY APPROACH RESPONSE TO CLIMATE CHANGE. (DEFRA, 2006).